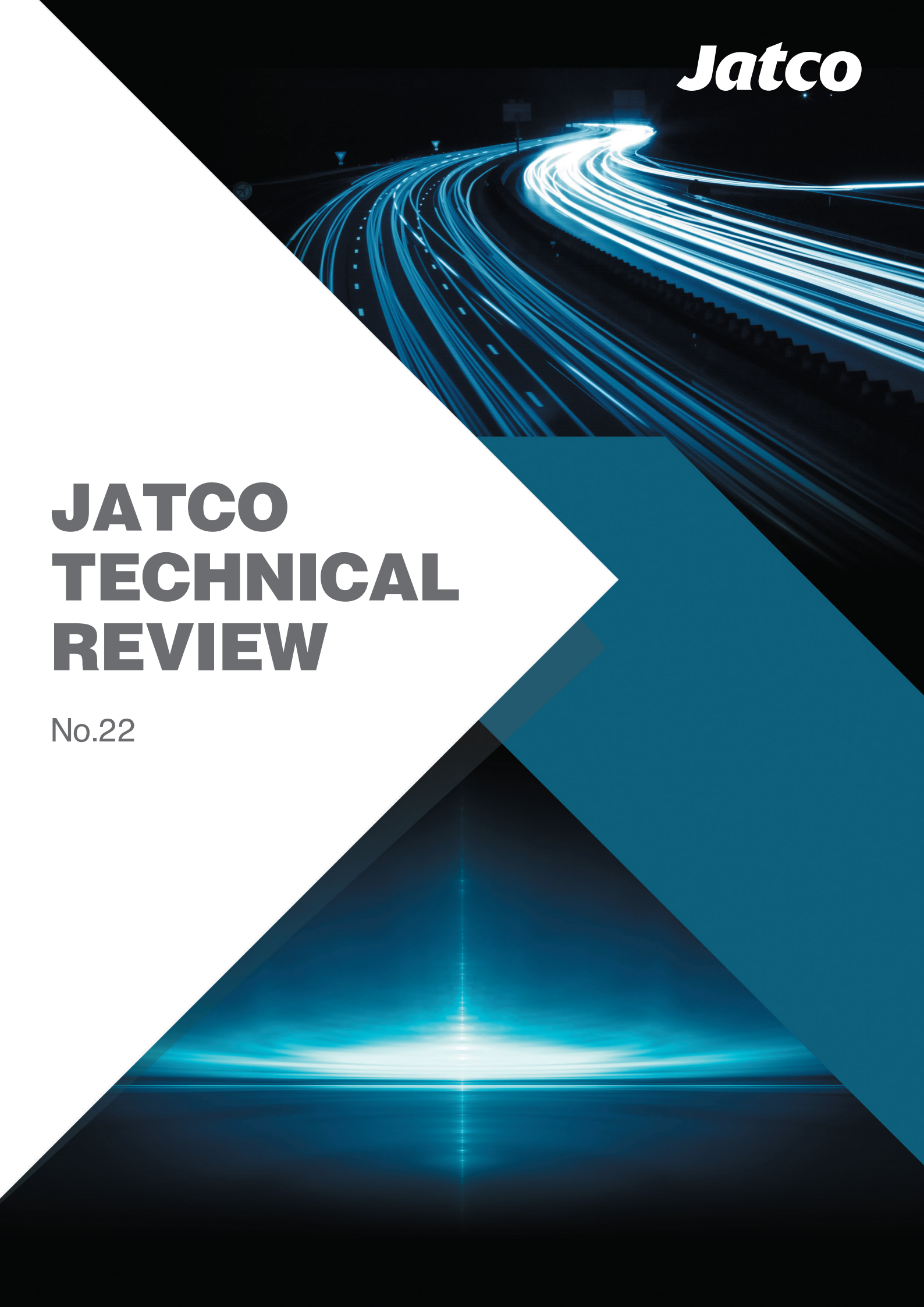

Jatco

JATCO TECHNICAL REVIEW

No.22

CONTENTS

Preface

Technical Reports

Introduction to Products

Patent

Global Changes and Purpose-driven Management

Tomoyoshi SATO
President and CEO

I wonder if I am the only one who feels that the pace of global change has become faster in recent years.

The issue of global warming prompted discussions about reducing CO_2 emissions at meetings of the Conference of the Parties (COP) to the United Nations Framework on Climate Change even before the outbreak of the COVID-19 pandemic. Now all of the developed countries have independently implemented their own emissions regulations while various speculations about climate change persist. In addition, consciousness of sustainability has risen, and the world is beginning to demand corporate governance that deals with discrimination, poverty and even human rights as typified by the Sustainable Development Goals (SDGs). Amid these historic changes, infections of the novel coronavirus have spread widely. That triggered advances in the remote world, accelerating the evolution of information technologies and inviting people into a virtual world where everything in daily life can be accomplished while staying at home. As a result, there is a feeling that this has changed even the industrial structure. Semiconductor shortages occurred in the midst of this transition in the industrial structure. Moreover, Russia's startling invasion of Ukraine has become a protracted struggle contrary to initial expectations, giving rise to problems concerning resources such as energy, grains and other materials and sparking global inflation. Considerable time has passed since the present day was first referred to as the age of VUCA, an acronym standing for volatility, uncertainty, complexity and ambiguity. In recent years, various drastic changes have occurred in a short period, creating a feeling that even time has become involved, and it is becoming harder to see the future.

During the past year since becoming president, I have continued to ask myself every day how our company can survive in the future. Even though we cannot see a definite future, can't we see the direction in which to proceed? If changes occur rapidly, shouldn't we acquire the strength and organizational capabilities to keep up with them? And wouldn't it be easier if we initiated change by ourselves instead?

It was against this backdrop that we reviewed our corporate philosophy this fiscal year. As a major pillar of our corporate philosophy, we newly established "driving the possibilities of mobility with technology and passion" as our purpose. This will serve as a compass showing the direction in which to proceed in our unpredictable voyage ahead. It will also be the foundation for perceiving and creating change. This purpose was defined to enable us to move forward in the direction we should proceed without losing our way and without being tossed about by the waves of rapid change. By making clear the significance of JATCO's presence and contributions to society, everyone within and outside the company will more easily understand JATCO's value, and also employees will have pride in their company and their work. Above all else, it signifies that we aim to confront change and initiate change by ourselves.

This is the 22nd issue of the JATCO Technical Review. Technology is a vital source of competitiveness in which we take pride. At JATCO, we are also expanding the scope of our technology to include electrification and digital transformation (DX) capabilities, in addition to our traditional technologies for automatic transmissions and continuously variable transmissions. This issue of the JATCO Technical Review also focuses on technologies for "driving the possibilities of mobility," so we hope that readers will also perceive the changes described here.

Large historical trends in the world are not easily changed, but one can understand their significance. By understanding change without resisting it and pursuing new technologies with passion, we intend to contribute to the formation of a new world of mobility based on those technologies.

JATCO will continue to initiate change based on our expressed purpose of "driving the possibilities of mobility with technology and passion."

Development of a new CVT featuring high efficiency and wide ratio coverage

Shingo SUZUKI* Kouhei TOYOHARA** Makoto OGURI *** Masaya MATSUMURA****

Summary

Higher efficiency and wider ratio coverage are demanded of continuously variable transmissions (CVTs) today in this transitional period toward electrification as a continuous environmental response. JATCO has developed a new high-efficiency CVT by adopting a twin oil pump system incorporating a high-output electric oil pump and simultaneously evolving existing technologies of the torque converter, chain, control valve and other components.

1. Introduction

The shift to electrification is accelerating toward the attainment of carbon neutrality. However, there are still many issues, including infrastructure aspects, that must be overcome in order for electrified vehicles without an internal combustion engine (ICE) to become popular throughout the world. Since ICE-powered vehicles will remain the mainstream for some time to come, it is absolutely essential to improve their efficiency. This article describes the technologies adopted for the new Jatco CVT-X (CVT-X), featuring wide ratio coverage, high efficiency and excellent compatibility with downsized turbocharged (DST) engines.

2. Overview of CVT-X

2.1 Development concept

Vehicle manufacturers are switching from naturally aspirated engines to DST engines as a measure for complying with global environmental requirements. The ratio coverage for the CVT-X pulley system was set at 8.2 in order to improve the acceleration response of DST engines before turbocharging provides boost and to lower the engine speed during cruising. A chain-driven variator system with high torque transmission efficiency was adopted to improve vehicle fuel economy. In addition, various measures were employed to reduce friction along with adopting a twin oil pump system that combines an electric oil pump (ELOP) with a mechanical oil pump (MOP), enabling the MOP to be downsized for reducing mechanical losses.

2.2 Specifications and major technologies

The specifications of the CVT-X and the existing Jatco CVT8 (CVT8) model are compared in Table 1. As shown in Fig. 1, the CVT-X has a standard CVT mechanism without an auxiliary transmission. It consists of a torque converter, forward-reverse clutch system, planetary gear set, pulley/chain assembly and 2 stage reduction gear pairs. As indicated in Fig. 2, the major technologies shown in Fig. 1 effectively reduce mechanical losses by 30% and achieve transmission efficiency of over 90%, thereby enabling the CVT-X to contribute to an 8% improvement in vehicle fuel economy under the U.S. city/highway combined driving mode. Among the major technologies adopted, the following section describes the attainment of ratio coverage of 8.2, twin oil pump system, control valve, torque converter, and resin baffle plates with a rubber seal.

* Control System Development Department ** Hardwarel System Development Department *** Unit System Development ****Unit Program Promotion Department

Table 1 Major specifications

Item		CVT-X (New CVT)		CVT8 (Current CVT)	
Torque capacity [Nm]		330		250 (mounted on previous car model)	380
Torque converter	Clutch / Oil flow route	Multiplate / 3-way		Single plate / 2-way	←
	Vibration damper	With pendulum damper	Long torsional damper	Long torsional damper	←
Variator system		Chain (3307 pitch)		Belt (28-10 layers)	Chain (3008 pitch)
	Ratio coverage	8.2 (2.95 - 0.36)		7.0 (2.64 - 0.38)	6.3 (2.43 - 0.38)
Gear ratios	Final gear	5.7 - 6.0		4.8 - 6.4	4.7 - 5.8
	Reverse gear	0.75		0.75	0.75
Size [mm]	Overall length	381	408	345	356
	Distance between prim.-sec. pulley shafts	180		173	173
Oil pressure control	Mechanical oil pump	12.7 cc/rev		14 cc/rev	18 cc/rev
	Electric oil pump	400 W		30 W (for stop-start)	-
Other	Shift-by-wire	○		○	-
	AT-CU	Integrated with case		Separately mounted (engine compartment)	←

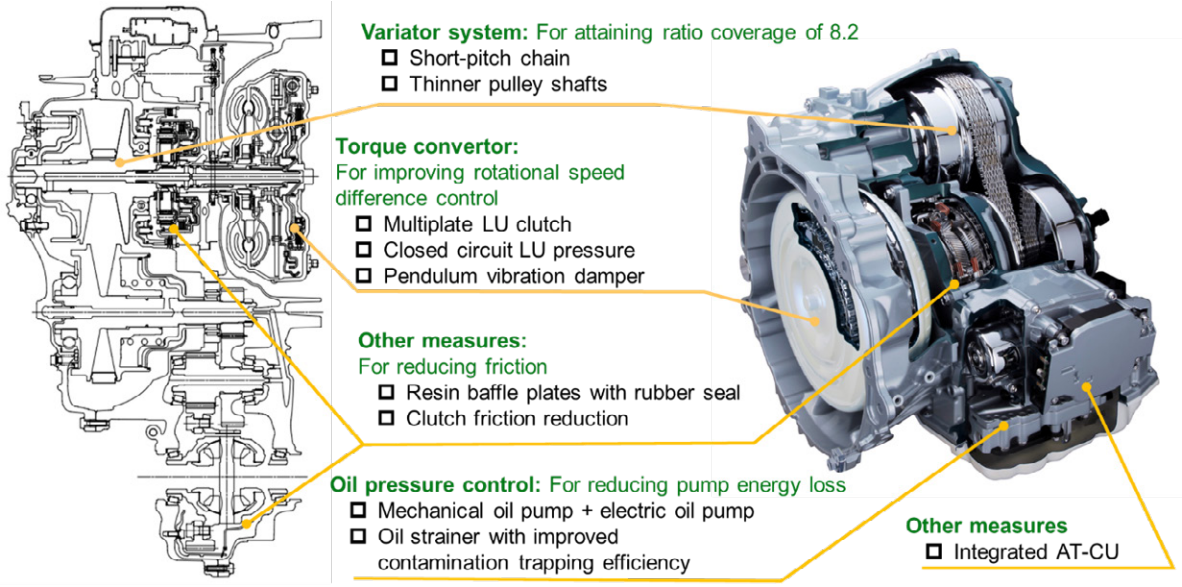

Fig. 1 Cross-sectional view and major technologies

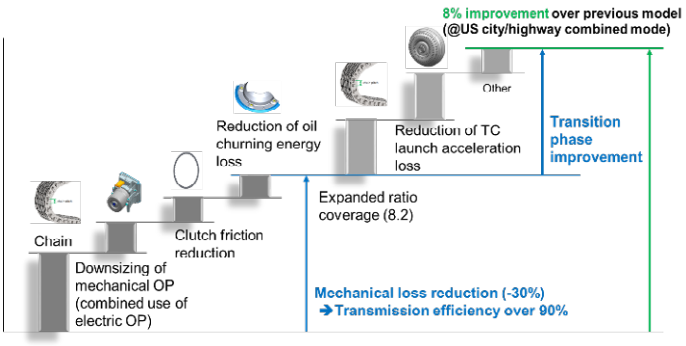

Fig. 2 Breakdown of 8% fuel economy improvement

3. Major technologies

3.1 Attainment of ratio coverage of 8.2

In order to expand ratio coverage, the radius ratio between the large and small wrap-around diameters of the chain must be increased on both the primary and secondary pulleys. It was desired to achieve ratio coverage of 8.2 while designing the CVT-X with the same minimum wrap-around radius on the small diameter side as that of the CVT8. To accomplish that, as shown in Fig. 3, the pulley outer diameter of the CVT-X had to be enlarged by 21% over that of the CVT8; in addition, the distance between the pulley shafts had to be increased by 37 mm from 173 mm for the CVT8 to 210 mm for the CVT-X. As shown in Fig. 4, the chain wrap-around radius on the small diameter side of the CVT-X was reduced by 15% from that of the CVT8 by adopting a short-pitch chain. Moreover, on the large diameter side, a chain wrap-around radius closer to the pulley outer diameter was achieved, thanks to the amount of chain stretch and management of the dimensional tolerances of the parts. That obtained a chain wrap-around radius ratio that effectively uses up to 98% of the pulley outer diameter. Consequently, the increase in the pulley outer diameter was kept to 4% and the increase in the center distance between pulley shafts was kept to 7 mm, increasing only from 173 mm for the CVT8 to 180 mm for the CVT-X. As a result, ratio coverage of 8.2 was achieved with good space efficiency.

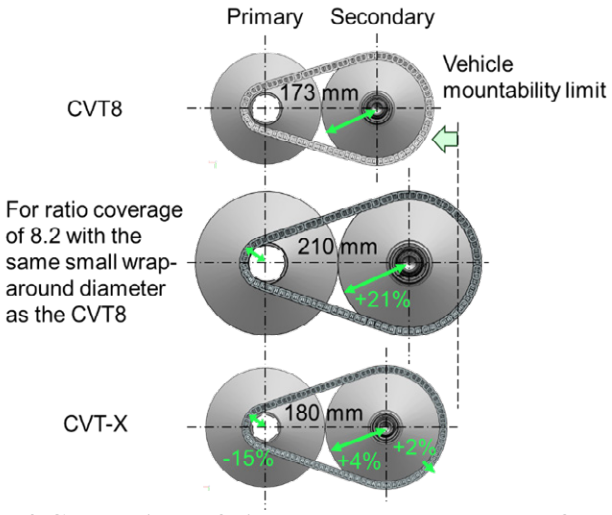

Fig. 3 Comparison of distance between pulley shafts based on wrap-around diameter

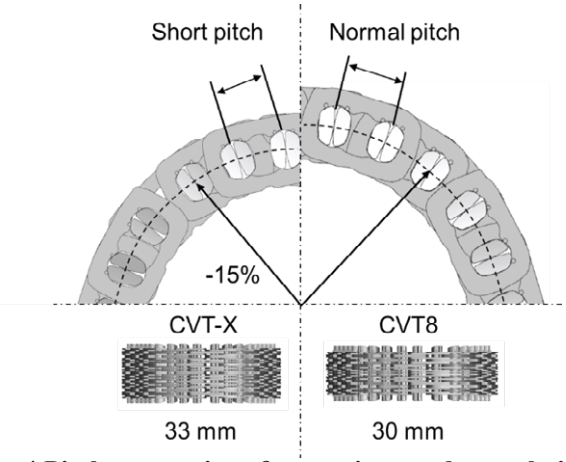

Fig. 4 Pitch comparison for previous and new chains

3.2 Twin oil pump system

As shown in Fig. 5, only the downsized MOP is used when driving with the flow of traffic in town; the ELOP is activated in situations where a large flow rate is needed to execute various quick shifts such as for kick-down acceleration or for sudden deceleration. It is also operated in other regions such as for stop-start driving and for stop-start coasting with the engine turned off. This system concept has made it possible to reduce mechanical losses by downsizing the MOP that is used in ordinary driving situations. For the CVT-X, the MOP was downsized by approximately 30% to reduce mechanical losses by 5.4% in driving situations where it alone supplies all the required flow rate.

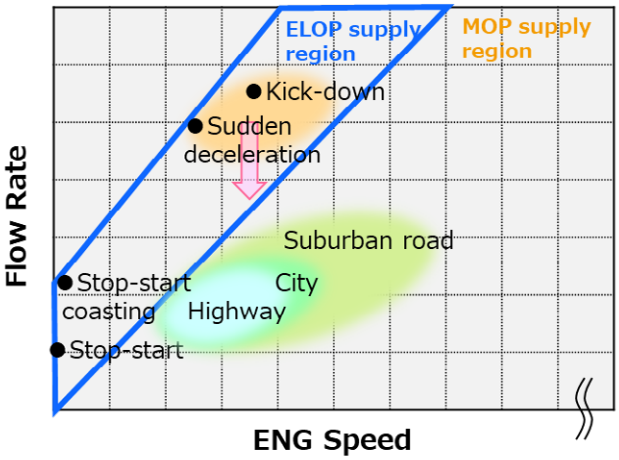

Fig. 5 Twin oil pump system concept

Both oil pumps are located inside the CVT case. As shown in Fig. 6, they suck up oil through a common oil strainer from a shared oil pan and supply it to various parts via the control valve. In situations where the driver presses the accelerator pedal hard with the intention to accelerate, the ELOP is activated to supply the flow rate to the pulleys that is needed to execute a quick shift, thereby achieving a highly responsive downshift. In deceleration situations due to sudden braking, the ELOP is also activated to complete the downshift in a short interval before the vehicle comes to a stop so as to ensure driving force for re-acceleration after the vehicle stops. This operation of the ELOP is shown in the time chart in Fig. 7. The system judges the flow rate needed from the ELOP based on the accelerator pedal position, vehicle speed, rate of deceleration and other factors. At the point where the system judges that the MOP alone can provide the required flow rate, it stops the ELOP to minimize the consumption of electric power.

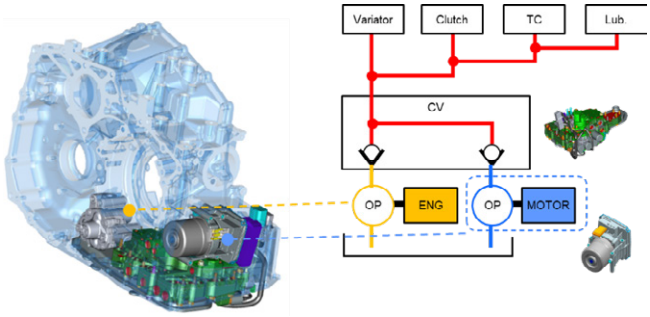

Fig. 6 Twin oil pump system layout

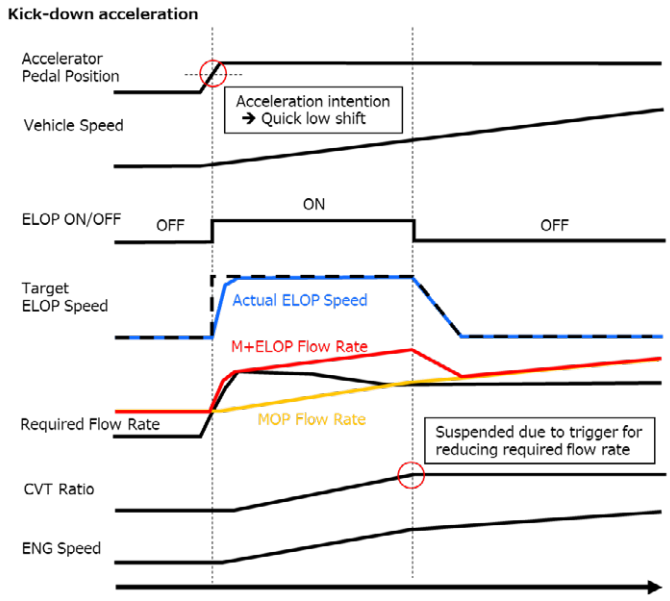

Fig. 7 ELOP time chart

3.3 Control valve

Control valve leakage and flow rate consumption must be reduced in order to improve fuel economy and ensure hydraulic pressure stability. For the CVT-X, the amount of leakage was reduced by 10% at representative operating points by optimizing the specifications of the valve body and spool. In addition, as shown in Fig. 8, a boring process was applied to the port involved in regulating the pressure, making it easy to control variation in the amount of lapping of the valve body and spool, thus enabling a design for suppressing hydrodynamic force. Moreover, wear resistance was improved by applying a high-consistency silicone to the valve body, thereby suppressing variation in the spool opening area characteristic and enhancing simulation accuracy of hydraulic pressure characteristics. As a result, it also became possible to simulate in advance the trade-off between stability and responsiveness, which was effective in improving pressure controllability as well.

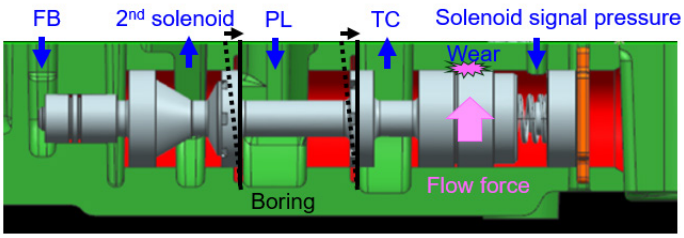

Fig. 8 Control valve (pressure regulator valve)

3.4 Torque converter

The torque converter transmits the driving force produced by the engine by means of the transmission fluid and engagement of the lock-up (LU) clutch. In order to obtain high levels of both driving force and fuel economy, the torque split between the fluid and LU clutch must be properly balanced. For the CVT-X, as shown in Fig. 9, a dedicated oil circuit was provided for the LU clutch as a means of improving the degrees of freedom for controlling torque transmission by the clutch. This made it possible to reduce the volume of the hydraulic pressure chamber by 58% to improve controllability of rotational speed differences between the engine and the turbine owing to LU clutch engagement. In addition, the LU clutch requires a thermal design because of the heat generated by sliding contact during rotational speed difference control. Accordingly, as shown in Fig. 9,

a multiplate clutch was adopted that reduces contact pressure on the LU clutch friction material by 56%. Suppressing the temperature rise at the sliding surface of the facing friction material has made it possible to use acceleration slip control in all speed ranges, as shown in Fig. 10. Previously, this control feature was applied only in the region of a small throttle valve opening. This change in the acceleration slip control system achieves a 1.3% improvement in fuel economy.

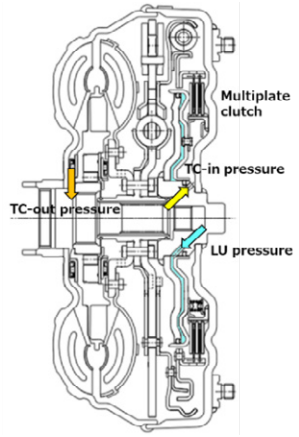

Fig. 9 3-way oil flow route of torque converter

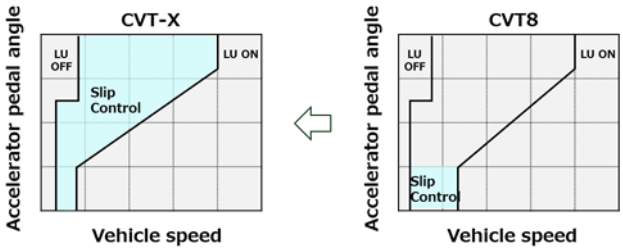

Fig. 10 Slip control region at vehicle launch

The CVT-X lineup is also intended to be combined with 3-cylinder DST engines, which experience greater torque fluctuation due to the reduced number of cylinders. As a countermeasure for this, a pendulum vibration damper was adopted as shown in Fig. 11. This type of damper provides damping force by activating the pendulum mass in the opposite phase of the input torque fluctuation frequency. In order to suppress any increase in the layout caused by the addition of the pendulum damper, it was combined with the main damper on the outer circumference side while the torque converter diameter was reduced by adopting the multiplate clutch. This created a compact layout that ensures sufficient torque transmission capacity without sacrificing performance.

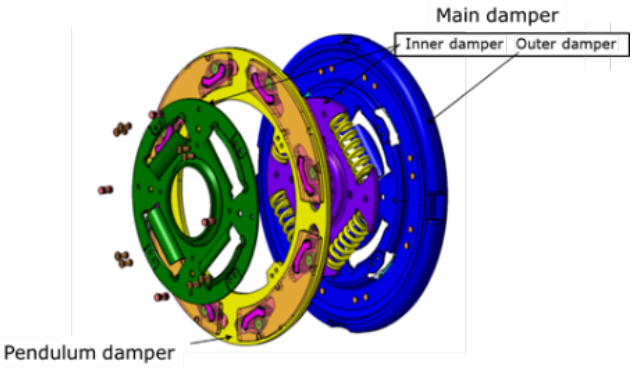

Fig. 11 Pendulum vibration damper

3.5 Resin baffle plates with rubber seal

The differential gear located in the bottom part of the CVT is its largest component and is a factor that worsens mechanical losses by causing oil churning. For that reason, baffle plates have previously been applied to suppress the inflow of oil to the differential gear chamber. To further reduce mechanical losses for the CVT-X, a rubber seal has been added to the baffle plates as shown in Fig. 12. The seal eliminates any gap to suppress the inflow of oil for reducing churning resistance, which achieves a 5.1% reduction in mechanical losses. In addition, molding the baffle plates of resin lightens their weight by approximately 300 g.

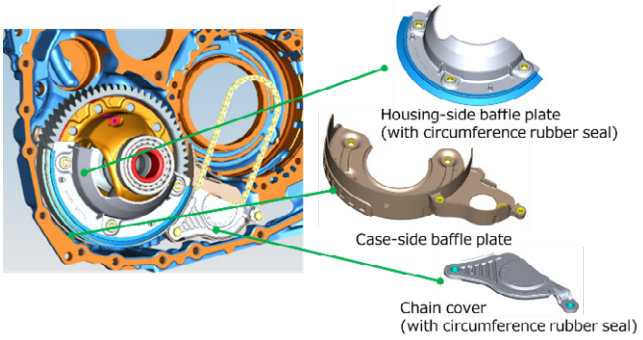

Fig. 12 Baffle plate

4. Conclusion

The new CVT-X achieves ratio coverage of 8.2 without adopting any auxiliary transmission or direct coupling device. Moreover, it reduces unit friction by 30% and achieves transmission efficiency surpassing the 90% barrier at representative management points of the U.S. city/highway combined driving mode to contribute to an 8% improvement in vehicle fuel economy. As such, it represents the ultimate CVT that has attained the final stage of evolution of mass-produced CVTs.

5. References

(1) Kouji OZAKI, Masatsugu ENDO, Satoshi WATANABE, Michinori MATSUO, “Development of a torque converter for the Jatco CVT-X mated to engines with fewer cylinders,” JATCO Technical Review, No. 21, pp. 89-94.

(2) Tomoyuki MIZUOCHI, Shigeru TOMODA, Youhei SHIMOKAWA, Jun SHIOMI, Hirofumi OKAHARA, “Introducing the fuel economy improvement technologies of the Jatco CVT8, JATCO Technical Review, No. 12, pp. 11-19.

(3) Shingo SUZUKI, Kouhei TOYOHARA, Takuro KAWASUMI, Masatsugu ENDO, Makoto OGURI, “Development of a new CVT featuring High Efficiency and Wide Ratio Coverage,” Proceedings of the 2022 JSAE Annual Congress (Spring), Document No. 20225135 (in Japanese).

■ Authors ■


Shingo SUZUKI


Kouhei TOYOHARA


Makoto OGURI


Masaya MATSUMURA

Development of a competitively priced lubrication system for JATCO's 1-axis e-Axle

Tomohiro NAGATA*

Summary

There are demands to reduce the size and cost of e-Axle systems used on electrified vehicles that have been spreading in recent years. A low-cost lubrication system with a simple structure and no oil pump has been built for JATCO's 1-axis e-Axle that uses a planetary gear set as the gearbox in order to downsize the system. Oil flow inside the unit was optimized to achieve both lubrication performance and excellent transmission efficiency.

1. Introduction

Advances are being made in downsizing and increasing the efficiency of e-Axle systems that integrate the drive motor, inverter and gearbox into one unit toward expanding the diffusion of electrified vehicles. Downsizing an e-Axle system produces many benefits with respect to improving vehicle packaging, including securing luggage space and interior roominess, obtaining space for mounting the battery pack, which has been increasing in volume in recent years, and providing collision safety space, among other things. The resulting improvement of mountability also reduces vehicle assembly costs. JATCO's 1-axis e-Axle uses a planetary gear set as the gearbox, which downsizes the unit by suppressing its height and longitudinal length compared with the previous 3-axis system.

This article describes the low-cost lubrication system adopted for the 1-axis e-Axle.

2. Structure of 1-axis e-Axle and lubrication system

2.1 Structure of 1-axis e-Axle

The structure of the 1-axis e-Axle is shown in Fig. 1. The 1-axis e-Axle uses a planetary gear set as the gearbox, with the motor rotating shaft and output shaft of the gearbox coaxially mounted. Lubrication oil is enclosed inside the gearbox, and oil seals are provided between the motor and the gearbox to prevent gearbox oil from penetrating into the motor chamber. The system is structured such that the output shaft passes through the hollow motor shaft. Because the interior of the hollow motor shaft is connected to the gearbox, a bearing and an oil seal are also positioned on the opposite side of the gearbox from the motor. This bearing is positioned on the left-hand (LH) side of the vehicle in the newly developed 1-axis e-Axle, so it is referred to here as the LH bearing. Lubrication is also provided to this LH bearing and oil seal that are located at some distance from the gearbox.

* Unit System Development Derartment

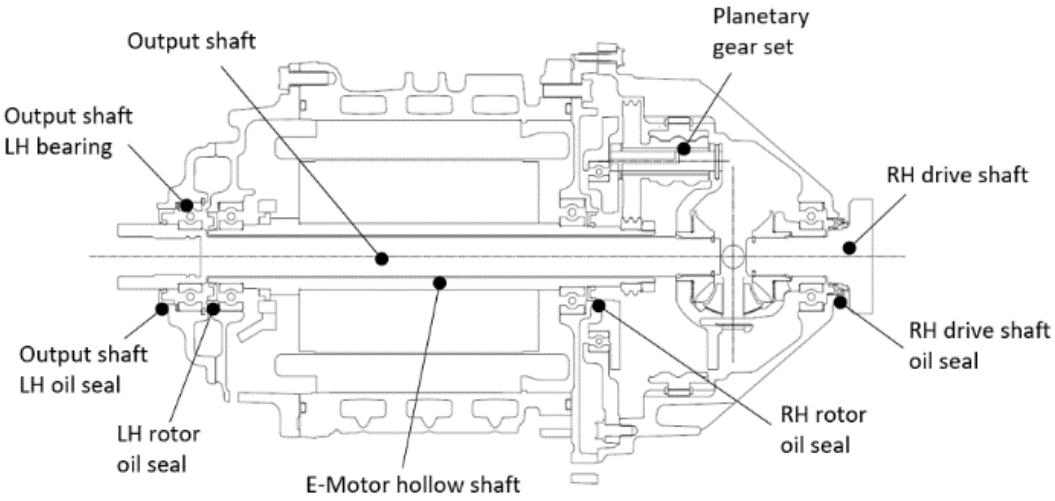

Fig. 1 1-axis e-Axle structure

2.2 Development concept of the lubrication system

The development concept of the lubrication system for the 1-axis e-Axle had the following three aims.

(1) The lubrication system does not use an oil pump in order to reduce the cost and size, whereas a planetary gear set ordinarily has an oil pump to forcibly lubricate the interior of the shafts.

(2) The lubrication system adopts an oil catch structure for circulating oil to lubricate the planetary gear set and the LH bearing.

(3) Oil churning resistance is kept to a minimum, thus achieving high transmission efficiency combined with lubrication performance.

2.2.1 Lubrication system using an oil catch structure

Figure 2 shows the lubrication system incorporating the oil catch structure.

Oil splashed by the rotating planetary gears is captured by the oil catch positioned at the top of the case. Captured oil is distributed though oil holes in the e-Axle case to lubricate the planetary gear set and the LH bearing.

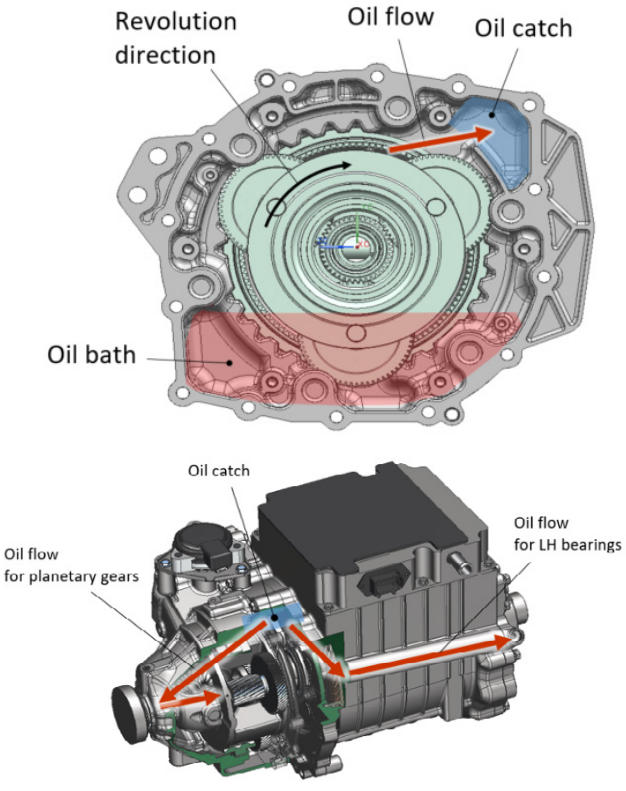

Fig. 2 Lubrication system for 1-axis e-Axle

2.2.2 Lubrication of the planetary gear set

The pinion gear of the planetary gear set revolves around the sun gear while rotating on its own axis. As shown in Fig. 3, the oil level is set so that the pinion gear is immersed in oil at low rotational speeds. Revolution of the immersed pinion gear churns oil toward the center of rotation of the planetary gears, thereby lubricating every part of the planetary gear set.

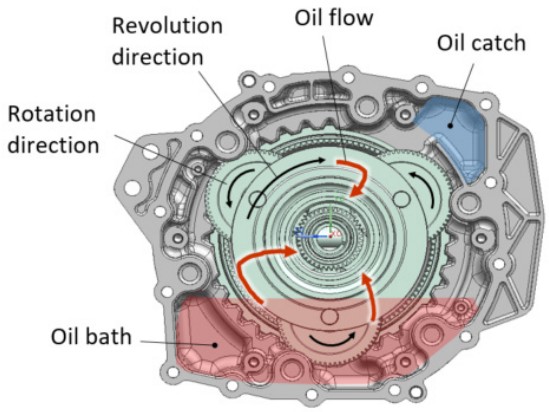

Fig. 3 Oil flow under low speed

As the rotational speed rises, centrifugal force reduces the amount of lubrication provided by churning caused by the pinion gear. However, because the quantity of oil splashed into the oil catch increases, oil captured by the oil catch is supplied through the case oil holes to the center of rotation of the planetary gears. As shown in Fig. 4, oil that reaches the center of planetary gear rotation is supplied to all parts of the planetary gear set by centrifugal force.

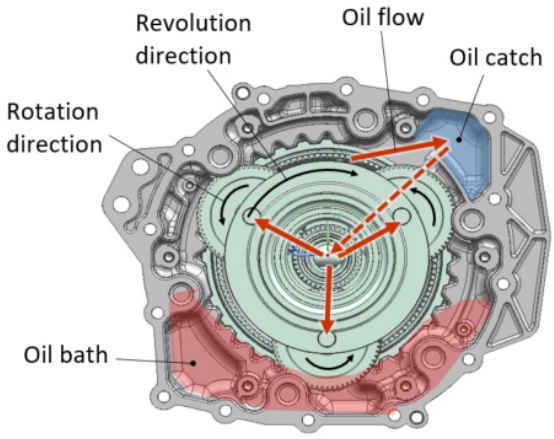

Fig. 4 Oil flow under high speed

2.2.3 Lubrication of LH bearing

The oil flow route to the LH bearing is shown in Fig. 5. As the rotational speed rises, lubrication oil from the oil catch reaches the LH bearing. However, there was concern that lubrication might be insufficient right after the start of rotation. To avoid that, the oil level on the LH bearing side is set higher than that on the gearbox side so that the lower half of the bearing is immersed in oil from a zero speed condition. Oil supplied from the oil catch is returned to the gearbox through the hollow rotating motor shaft, which provides a structure for circulating the oil.

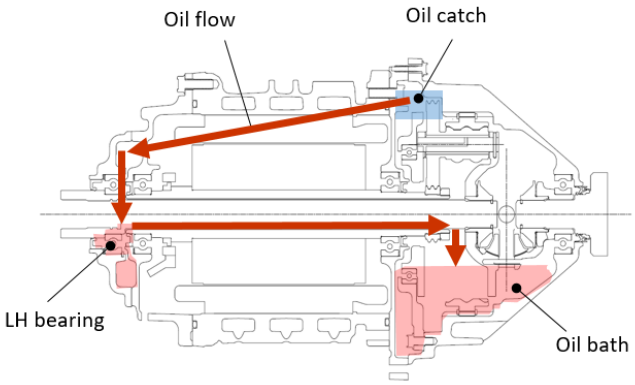

Fig. 5 Oil flow for LH bearing

3. Lubrication system issues and feasibility

3.1 Feasibility of lubrication system using the oil catch structure

To ensure the feasibility of the lubrication system using the oil catch structure, the oil catch had to be designed so that it could efficiently capture oil splashed by the rotating planetary gear set. Oil flow inside the gearbox was simulated using computational fluid dynamics simulation software. An oil flow visualization test was conducted to verify the validity of the simulation results. Figure 6 shows the oil flow simulation results, and Fig. 7 shows the appearance of the oil flow visualization test using a transparent resin case. The simulation results were validated experimentally using a test gear set, enabling the oil catch to be designed with the optimal geometry and optimally positioned.

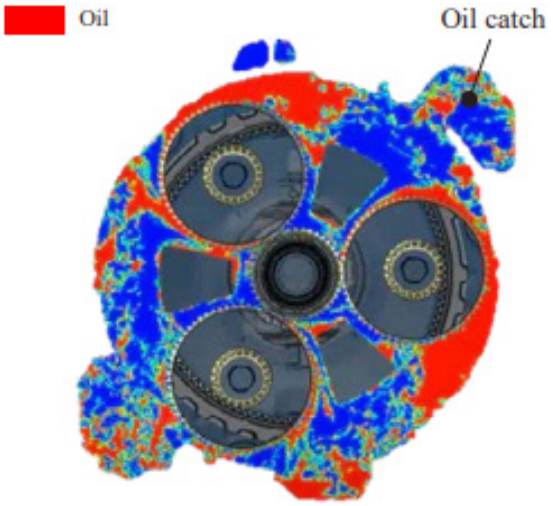

Fig. 6 Oil flow simulation

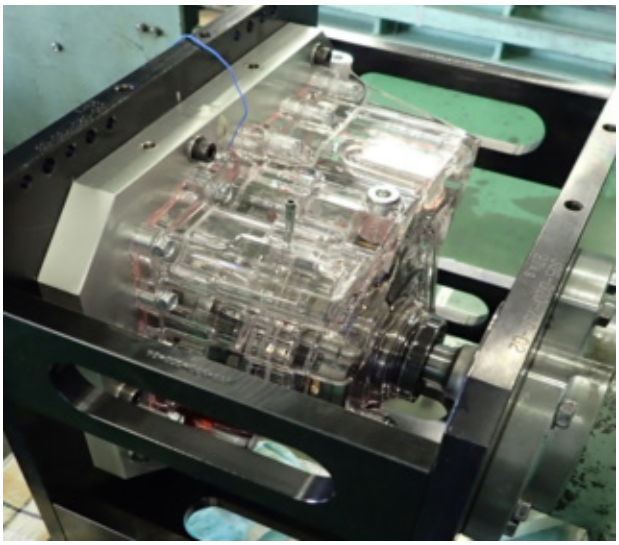

Fig. 7 Oil flow visualization test

3.2 Issues and feasibility of planetary gear set lubrication

As described in section 2.2.2, lubrication provided by pinion gear churning is dominant from a zero speed condition to the low-speed range, and oil catch lubrication is dominant in the medium- to high-speed ranges. The two lubrication methods have contradictory characteristics relative to their respective rotational speed. Accordingly, one issue was to ensure a stable supply of the lubrication volume required by the planetary gear set in all speed ranges.

The lubrication volume provided by pinion gear churning and that provided by oil catch lubrication were measured. Figure 8 presents the measured results that validated the feasibility of these methods of lubricating the planetary gear set. The results confirmed that the combination of lubrication by pinion gear churning and oil catch lubrication stably supplied lubrication to the planetary gear set in all speed ranges.

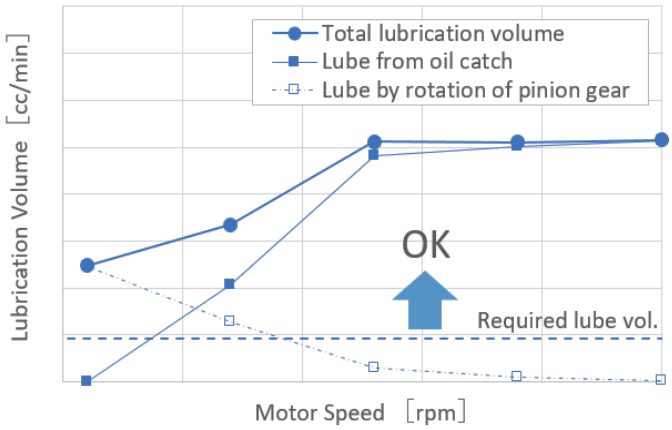

Fig. 8 Results of planetary gear lubrication volume measurement

3.3 Issues and feasibility of LH bearing lubrication

There was concern about an increase in oil churning resistance because the LH bearing would be immersed in oil from a zero speed condition, as mentioned in section 2.2.3. Therefore, oil churning resistance was reduced by actively retaining oil in the oil catch so as to lower the dynamic oil level on the gearbox side. The oil catch capacity was designed so as to ensure the desired lubrication performance and also reduce oil churning resistance by lowering the dynamic oil level.

The effect of retaining oil in the oil catch on lowering the oil level was validated by conducting a visualization test of the oil catch and by measuring the oil level in the gearbox. The transmission efficiency of the gearbox was also measured and was confirmed to be superior to that of the conventional 3-axis system.

Figure 9 shows the results of the oil level measurement. For comparison, the oil level was also measured for a unit with an ineffective oil catch. The visualization test results and the measured oil level results confirmed that the dynamic oil level was reduced as expected.

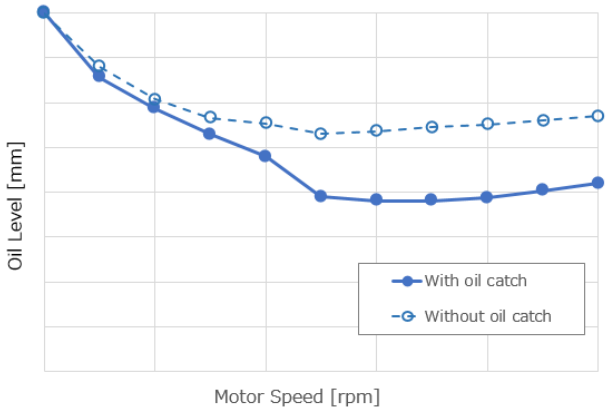

Fig. 9 Results of gearbox oil level measurement

Figure 10 compares the torque loss of the gearbox of the 1-axis e-Axle with that of the conventional 3-axis e-Axle. The torque loss of the 1-axis e-Axle has been reduced to approximately one-half that of the 3-axis unit. That reduction is attributed to the effect of reducing oil churning by lowering the oil level and the effect on reducing mechanical loss by the bearing structure of the 1-axis e-Axle which does not use tapered roller bearings.

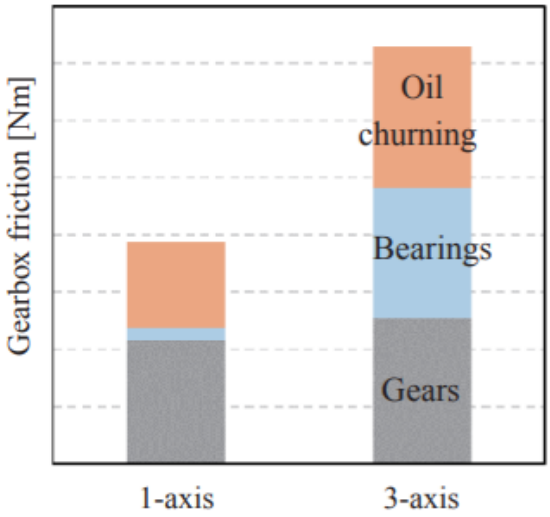

Fig. 10 Gearbox friction loss

4. Conclusion

A lubrication system with a simple structure was built for the 1-axis e-Axle by using a planetary gear set instead of adopting an oil pump. Oil flow inside the unit was optimized so as to both ensure lubrication performance and reduce churning resistance. That worked to achieve a low-cost, compact and high-efficiency 1-axis e-Axle system.

5. References

(1) Hiroki UEHARA, Shota OIKAWA, Kazuhiko YOKOYAMA, “Compact and high-efficiency 1-axis e-Axle with a planetary gear set,” JATCO Technical Review, No. 21, pp. 77-80, 2022.

■ Author ■

Tomohiro NAGATA

Core model process for improving drivability development efficiency

Junya AIZAWA*　Takurou KAWASUMI**　Koshiro SUGIYAMA***

Summary

In recent years, it has been necessary to shorten the development period for powertrain units. Toward that end, JATCO has been advancing reform of the development process by applying model-based systems engineering. In development activities to achieve drivability targets, we have started to shorten the development period by reducing the amount of rework. However, in order to maximize the benefits of model-based systems engineering, designs must be executed using highly accurate models at the initial design stage of the system and sub-systems. A new model development process was implemented in this project that has led to improvement of drivability development efficiency. This article describes the new process and presents examples of its benefits.

1. Introduction

Designers' familiarity with model-based systems engineering (MBSE) has improved in recent years, increasing the use of models. As a result, repetitive cycles of design, build and test have been reduced.

The range of model use extends from the design phase of the system and sub-system levels on the left side of the V-shaped development process to the validation phase on the right side involving parallel use of actual hardware, including a hardware in the loop system (HILS). Models have been utilized over a wide range of the V-shaped development process (Fig. 1).

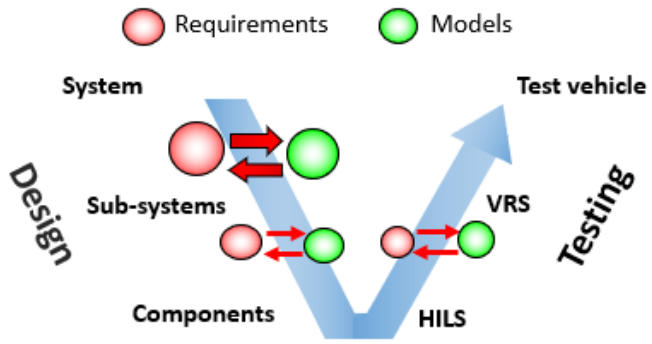

Fig. 1 Model application to V-shaped development process

In order to maximize the benefits of shortening the development period, models must by constructed that ensure an accurate response to the requirements and match the development plan.

This article describes activities undertaken to create a new model development process for improving model construction efficiency and model accuracy.

2. Model issues in drivability development

Drivability is an index for achieving performance that does not cause drivers any feeling of discomfort when a vehicle accelerates or decelerates or changes between forward and reverse motion. It is a critical design criterion that determines the product value of a transmission.

There are many driving conditions for evaluating drivability involving combinations of factors such as a vehicle's driving environment, vehicle speed condition and the driver's operations. Accordingly, the models used in design activities must enable highly accurate, wide-ranging studies in order to design drivability using models (Fig. 2).

* Hardware System Development Department, JATCO Engineering Ltd ** Innovative Technology Development Department *** Hardware System Development Department

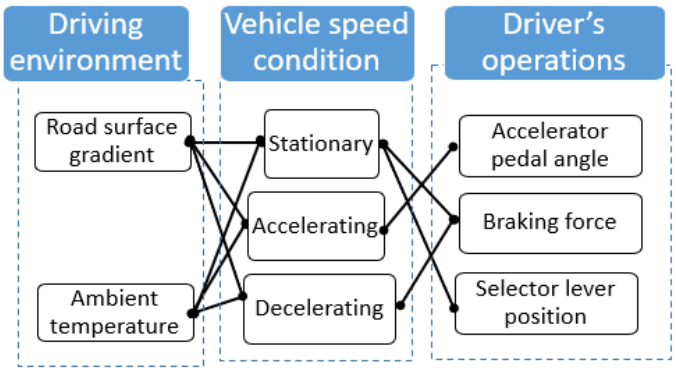

Fig. 2 Combinations of driving conditions

However, the models constructed and used in design activities heretofore have not necessarily provided sufficient design accuracy, giving rise to design specification changes in the later stages of the development process. Issues involved in model construction are described below.

2.1 Increase in model construction man-hours

In constructing models to date, the aim has been to achieve the same level of accuracy as the test results measured under each driving condition. Because each condition has been modeled separately, only a narrow range of studies can be conducted with a single model. The number of models used has also continued to increase as the driving conditions for which performance predictions are desired have been expanded (Table 1).

Table 1 Modelling according to driving conditions

		Vehicle speed condition		
		Stationary	Accelerating	Decelerating
Accelerator pedal angle	Large	·	Model A	·
	Small	·	Model B	·
Braking force	Strong	Model C	·	Model D
	Weak	·	·	Model E
Selector lever position	D	Model F	·	·
	R	Model G	·	·

In cases where part specifications are changed or new functions are added in the process of conducting design studies using models, the model composition and parameters must be modified. Because modifications are made for each model, the man-hours required for updating the models have expanded enormously as the number of models has increased.

Additionally, information exchanged between the model developers and designers for updating the models has remained only at the level of recognition between the individuals involved and has not been shared throughout the company.

Consequently, every time the scope of model construction or the designers change, parameter revision histories and details must be researched by asking around among the people involved. It has taken a lot of time to obtain the information because the sources of the information must be confirmed, mutual recognition of the assumptions underlying the parameters is needed, and there is waiting time before getting the answers.

As a result, there have not been enough man-hours for model construction, making it impossible to sufficiently secure the models needed in design studies.

2.2 Decline in design accuracy owing to the use of separate models

In order to guarantee model accuracy, the information of the model parameters must be properly defined. As development work progresses, parameters change owing to the dimensional tolerances of parts, their state of deterioration, and differences that occur between the required design values and the test data.

In this regard as well, there are times when confirmation is overlooked because the sharing of information depends on individuals, and models may be created that contain parameters unsuitable for design studies, leading to a decline in design accuracy.

Moreover, models have so far been created by individual model developers and designers, and the latter have selected and used models based on their own personal judgment. They have not always recognized whether models suitable for design studies are available or not. This has led to design studies being conducted using models that lack sufficient accuracy.

To resolve the foregoing issues, it was decided to implement a process for efficiently constructing high-accuracy models.

3. Concept of core model process

Let us consider the form desired of a model. If the parameters and characteristics of a model reflect the range of diving conditions for reproducing the behavior of the actual objects, predictive studies can be conducted without dividing the model. However, so far many models have been constructed separately for each driving condition, so the desired model form has not been obtained.

Our aim is to cut the man-hours needed for updating models through a reduction of their number as much as possible by periodically integrating them to create a model of the entire system, while expanding the scope of the studies that can be conducted.

Expanding the scope of a model increases the number of part elements, leading to an expansion of driving conditions that could not be examined previously. Assuming that this would improve design accuracy for overall development of drivability, we adopted this approach as the direction that should be taken for model construction (Fig. 3).

The model is positioned as a core model and is used in the overall development of drivability.

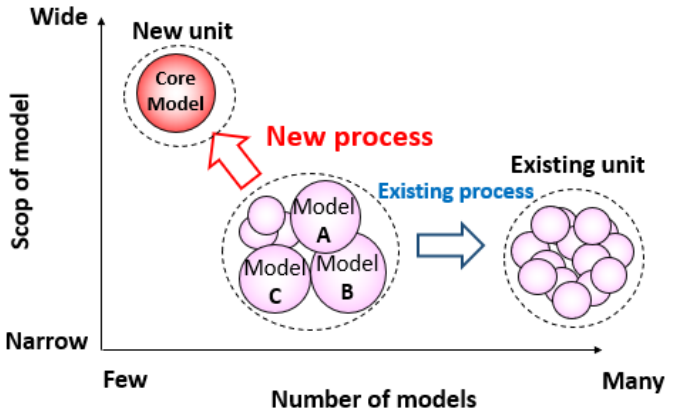

Fig. 3 Direction for model construction

As the development work progresses, the level of design detail increases, giving rise to a revision of the study conditions and parameter changes. Accordingly, after the design study, the model developers must reflect the specification changes and newly required conditions in the model immediately so as to increase its accuracy. It is essential for the designers to reduce any redoing of development work by conducting design studies using the updated model.

A core model process was constructed as a new method for efficiently carrying out the cycle of using and updating the core model. The specific activities for accomplishing this new process will be described in the following section.

4. Measures for accomplishing the core model process

4.1 Improving accuracy by standardizing the model

The concept of the core model is that it should achieve both high accuracy and broad flexibility. Ideally, the core model should reproduce response changes to inputs/outputs in line with the design study that are equal to those of the actual objects. The element levels needed to accomplish that were defined as shown in Table 2. Based on these definitions, the individual models to be integrated were selected, and new characteristic values were obtained for any places that were deficient.

Table 2 Definitions of model elements

Model scope	LV.1 Linear elements (Map)	LV.2 Nonlinear elements (fundam. eqs.)	LV.3 Nonlinear elements (fundam. eqs. + characteristics)
Hydraulic pressure elements		Pressure Transfer function $P(s)=G(s)\cdot Q(s)$	·Pressure loss in passages ·Oil leakage amount ·Lack of balance in oil supply volumes
Launch elements		Hydraulic coupling Torque transmission eq. $T=\tau\cdot Ne^2$	·Damping coef. ·Volume transient change ·Pressure response/balance
Forward/ reverse changeover elements		Clutches Torque transmission eq. $T=\mu\cdot R\cdot F$	·Vehicle sensitivity ·Pressure response/balance

A quick pressure response matching the driver's intention can improve a vehicle's shift performance and drivability when changing between forward and reverse motion.

As such, the hydraulic pressure elements contribute significantly to the overall drivability of a transmission, so

priority was put on improving their model. The details are explained below.

The hydraulic pressure system consists of multiple valves and complexly shaped oil passages. Nonlinear elements that must be considered in the model include pressure losses caused by oil passage bends and constrictions, oil leakage from the passages, and the lack of balance among the oil volumes supplied to the various parts of the system.

Previously, no definite criteria were determined for optimally modeling these nonlinear elements.

Using hydraulic pressure designs executed heretofore and empirical rules based on experimentation, pressure losses were modeled in this project only as a structure exceeding the criterion. This made it possible to construct a model without imposing any unnecessary computational load while still maintaining high accuracy (Fig. 4).

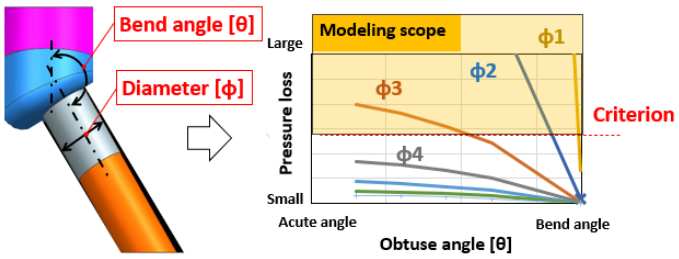

Fig. 4 Standardization of hydraulic pressure model

For oil leaks between parts and for passages with complex branching, 3D computational fluid dynamics simulations were conducted to accurately derive characteristic values in order to make accurate predictions (Fig. 5).

The characteristic values obtained for the nonlinear elements were reflected in a 1D model of the entire system, which led to improved accuracy.

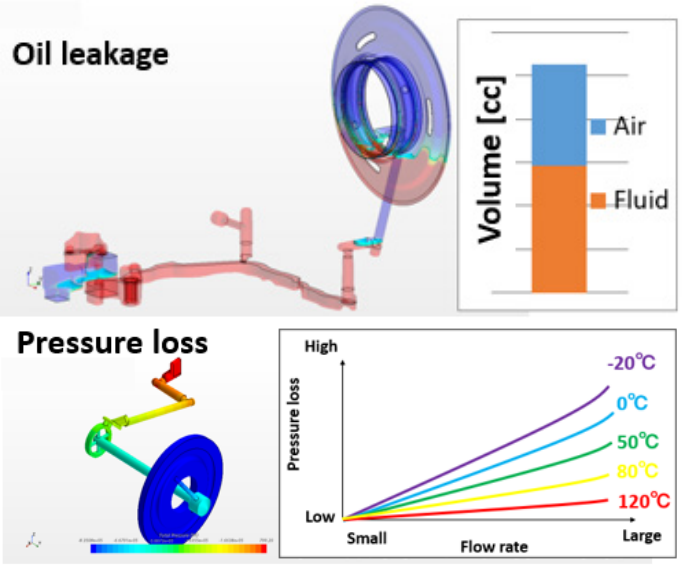

Fig. 5 Characteristics obtained by 3D CFD simulation

4.2 Reduction of model construction man-hours using the core model process

In order to reduce the time spent gathering the information described in section 2.1, model parameter information must be easy to find. Therefore, a single standard format was created that lists all the parameters defined in the core model.

The model developers describe in detail the constituent elements of the model and parameter information in this format. This makes it easy for the designers to recognize the information needed for the model.

When parameter changes are made, the designers take the initiative to share that information, thereby reducing the number of mutual inquiries and responses and enabling information to be shared efficiently.

To make sure that these measures are carried out without any omissions, the roles of the development engineers involved with the model and the details of the documents to be exchanged have been clearly defined (Fig. 6).

A process for continually improving design accuracy while continuing to evolve the core model has been adopted for development projects.

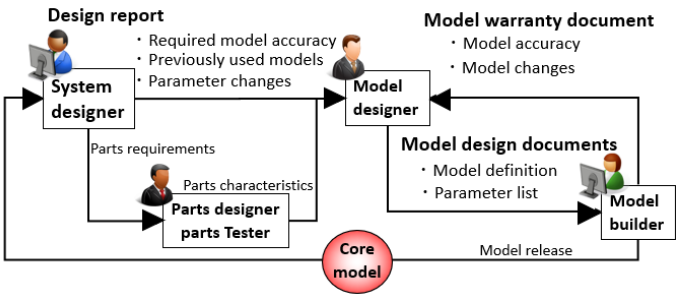

Fig. 6 Core model process

5. Benefits of applying the core model development process

Transmission functions for ensuring drivability include forward/reverse changeover by the clutches, pulley speed changes necessary for acceleration/deceleration, and torque converter lockup, among others. The core model was applied to execute a model design for each function.

Previously, design changes occurred in the latter stages of development especially regarding transmission performance for changing between forward and reverse motion. It was decided to use the model intensively for designing this performance, examples of which are described below.

Transmission performance for forward/reverse changeover is evaluated using two indices. One is the lag time from the driver's operation of the selector lever to the generation of driving force at the tires; the other is torque fluctuation that occurs at the time of clutch engagement. It is necessary to reduce both indices simultaneously, though they have a trade-off relationship.

In order to execute a feasible design for accomplishing that reduction, it is necessary to predict piston travel, which functions to engage and release the clutches, and also torque fluctuation at the time of clutch engagement.

Elements that contribute greatly to lag include the oil passage orifice that functions to suppress the inflow volume of oil for moving the piston (Fig. 7).

A part element that contributes greatly to torque fluctuation at the time of clutch engagement is the stiffness of the dish-shaped clutch spring (i.e., dish) that has a counteracting force proportional to the pressing force of the piston.

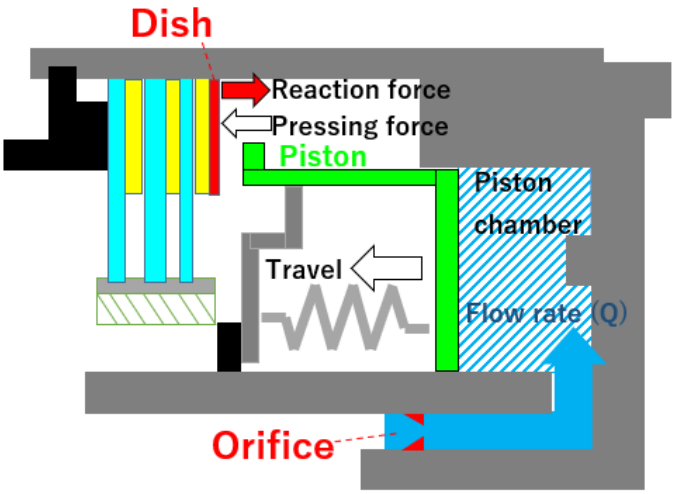

Fig. 7 Configuration of forward/reverse changeover system

Previously, it was not possible to accurately predict the effects on performance of the oil volume flowing into the piston chamber and specification differences of clutch engagement parts. Consequently, there was a repeated trial and error process of design and testing.

Use of the core model in this project enabled accurate prediction of lag and torque fluctuation due to changes in the orifice diameter and dish stiffness. As a result, the core model made it possible to determine optimal specifications for satisfying transmission performance for changing between forward and reverse motion (Fig. 8).

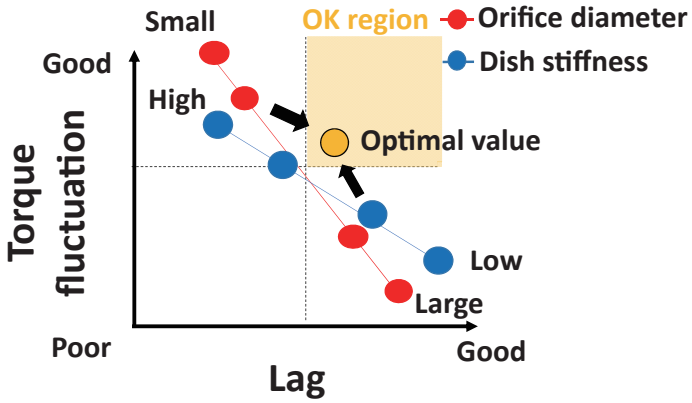

Fig. 8 Optimal design for selector lever performance

The results of verification tests conducted subsequently were equal to those obtained with the core model, thus confirming that the required performance was satisfied. This demonstrated the effectiveness of the core model process on improving design accuracy.

In addition, the core model process reduced the man-hours for collecting model information and the number of models created. As a result, it had the effect of reducing model construction man-hours by 75% compared with the existing process.

As described here, the implementation of the core model process has contributed greatly to improving development efficiency by reducing the repetition of design and testing in the drivability development process.

6. Conclusion

Design studies are conducted every day in the development process. Previously, there was an issue that models were not being developed simultaneously in a short period of time and were not available on a timely basis.

The core model process implemented in this project is an effective method enabling the many employees involved in development work to efficiently construct and use models.

It has reduced development man-hours especially for the hydraulic pressure system that was previously a major factor causing insufficient design study accuracy. That was achieved by enabling definition of the model criteria and model construction, thereby improving the accuracy of drivability studies and suppressing the occurrence of rework.

The aim going forward is to expand the application of this process to all areas of performance so as to increase overall development work efficiency.

■ Authors ■

Junya AIZAWA

Takurou KAWASUMI

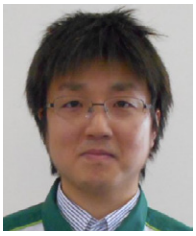

Koshiro SUGIYAMA

Development of a fuel efficiency analysis tool that shortens the development period

Chadol KIM* Sunho LEE* Jaeseok LIM* Sungyub HAN*
Keunsoo KIM* Jaesang LEE** Hyeongbeom HEO**

Summary

In recent years, not only society's environmental needs, but also the needs of vehicle manufacturers that are our customers for shorter development periods and reduced development costs have been continually increasing. The newly developed fuel efficiency analysis tool described here shortens the lead time from analysis to the determination of specifications. As a result, it makes it possible to achieve the targeted fuel efficiency and to reduce the number of fuel efficiency tests conducted, thus not only contributing to the environment, but also enabling an effective response to the needs of vehicle manufacturers. This article describes in detail the development of this fuel efficiency analysis tool.

1. Introduction

Demands for a reduction of CO_2 emissions as one of society's environmental needs have become increasingly more numerous in recent years. Transmission (TM) development activities have been helping to resolve this environmental need by discovering and proposing various measures for improving vehicle fuel economy.

At the same time, vehicle manufacturers that are our customers need shorter development periods and reduced development costs. It is also necessary to respond to their needs as well as to society's environmental needs.

A fuel efficiency analysis tool has been developed in this project as a measure for addressing these issues by shortening the development lead time from the analysis of fuel efficiency waveforms to the determination of the related specifications. As a result, the lead time for proposing specifications contributing to improving fuel economy has been shortened (Fig. 1). It has also contributed to cutting development costs by reducing the number of tests conducted. This article describes the details of the development of this fuel efficiency analysis tool.

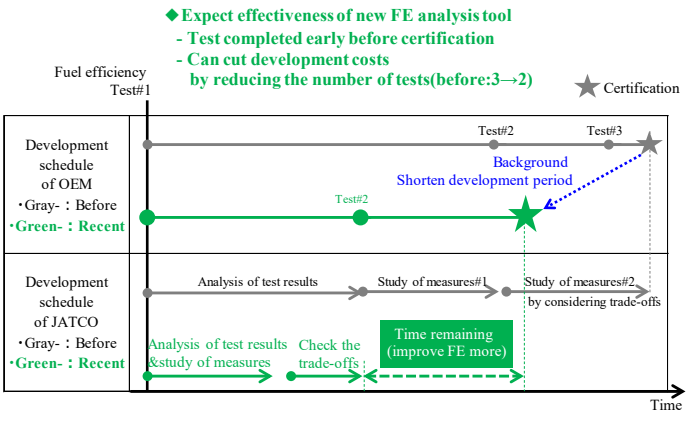

Fig. 1 Previous and recent development schedule

2. Issues and approaches to improvement

In proceeding with TM development work at JATCO, we have adopted the concept of the V-process, which is one systems engineering (SE) approach. The left side of the V-process consists of the design phase and right side is the testing phase for design validation. This V-process has the following issues.

- Design phase

  Measures for building a TM so as to attain the required vehicle fuel efficiency are designed and studied. In this process, it is necessary to link the TM hardware specifications and software specifications.

  1) In order to develop the design, the specifications

* System Performance & Control System Development Office, JATCO Korea Engineering Corporation
**Digital Engineering Promotion Office , JATCO Korea Engineering Corporation

of the selected vehicle, engine and TM must be coordinated in advance with the vehicle manufacturer.

2) It is necessary to ensure the accuracy of fuel efficiency simulations.

- Validation/calibration phase

In case the fuel efficiency improvement intended by the design is not achieved, the cause must be immediately and accurately analyzed so the results can be fed back to the design parameters.

1) Test waveforms are analyzed to see if there was any behavior other than the design intention or any differences between the test stand conditions and the assumed specifications at the time of design development. Nothing must be overlooked in the analysis, and the results are linked to a study of countermeasure specifications to be developed in a shorter lead time.

2) The TM calibration parameters that determine fuel efficiency performance have many trade-offs with the parameters for drivability, noise and vibration, and reliability. When calibration parameters are changed, countermeasure specifications must be presented that take into account such trade-offs (Fig. 2).

This project was focused on improvement of the validation/calibration phase. The studies conducted by the engineers in charge were sorted out; it was decided that the fuel efficiency analysis tool would automate an analysis of the measured fuel efficiency waveforms and an analysis of the contributions of the calibration parameters to fuel efficiency.

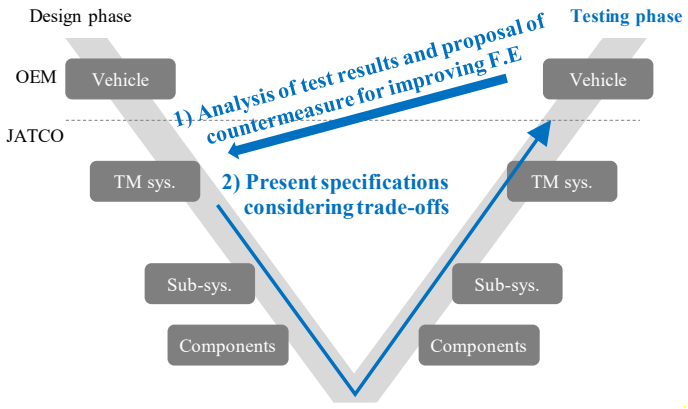

Fig. 2 Issues and V-process

3. Key points of improvement

3.1 Definition of functions needed by the fuel efficiency analysis tool

The fuel efficiency analysis tool has the following three purposes.

1) To eliminate any differences in analysis quality among employees.

2) To automatically visualize the analysis results for early determination of countermeasure specifications on the basis of effective coordination with the vehicle manufacturer.

3) To shorten processes that have previously been time-consuming.

The necessary functions for accomplishing these purposes were defined from the following perspectives

1) The process flow of the development activities at the work level of the engineers in charge was clarified (Fig. 3), and a study was made of the functions needed by the fuel efficiency analysis tool.

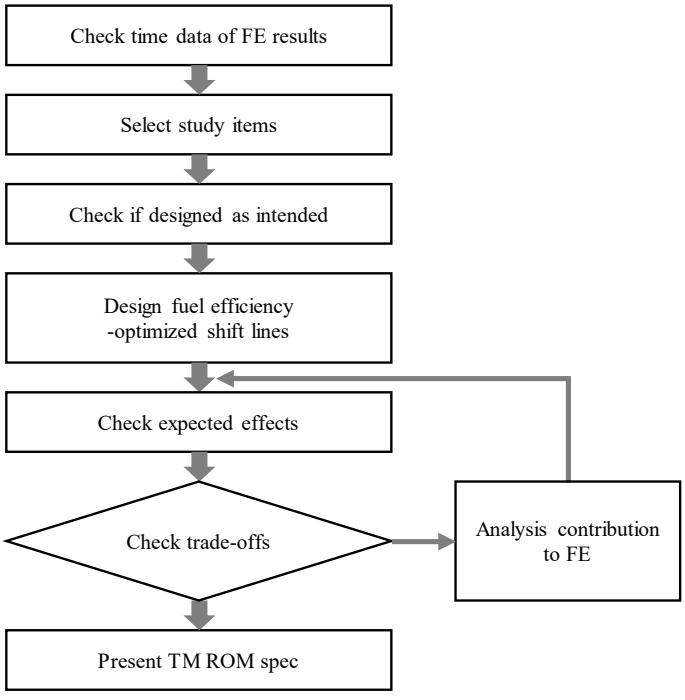

Fig. 3 Previous process flow

2) The TM factors influencing fuel efficiency were identified (Fig. 4) and the tool should be able to analyze quantitatively the items related to each influential factor.
3) Based on experience to date, the tool should be able to automatically generate the graphs and tables frequently used in coordinating with the vehicle manufacturer.

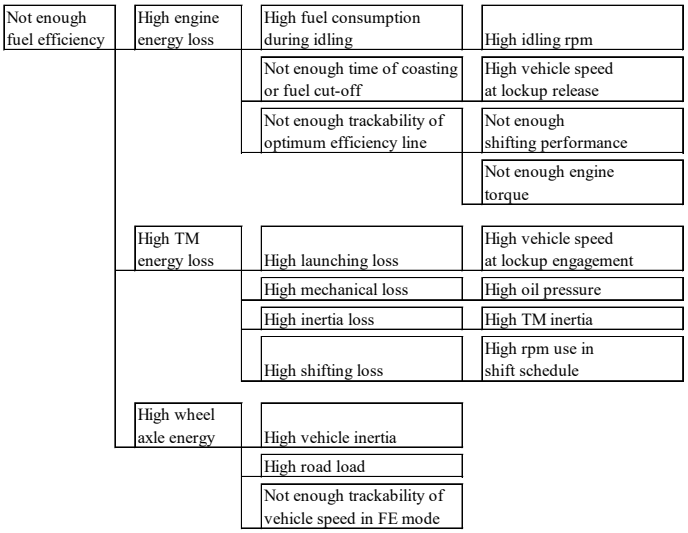

Fig. 4 Factors influencing fuel efficiency

The necessary functions were organized in terms of requirements, functions and logic (RFL), making it possible to complete the composition and structure of the fuel efficiency analysis tool to be developed (Table 1).

Table 1 Requirements and functional methods

Requirement	Function1	Function2
No change in analysis quality among employees	Compare design intent and test results	Check the intention of shift schedule
		Check the intention of lockup engagement
		Check the intention of sub-gear schedule
	Energy analysis in test results	Analysis of engine energy loss
		Analysis of transmission energy loss
		Analysis of transmission output energy
	Compare with F.E optimized shift schedule	
Decide the specifications for early contermeasures	Analysis of contribution to FE	Check the frequency of time use in test
		Check the frequency of energy use in test
Shorten the time of studying test results	Arrangement of study specifications	Select specifications of vehicle and TM
		Import control constant from ROM file
	Arrangement of test results	Automatically convert to proper format
		Match the time of test results
		Match the name of label
	Accumulate analysis results for experience	Save analysis results

3.2 Creation of fuel efficiency analysis tool

The tool was designed to shorten the lead time from fuel efficiency waveform analysis to the proposal of specifications for improvement by enabling anyone to study the processes from analysis to specification proposal without overlooking anything. Moreover, all of the necessary functions were incorporated into one tool (Fig. 5).

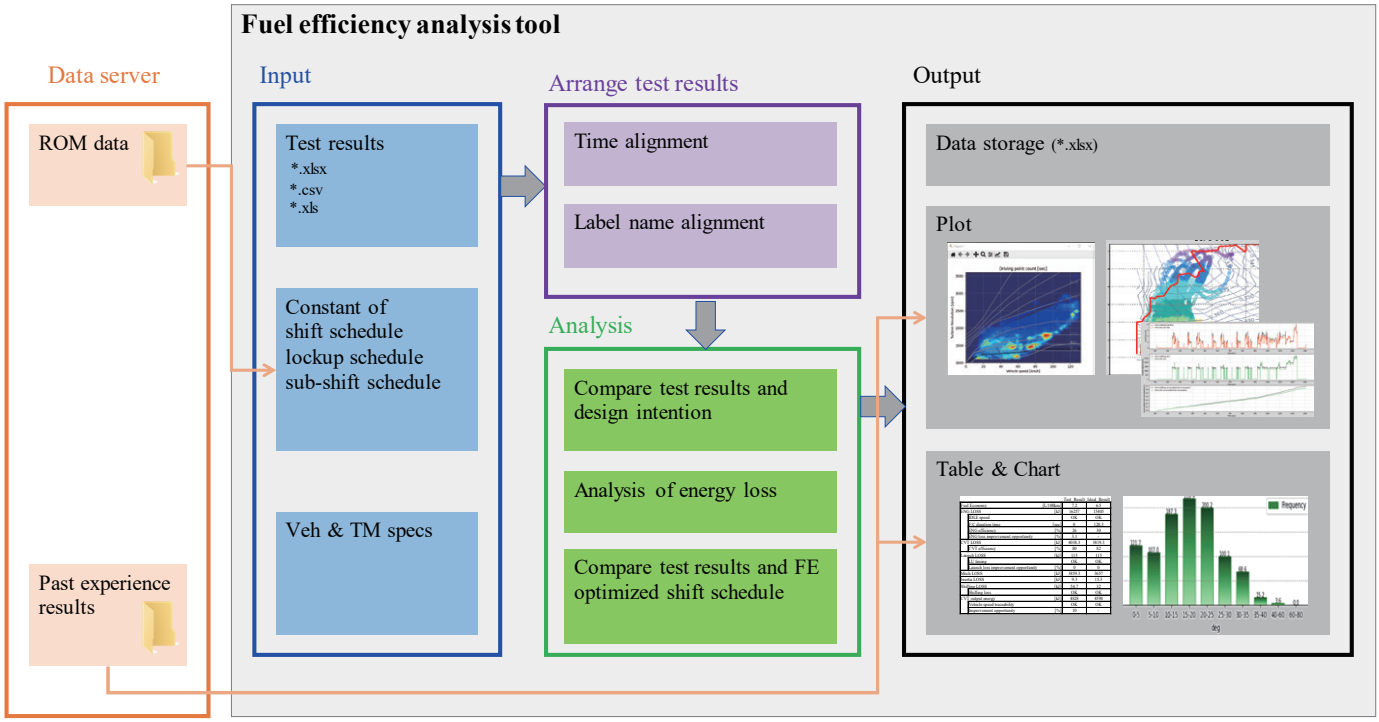

Fig. 5 Flowchart of inputs & outputs

- Shortening lead time

  1) By simply inputting the waveform, the tool can automatically search for the zero-point marking the start of fuel efficiency measurement (Fig. 6).

  2) Linking the tool to the data server has shortened the time for importing the TM ROM specifications and the time for confirming actual market trends.

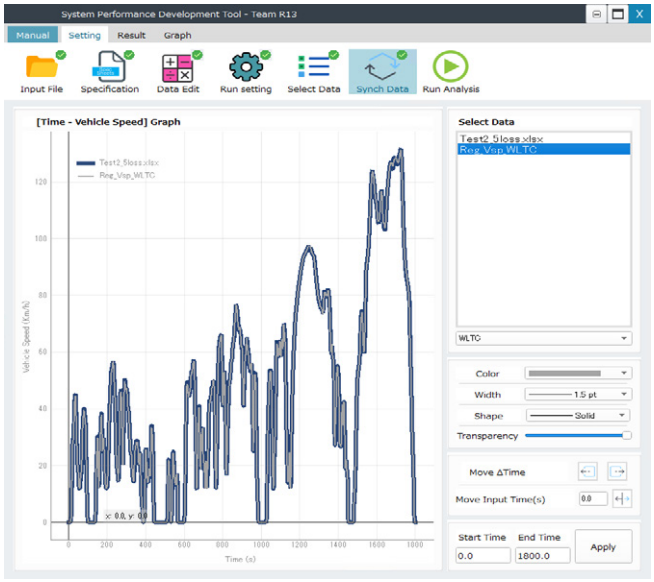

Fig. 6 Function to match the time of test results

- Every employee's analysis quality is equal to or better than before.

  1) A user interface was developed for the tool that enables anyone to conduct a fuel efficiency analysis with just simple operations.

The newly developed tool makes it possible to analyze fuel efficiency with just one user interface and simple operations for inputting specifications (Fig. 7).

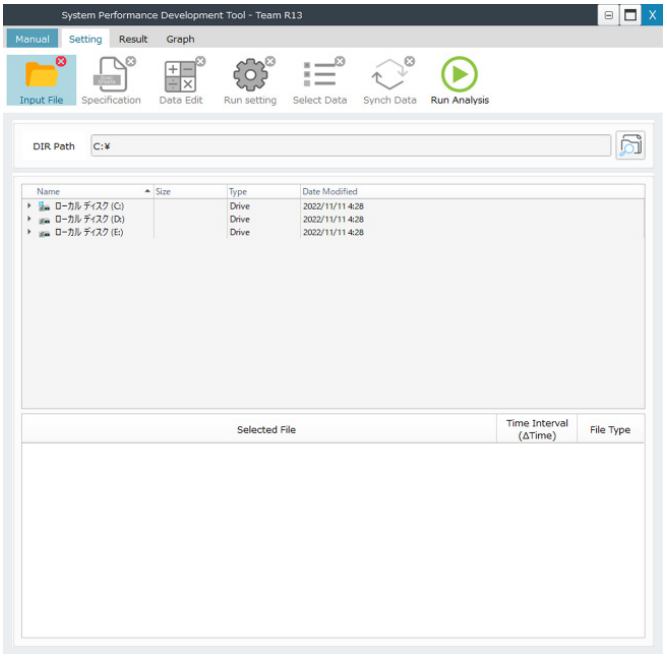

Fig. 7 Main interface display of new fuel efficiency analysis tool

3.3 Function for automatic analysis of TM factors influencing fuel efficiency

The TM factors influencing fuel efficiency can be broadly categorized as follows:

(1) Mechanical loss

(2) Shifting loss

(3) Launch loss

(4) Inertia loss

The influence of these four factors is quantitatively calculated from the measured fuel efficiency waveform and comparisons are made with the design plan values and general trends. On that basis, it must be possible to identify the factors contributing to non-attainment of the fuel efficiency target. In case the unattained factors do not have the targeted values, it is necessary to be able to identify the causes involved.

The fuel efficiency analysis tool incorporates the following four measures for accomplishing these tasks.

1) It can calculate the loss from the four factors influencing fuel efficiency as a result of inputting the fuel efficiency waveform.
2) It automatically calculates the shift lines and lockup clutch engagement values imported from the TM ROM and is equipped with a function that can compare the measured values and the intended design values.
3) It imports previous results from the data server and can compare the losses of the four factors influencing fuel efficiency obtained from the fuel efficiency waveform with the general trends.
4) If the losses deviate from the design plan values, the tool incorporates a function for analyzing the factors involved (Table 2). Examples here include the shift lines and engagement region of the lockup clutch

Table 2 Results of energy loss analysis

			Test result	Ideal result
Fuel efficiency		[L/100km]	7.2	6.5
Engine loss		[kJ]	16257	15405
	Idle speed		OK	OK
	Fuel cut-off duration time	[sec]	0	128.3
	Engine efficiency	[%]	26	30
	Engine loss improvement opportunity	[%]	3.1	-
CVT loss		[kJ]	4038.3	3819.3
	CVT efficiency	[%]	80	82
Launch loss		[kJ]	115	115
	Lockup timing		OK	OK
	Launch loss improvement opportunity	[%]	0	0
Mech loss		[kJ]	3859.3	3657
Inertia loss		[kJ]	9.3	15.3
Shifting loss		[kJ]	54.7	32
	Shifting loss		OK	OK
CVT output energy		[kJ]	4828	4598
	Vehicle speed traceability		OK	OK
	Improvement opportunity	[%]	10	-

The tool is capable of comprehensively analyzing the TM factors influencing fuel efficiency automatically. Accordingly, anyone can identify the factors contributing to the non-attainment of the fuel efficiency target in a shorter period of time without overlooking anything.

3.4 Automatic visualization of frequently used graphs

In order to quickly plan countermeasure specifications based on the analyzed results, it is necessary to determine specifications that take into account trade-offs resulting from specification changes. For that purpose, the related departments must coordinate with the vehicle manufacturer. The tool is equipped with a function for visualizing frequently changed parameters in order to coordinate them preferentially in the validation/calibration phase.

- Shift calibration

1) The tool can plot contour graphs showing the proportion of fuel efficiency mode driving and the fuel consumption rate on the shift schedule lines (Fig. 8).

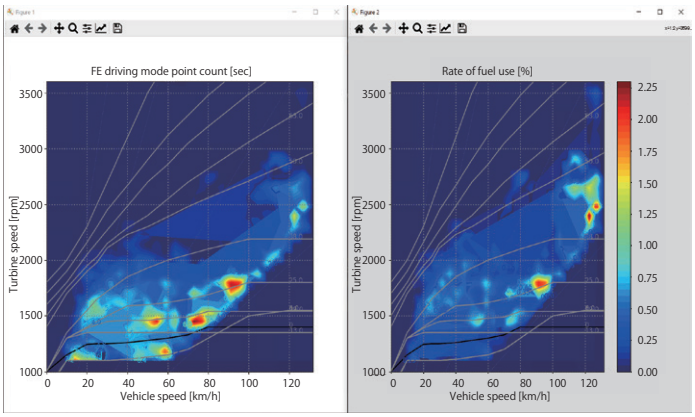

Fig. 8 Contours of proportion of FE driving mode and fuel use in shift schedule

2) The tool is equipped with a function for superimposing the predicted design speed and actual speed on a time chart and highlighting the places that deviate from the design prediction (Fig. 9).
3) The tool can superimpose the ideal speed for fuel efficiency and the measured speed on a time chart and highlight the places where the measured values deviate from the ideal values. Moreover, it can automatically calculate how much improvement in fuel efficiency can be expected by approaching the ideal values (Fig. 10).

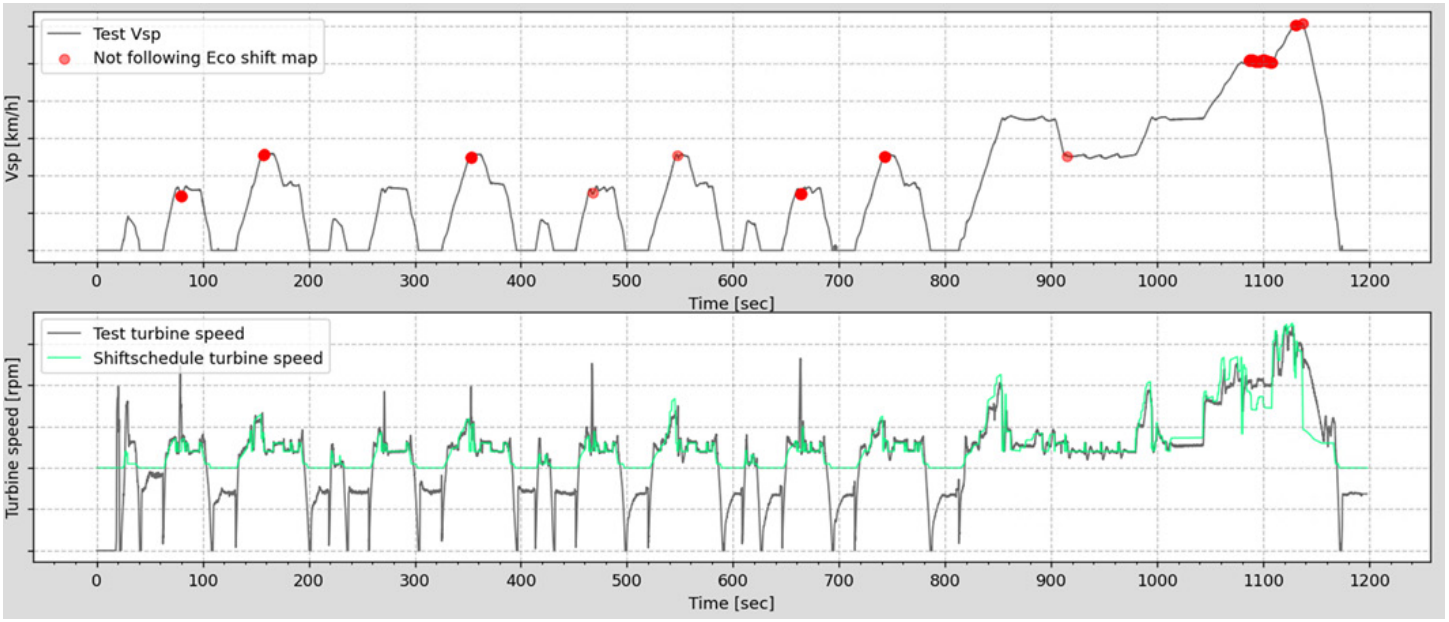

Fig. 9 Function to check the intention of shift schedule

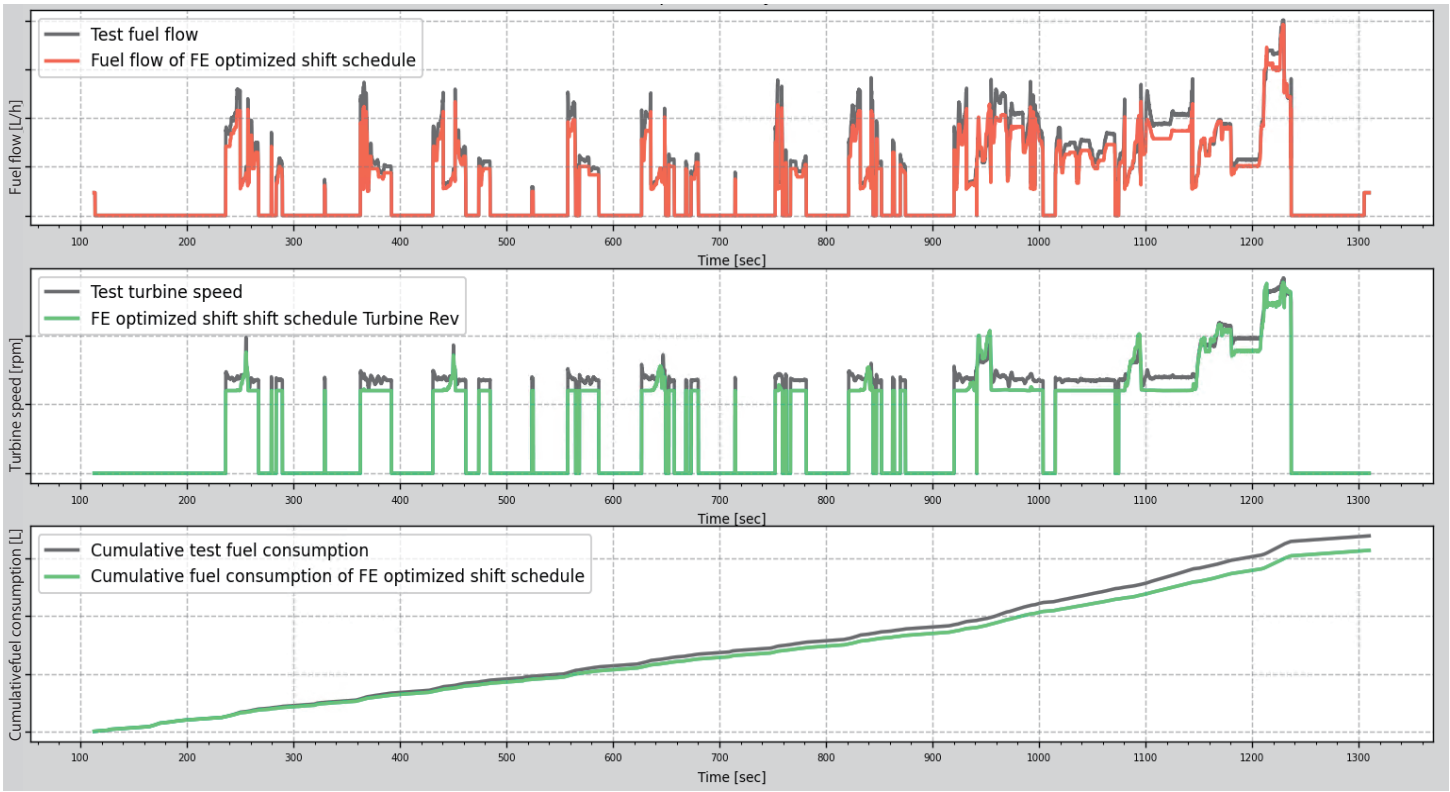

Fig. 10 Function to compare test results and FE optimized shift schedule

- Lockup calibration

1) The tool is equipped with a function for superimposing the designed lockup clutch engagement region and the measured region on a time chart and highlighting the places where the lockup behavior deviates from the design intention (Fig. 11).

By automatically visualizing frequently used graphs, the tool makes it possible to distinguish regions having a large impact on fuel efficiency and regions of high priority. In addition, in regions where the measured behavior deviates from the design intention, it can narrow down the places requiring a detailed factor analysis, thus enabling studies to be conducted efficiently.

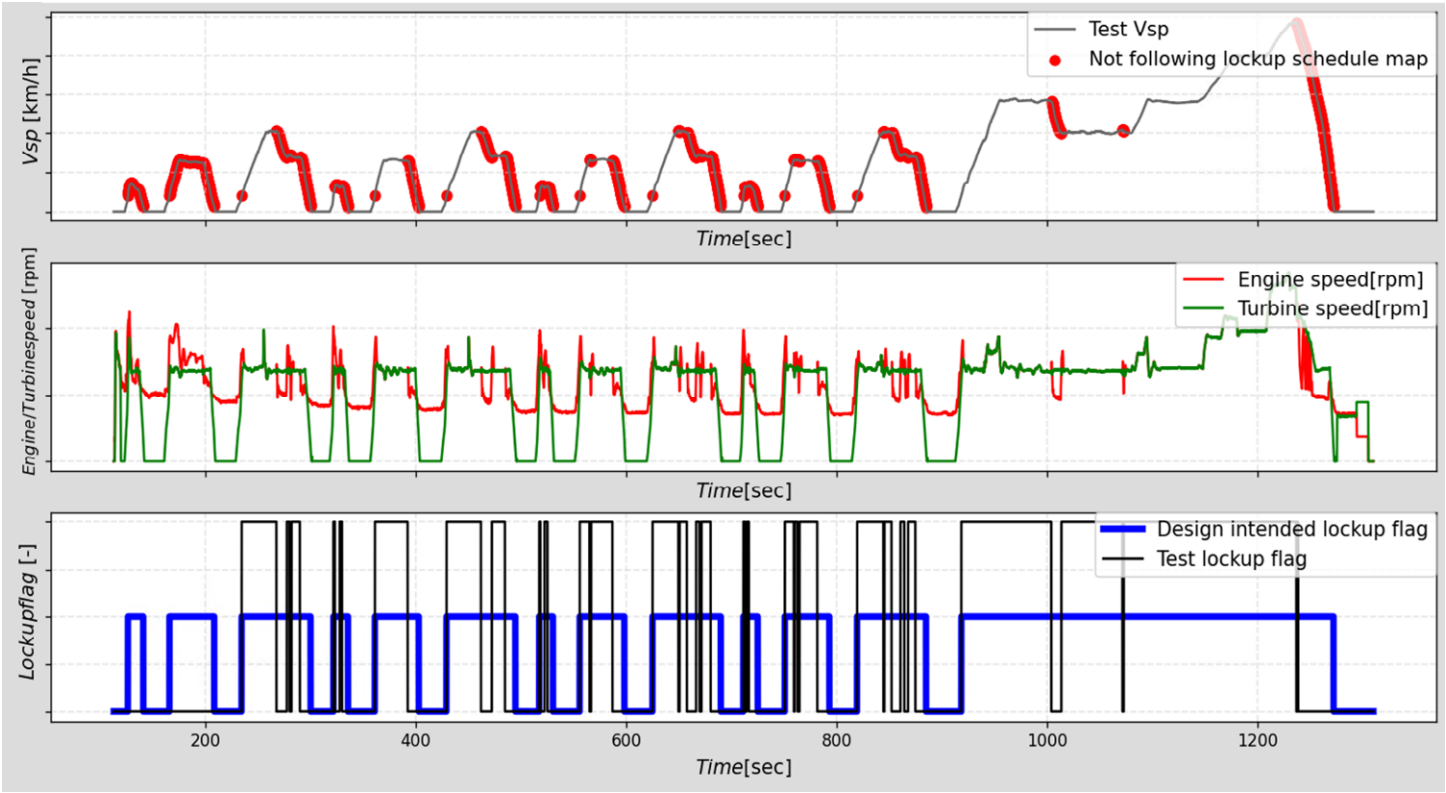

Fig. 11 Function to check the intention of lockup engagement

4. Conclusion

The use of the newly developed fuel efficiency analysis tool has improved the lead time efficiency of work processes by 60%, thereby reducing the time required for waveform analysis and examination of improvement measures (Fig. 12). In addition, using this tool has made it possible to achieve the targeted fuel efficiency in a short period of time. It has reduced the number of tests needed to attain the targeted fuel efficiency, enabling the remaining time until fuel efficiency certification to be used effectively for discovering further measures for improving fuel efficiency. Moreover, when a trade-off occurs in the development process, the tool makes it possible to quickly confirm if there is any resultant impact on fuel efficiency, thus enabling smooth adjustment of specifications toward the attainment of fuel efficiency certification.

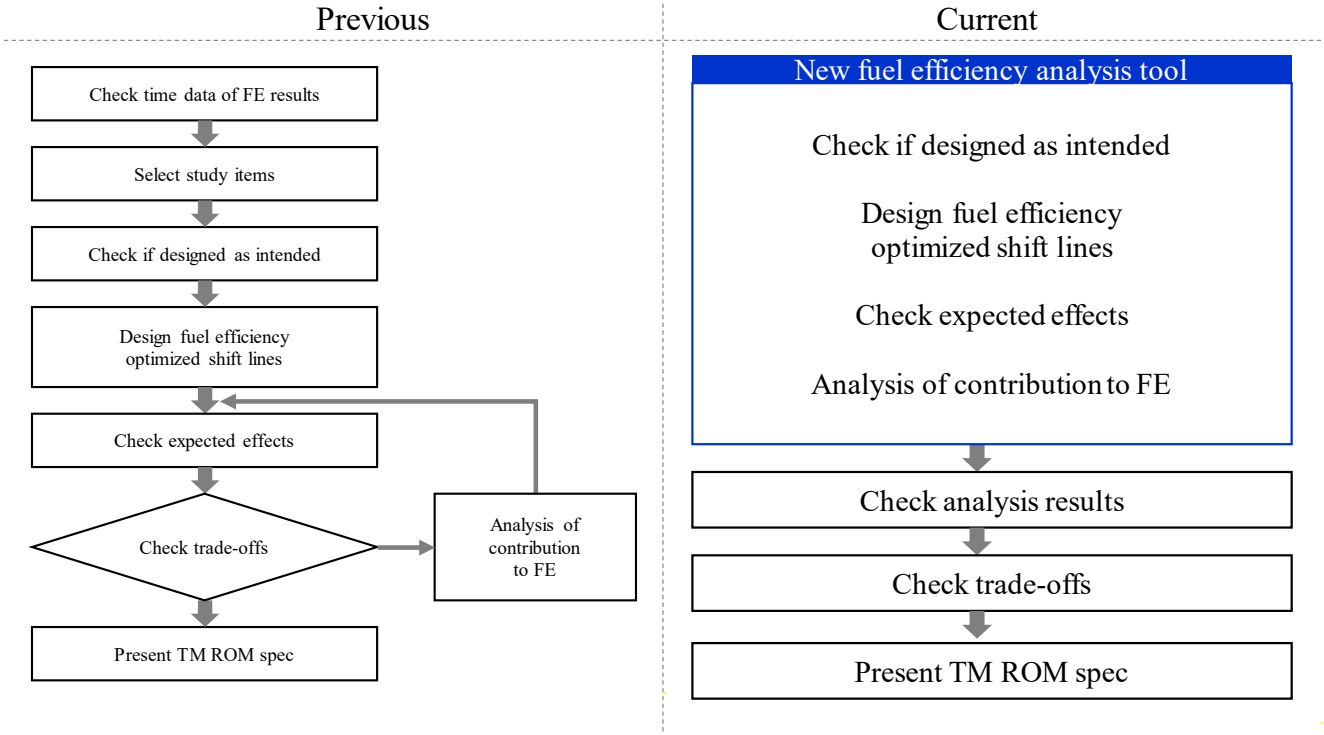

Fig. 12 Previous and current process flow

■ Authors ■


Chadol KIM


Sunho LEE


Jaeseok LIM


Sungyub HAN


Keunsoo KIM


Jaesang LEE

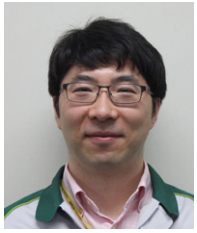
Hyeongbeom HEO

Implementation of asymmetric tooth root geometry for downsizing automotive transmission gears

Kunihiko FUKANOKI* Koji MATSUO* Yoshitomo SUZUKI**

Summary

This article proposes a design method for improving the tooth root breakage strength of automotive transmission gears. This method for improving tooth root breakage strength involves increasing the tooth root radius of curvature so as to relax tooth root stress. The tooth root radius of curvature is limited by the symmetric geometry of the cutting tool tip radius for both the driving- and coasting-side tooth flanks.

In this study, a method is proposed for designing gears with an asymmetric tooth root geometry along with a method for designing cutting tools for machining such gears with stable quality. The effectiveness of the proposed methods was validated, and it was confirmed that gear service life can be lengthened against tooth root breakage. The results verified that the implementation of the proposed design methods is effective for improving tooth root breakage strength and extending gear service life.

1. Study background

There have been demands in recent years for further reduction of automotive transmission size and weight from the standpoints of improving vehicle fuel economy and ensuring collision safety, among other requirements. As a result, the durability and reliability of transmission gears must be ensured under even more severe operating environment conditions.

This article focuses on tooth root breakage strength, as breakage is a principal failure mode of automotive transmission gears. A new method of designing gears is proposed that can improve tooth root breakage strength. The traditional approach to designing tooth root breakage strength has been to use S-N diagrams of tooth root fatigue breakage. The modified Miner's rule is used to define the target number of load cycles for gears based on the input torque and input frequency that occur in real-world driving situations (referred to here as the field loading frequency). Tooth root bending stress is defined as the criterion for satisfying this target performance. Gear specifications are then designed so as to satisfy this criterion.

In order to improve tooth root breakage strength, tooth root bending stress must be reduced. A key factor in this regard is to relax the stress concentration by increasing the tooth root radius of curvature. The size of the tooth root radius of curvature is limited by the conditions needed for a viable hob as the gear tooth cutting tool. This limitation stems from the symmetric geometry of the hob cutting edge radius for both the driving- and coasting-side tooth flanks. Moreover, because the field loading frequency is larger on the driving side than on the coasting side, the gear size is determined by the tooth root breakage strength required by the driving-side tooth flanks. Accordingly, it was reasoned that gears could be downsized if they could be designed with an asymmetric tooth root radius of curvature, that is, by designing the driving-side and coasting-side tooth flanks with a large and small radius of curvature, respectively.

Therefore, this article proposes a method of designing gears with an asymmetric tooth root geometry and a method of designing hobs for machining such gears with stable quality in mass production. The validity of the proposed design methods has been verified by conducting durability tests on CVT units built with gears designed and produced using these methods. The test results

*Hardwarel System Development Department **Engineering Management Department

confirmed that the tooth root breakage life of the tested gears was lengthened. Finally, the implementation of mass production of gears having an asymmetric tooth root radius of curvature will be described.

2. Concept of strength design for an asymmetric tooth root radius of curvature (R)

As mentioned above, it is well known that tooth root bending stress is a key factor of tooth root breakage strength. The authors applied the method proposed by Kubo and Umezawa in (Fig. 1)[1] to calculate the load distribution on a simultaneous line of contact. Tooth root bending stress was then calculated from the load distribution, and tooth root breakage strength was designed on that basis.

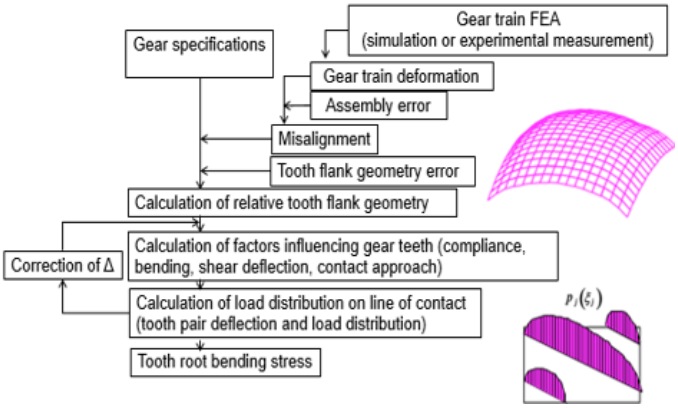

Fig. 1 Flow chart of the calculation of tooth root stress using the equation proposed by Kubo and Umezawa

The tooth root bending stress used in this calculation method can be calculated using the following expression proposed by Aida and Terauchi[2] for calculating tensile bending stress.

$$\sigma_t = \left(1+0.08\frac{S}{\rho}\right)(0.66\sigma_{Nb}+0.40\sqrt{\sigma_{Nb}^2+36\tau_N^2}+1.15\sigma_{Nc}) \quad \cdots\cdot (1)$$

where S is the tooth thickness at the position of the critical cross section, ρ is the tooth root radius of curvature, σNb is nominal bending stress, τN is nominal shear stress and σNc is compressive stress. The value of ρ in the equation must be given as a dimension that allows viable hob cutting edge geometry.

Equation (1) is an expression derived on the basis of gears having a symmetric tooth root radius of curvature. However, it was reasoned in this study that Eq. (1) was applicable even to gears having asymmetric tooth root geometry so long as tooth deflection did not change. Specifically, it was assumed that the bending stress of gears having an asymmetric tooth root radius of curvature can be calculated by making the tooth thickness S at the position of the critical cross section the same as that of conventional gears with symmetric tooth root geometry and applying the respective tooth root radius of curvature ρ of the driving- and coasting-side tooth flanks to Eq. (1).

3. Construction of a method for designing gears with asymmetric tooth root geometry

The proposed design method was constructed using the second reduction gear pair shown in Fig. 2 of a CVT for use on midsize to large passenger vehicles. The specifications of the target gear pair are listed in Table 1.

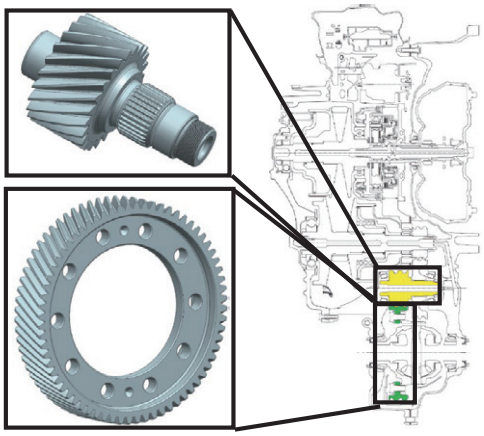

Fig. 2 Continuously variable transmission unit for medium to large passenger cars and a second reduction gear pair.

Table 1 Geometries of target gear pair

			Reduction gear	Final gear
Module	m_n	mm	2.48	←
Pressure angle	α_n	deg.	19	←
Helix angle	β	deg.	28(LH)	28(RH)
Number of teeth	z	-	23	68
Tip diameter	d_a	mm	71.9	195.3
Root diameter	d_f	mm	58.24	181.84
Facewidth	b	mm	38.9	38

Transmission gears are not used under steady torque inputs during real-world driving. Various torque levels are input to the transmission, acceleration and deceleration events are repeated, and the torque input to the gears differs between the driving side and the coasting side. An example of the field loading frequency is shown in Fig. 3.

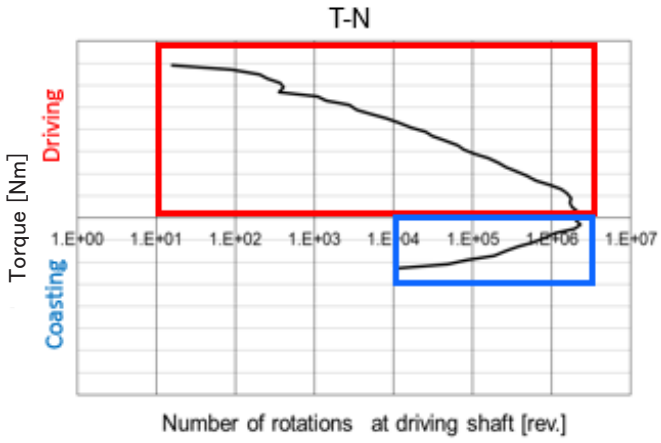

Fig. 3 Field loading frequency

The figure indicates that the predominant share of the field loading frequency is input to the driving side compared with the coasting side. Because the field loading frequency is small on the coasting side, the tooth root breakage strength of the coasting-side tooth flanks under this loading frequency is designed on the basis of the fatigue limit. Accordingly, it is not necessary for driving-side and coasting-side tooth flanks of transmission gears to possess the same tooth root breakage strength.

Therefore, the target gear pair is intentionally designed with a different size of fillet radius of curvature for the driving- and coasting-side tooth flanks, enabling the necessary strength to be secured on each side. Specifically, the gears are designed with a large radius of curvature for the driving-side tooth flanks and a small radius of curvature for the coasting-side tooth flanks. The gear tooth root radius of curvature is determined based on the field loading frequency (horizontal axis) on the driving side so that the tooth root bending stress is below the criterion; the radius of curvature for the coasting-side tooth flanks is designed based on the coasting-side field loading frequency so that the tooth root bending stress is below the fatigue limit.

Tool life and the machined accuracy of tooth flanks after the hobbing process are taken into account in designing hobs for machining gears with different radii of curvature for the driving-side and coasting-side tooth flanks. If the radius of curvature R of the hob cutting edge is excessively small, it can be expected that hob edge chipping or early crater wear may occur, resulting in a substantial reduction of tool life and increased costs. Accordingly, care is taken when manufacturing hobs to ensure the minimum necessary radius of curvature R of the hob cutting edge for coasting-side tooth flanks. In addition, in cases where the radius of curvature of the hob cutting edge differs between the driving- and coasting-side tooth flanks, care is taken so that the same amount of stock is removed from the tooth roots of the right and left tooth flanks in the tooth flank finishing process. If it is not identical, tools used in the tooth flank finishing process for gears with asymmetric tooth root geometry would be subjected to different cutting loads on their right and left cutting edges. It can be expected that this condition could cause vibration and produce undulations on machined tooth flanks. Therefore, as shown in Fig. 4, a protuberance geometry was designed for unifying the diameter at the start of undercutting following hobbing in order to ensure that stock removal on the tooth root side is identical even for gears having an asymmetric tooth root radius of curvature.

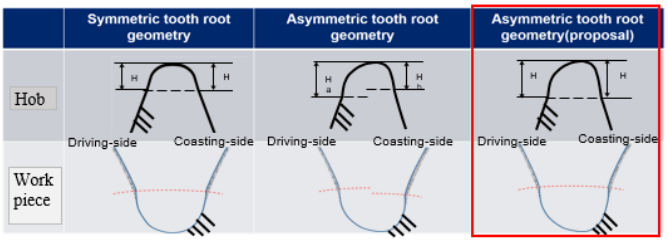

Fig. 4 Comparison of hob and workpiece

A concrete design was then executed based on the concept described above. The criterion for the tooth root bending stress of the driving-side tooth flanks was set at 1,220 MPa based on the field loading frequency of a vehicle fitted with symmetric gears, and a fatigue limit design was adopted for the coasting-side tooth flanks. To satisfy these values, the tool cutting edge was designed

with radii R of 1.116 mm for the driving-side tooth flanks and 0.372 mm for the coasting-side tooth flanks.

If these tool cutting edge radii R are ensured, the desired tooth root breakage strength can be satisfied and also productivity can be secured. The hob design method was also applied to unify the diameter at the start of undercutting of the target gear pair in order to obtain stable machining accuracy in the tooth flank machining process. The specific tool dimensions and tooth root geometry are shown in Figs. 5 and 6, respectively.

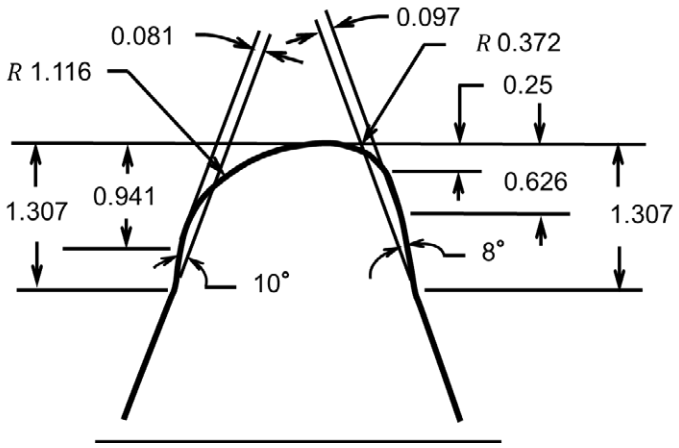

Fig. 5 The specific tool dimensions

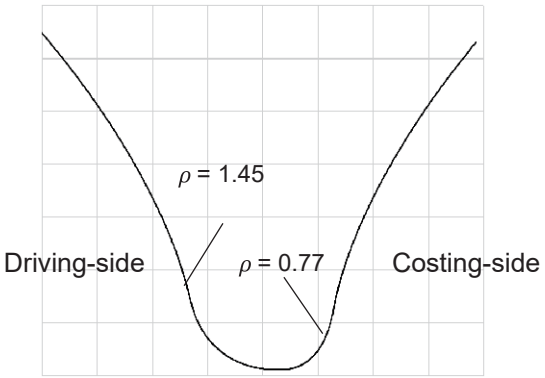

Fig. 6 Tooth root geometry

An estimation was made of the effects of applying an asymmetric tooth root radius of curvature to the target gear pair. Two types of target gear pairs were designed for the gear specifications in Table 1. One gear pair had a symmetric tooth root radius of curvature and the other pair had an asymmetric radius of curvature. The face width was designed to satisfy the criterion for tooth root bending stress. The gear volume was calculated from the difference in the face width, and the effect of the asymmetric design on improving torque density is shown conceptually in Fig. 7. The results indicate that a size reduction of 9.5% can be expected, thus confirming that an asymmetric tooth root radius of curvature can contribute significantly to downsizing transmission gears.

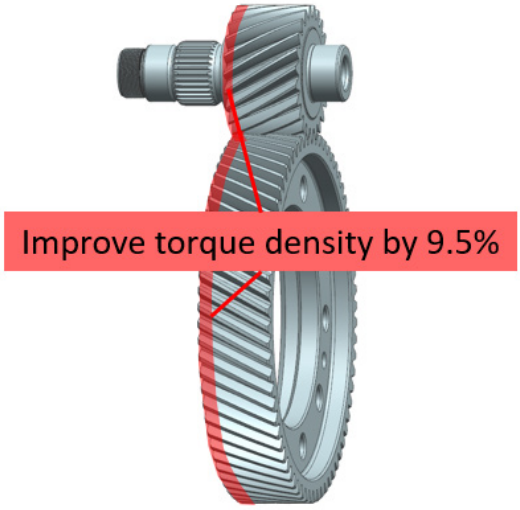

Fig. 7 Concept for improving torque density

In conducting durability tests, it is essential to know the accuracy of the gears being evaluated because that information is critical for the durability evaluation. Because this study focused on tooth root breakage strength, measurements were made of the tooth root geometry.

The tooth root geometry of the test gears was machined with hobs that were designed as explained earlier. In order to evaluate whether the tooth root geometry was machined according to the design intention, it had to be represented geometrically. The tooth root geometry was evaluated in a cross section perpendicular to the axis. Therefore, an equation was calculated for the tooth root fillet curvature in the cross section perpendicular to the gear axis based on the hob tooth profile dimensions. A simulation for calculating the tooth root geometry was created, and the theoretical geometry and the actual geometry were superimposed as shown in Fig. 8. As seen in Fig. 9, the actual and calculated tooth root geometries showed good agreement, indicating that the test gears had the desired tooth root geometry as expected.

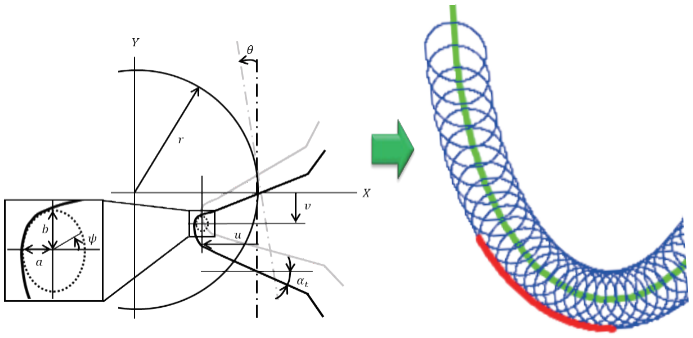

Fig. 8 Simulation for calculating the tooth root geometry in the perpendicular cross section

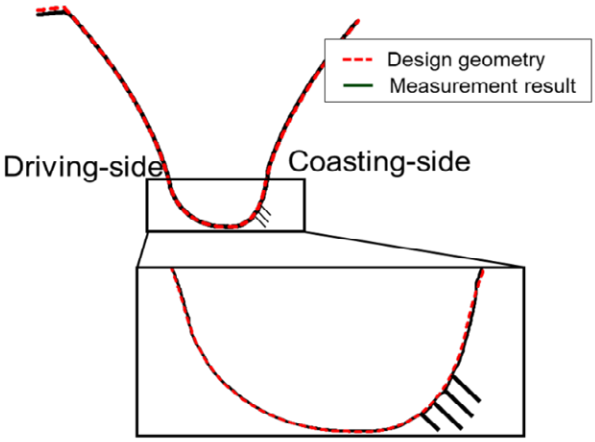

Fig. 9 Comparison of calculated and measured geometries

4. Experimental validation

Evaluations of tooth root breakage strength were conducted using the motor-dynamo testing system outlined schematically in Fig. 10. A photograph of the test stand is shown in Fig. 11.

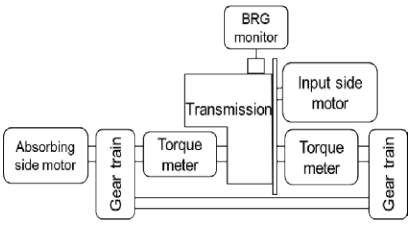

Fig. 10 Outline of test stand

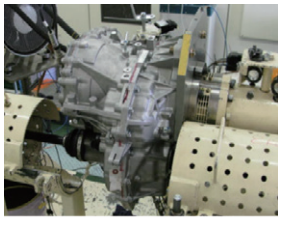

Fig. 11 Photo of test stand

The target gear pair was incorporated in a CVT unit installed on the motor-dynamo. Rotation was applied by the input-side motor and the absorbing-side motor was braked to generate the desired input torque. Durability tests were conducted under conditions of a specified rotational speed and torque until tooth root breakage occurred.

4.1 Test results

The number of cycles to tooth root breakage and the calculated tooth root stress were summarized in an S-N diagram; an example of results is presented in Fig. 12. The red circles in the diagram are for gears with an asymmetric tooth root radius of curvature and the black circles are for gears with a symmetric tooth root radius of curvature.

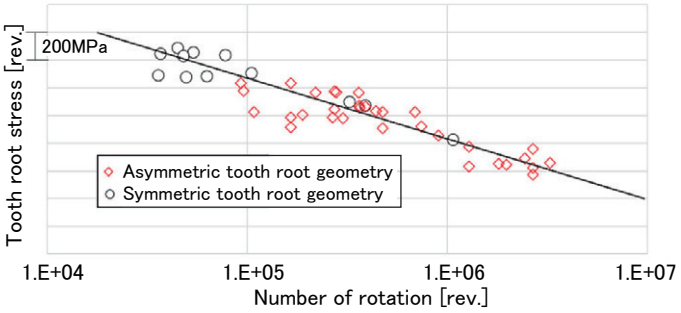

Fig. 12 S-N diagram

It is seen that the test results for both the symmetric and asymmetric tooth root geometries are plotted on the same S-N curve. Consequently, the results confirm that the method proposed for calculating tooth root stress is also applicable to gears having an asymmetric tooth root radius of curvature.

The calculated values for the stress ratio and the volume ratio of the target gear pair are compared in Table 2 with the values calculated from the test results in order to show the effects of applying asymmetric gear tooth root geometry.

Table 2 Comparison of estimated and experimental results for calculating size effect accurately

	Volume reduction ratio [%]
Estimated	9.5
Experimental result	10

The results indicate that the differences between the two sets of values were small, thus verifying the effectiveness of asymmetric tooth root geometry for downsizing transmission gears.

5. Conclusion

A method of designing automotive transmission gears with an asymmetric tooth root radius of curvature was investigated taking into account the field loading frequency during real-world vehicle use. The aim of this design method is to enable automotive transmission gears to be downsized by improving tooth root breakage strength.

This design method makes it possible to reduce the gear size and weight by 10% compared with conventionally designed gears. CVT units are now being mass produced with gears having an asymmetric tooth root radius of curvature.

6. References

(1) Kubo, A. and Umezawa, K., On the Power Transmitting Characteristics of Helical Gears with Manufacturing and Alignment Errors (1st Report): Fundamental Consideration, Transactions of the JSME (in Japanese), Vol. 43, No. 73, (1977), pp. 2271-2783.

(2) Aida, T., and Terauchi, Y., On the Bending Stress of Spur Gears (2nd Report): The Stress Concentration Factor and the Equation for the Calculation of Bending Stress of Gear Teeth), Transactions of the JSME (in Japanese), Vol. 27, No. 178, (1961), pp. 868-876.

(3) Fukanoki, K., “Practical application of asymmetric tooth root geometry for downsizing automotive transmission gears,” VDI International Conference on Gears 2022, September 12-14, 2022, Germany, pp. 197-213.

■ Authors ■

Kunihiko FUKANOKI

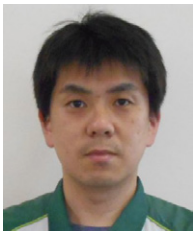

Koji MATSUO

Yoshitomo SUZUKI

Clutch texture technology inspired by two types of creatures: From conception to design to mass production method

Michinori MATSUO*

Summary

JATCO has improved clutch friction stability and extended clutch service life by machining a texture on the mating steel plate instead of on the conventional friction material. This texture was inspired by two creatures to address stick-slip that is a fundamental issue of clutches. This article describes the new engineering method from the perspectives of conception, design and mass production.

1. Introduction

In order to maintain a habitable global environment for people, there is a greater need than ever before for society to use sustainable things. The automotive industry also has a large responsibility in this regard. Reforms are necessary not only for achieving carbon neutrality but also in various fields, including extending the usable lifetime of vehicles.

Currently, I am engaged in the creation of innovations and the development of fundamental technologies. Being in a position that demands unprecedented technological concepts, I have focused on biomimetrics, i.e., nature-inspired innovation.

Living things have undergone a long history of evolution to reach their present forms since the earth was formed. Learning from and drawing upon that evolution, I believe, can provide approaches for pursuing innovations in the process of studying sustainability. The surface texture technology developed in this project was inspired by two types of creatures.

The hexagonal arrays seen on the feet of katydids and frogs are thought to function for stick-slip control and grip enhancement. Accordingly, a technology was developed for machining a texture of fine hexagonal grooves on the steel plate that is a constituent part of transmission clutches.

As a result, a substantial improvement of clutch friction characteristics was accomplished as a benefit gained from nature. This article describes the details of this development from conception to the establishment of a mass production method.

2. Conception and selection of part for application

2.1 Conception

Information on nature was researched focusing on inspiration from outside the automotive industry in seeking concepts for unprecedented technologies. Borrowing the wisdom of creatures that have accumulated a long evolutionary history was assumed to be the most suitable approach to finding things that vastly exceed the realm of human thought.

A search was made for information especially related to insects in the natural world. The shells of insects seemed to be like a robot in having simplicity combined with complexity. This gave the impression that much can be learned from them, making it easier to come up with ideas applicable to industrial products.

In the course of investigating insects and technologies and other ideas derived from them, I came across the genre called biomimetrics. I found that extremely interesting studies are under way in a variety of fields, including robots based on the ecosystem of ants, the brains of flies and the feet of sea lice. Among these studies, there was an

* Innovative Technology Development Department

article about the bottom of katydid feet.

The bottom of katydid feet has a hexagonal texture that has an expected value of stick-slip control. The results of friction experiments conducted using a silicone material showed that stick-slip was eliminated, yielding smooth friction characteristics (Fig. 1).[(1)-(2)]

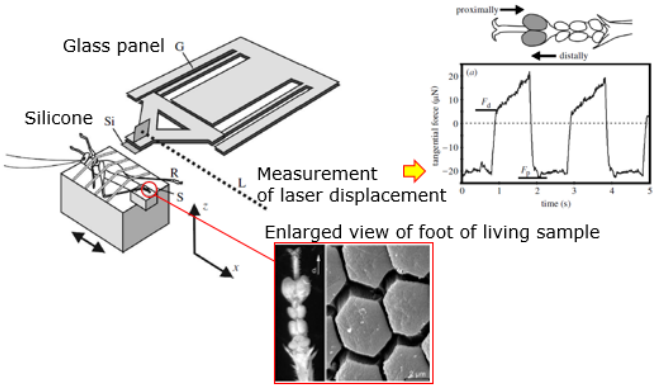

Fig. 1 Information extract for the bottom of katydid feet

Further research was then conducted on the bottom of creatures' feet. A close examination of grasshoppers, which give the impression of being similar to katydids, revealed that they apparently did not have any hexagonal pattern on the bottom of their feet. This suggested that grasshoppers flee by flying away while katydids flee by running away.

A close examination of frogs, which, like katydids, jump on their hind legs, revealed a hexagonal structure on their feet. Frogs have been researched in the medical field. Reports have mainly been written about the function of this structure for improving gripping ability (Fig. 2).[(3)]

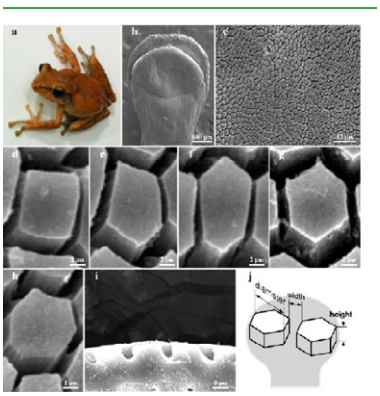

Fig. 2 Information extract for the bottom of frog feet

One point of interest here is that both types of creatures, an insect and an amphibian, have a hexagonal pattern on the bottom of their feet, though they are different species and also live in different environments. Another point is that the function of the pattern of each one is different. It was inferred that the hexagonal pattern imparts multiple positive effects on frictional surfaces, so it was decided to investigate this texture.

2.2 Applied

2.2.1 To which part should the texture be applied?

The question of to which transmission parts the texture should be applied in order to use it effectively for our products was also an extremely important point for increasing the likelihood of obtaining the desired effect.

Frictional surfaces are found at a variety of places inside a transmission, including the shafts, belt, pulleys, gear surfaces and clutches, among other locations. It was concluded that clutch parts were suitable locations where the functionality of the hexagonal pattern was desired (Fig. 3).

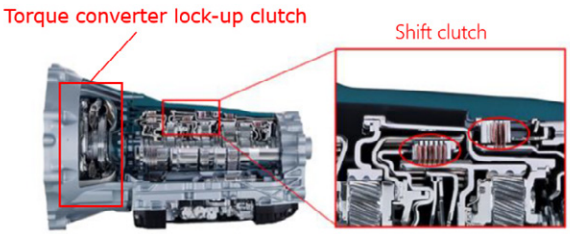

Fig. 3 Candidate parts for texture adaptation

Why are clutches suitable? Clutches engage and disengage repeatedly in the process of shifting gears. Clutches are engaged by gradually applying pressing force to achieve engagement. A slipping state occurs during the transition. When there is slipping, stick-slip can occur as a natural phenomenon at frictional surfaces. Stick-slip is an issue because it causes vehicle occupants to feel an unpleasant vibration.

Clutch friction is usually under design control, so the likelihood of stick-slip occurring is very small. However, stick-slip can occur accompanying deterioration with use.

Since katydids suppress stick-slip in nature, it was

decided it would be worthwhile to attempt a similar application to the stick-slip phenomenon in JATCO's transmissions. Moreover, it was expected that it would also improve gripping force as noted earlier for frogs.

Clutches are engaged by friction to transmit driving force, and energy is also required during engagement. An increase in gripping force would result in a higher friction coefficient, and it could be expected that pressing force would also be reduced.

2.2.2 To which clutch parts should the texture be applied?

The clutch friction material and steel plate were considered as two conceivable places for applying the texture. In this study, the steel plate surface was selected. In a conventional sense, there was concern that machining the texture on the steel plate would produce a file-like effect that would abrade the cellulose and other components of the friction material. However, considering that the two types of creatures live on the tops of leaves containing cellulose, it was envisioned that the texture might be viable if the surface pressure was reduced to the level occurring in nature (Fig. 4).

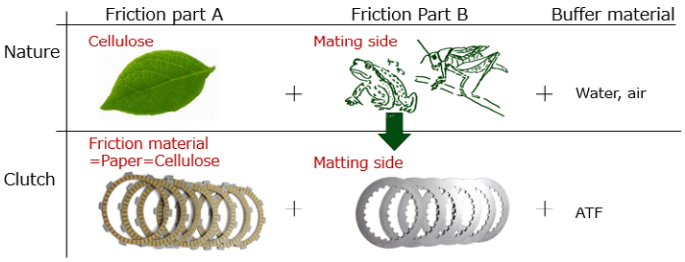

Fig. 4 Conceptual representations of adaptation locations

3. Design

3.1 Calculation of surface pressure

The detailed dimensions were calculated by making a Fermi estimate. Taking into account all the aspects up to mass production, it would be virtually impossible to calculate everything because there are so many points that differ from the living environment of the two types of creatures, including clutch immersion in oil and the stiffness of steel, among other things. As the development concept, it was decided to use the approximate surface pressure that the creatures would experience in their natural environment on the earth (Fig. 5).

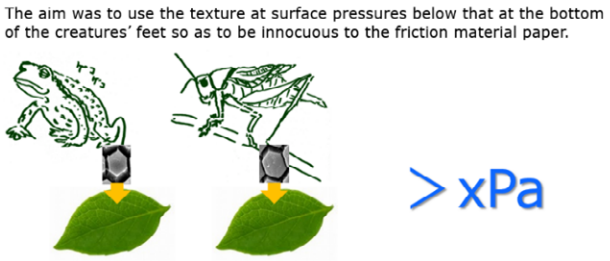

Fig. 5 Representation of concept

There are blogs on the Internet by people who like insects, so it was possible to find some information about the mass of katydids. The testes of katydids account for about 1-13.8% of the mass and weigh about 2.7-70.1 mg. From these data, the body weight was calculated to be 491.9 mg.

A technical paper[(3)] concerning research on katydids contained image data for the bottom of their feet. The area of the hexagons was measured and provisionally assumed to be $1.67576 \times 10^{-11} m^2$. The size of one foot was deduced from the overall length and the number hexagons was estimated for one foot (Fig. 6).

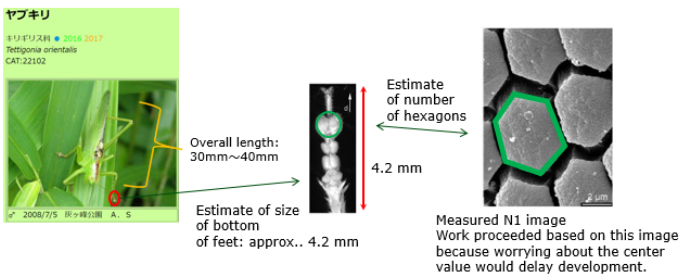

Fig. 6 Enlarged view of the bottom of katydid feet

Next, it was decided to calculate the total number of the hexagons that do the functional work. While katydids have six legs, it was hypothesized that their center of gravity is probably concentrated on the two thick rear legs when they move, not when they are stationary. Under that assumption, the surface pressure concentrated on their rear feet was calculated in this study. Based on this information,

it was hypothesized that there were approximately 70,000 hexagons on the bottom of the feet supporting the body weight. The surface pressure on one hexagon was then determined as an index.

A similar investigation was also conducted for frogs. Because the order of magnitude was similar for both the hexagon size and surface pressure, it was decided to use the calculated results for katydids.

3.2 Resizing the hexagons for application to automotive parts

A study was conducted regarding the application of the texture to transmission clutches, based on the surface pressure of the single-plate lock-up clutch of a torque converter, which experiences high surface pressure. The hexagons of the creatures were expanded in size to match the lock-up clutch design, resulting in hexagons that measured approximately 120 μm on one side.

3.3 Design of groove width and depth

The groove width and depth were set at 50 μm and 20 μm, respectively. Because the dimensions could not be measured from photographs of the creatures' feet, they were provisionally determined from the oil film thickness and a margin allowing the transmission fluid to flow through the grooves easily. The dimensions were comprehensively determined taking into account prototyping and mass production methods and in reference to cost and other factors.

3.4 Orientation of hexagons

A technical paper(5) concerning research on frog legs stated that fluid flow differed depending on the orientation of the hexagons as to whether the corners or sides pointed forward. Hexagons with corners pointed forward were referred to as corner-sliding (CS) and those with sides pointed forward as side-sliding (SS). Those designations are used in this article.

In addition, the adaptation of micro-grooves on the clutch plate was also expected to have the effect of improving micro-cooling by the transmission fluid flowing through the grooves. However, because clutches are rotating parts, the positioning of regular hexagons without any modification would cause their orientation to differ at the 12 and 6 o'clock positions and at the 3 and 9 o'clock positions. It was thought that the effects of rotation on the state of the fluid and frictional surface might differ at each position. Therefore, the angles of the hexagons were slightly varied radially, and the hexagons were positioned so that their orientation would be identical in relation to the direction of rotation (Fig. 7).

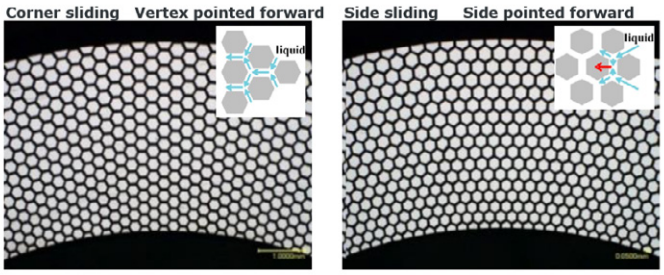

Fig. 7 Prototype test pieces directionally aligned (Left: CS; right: SS)

4. Investigation results

4.1 Prototyping

First, a femtosecond laser was used to machine an initial prototype of the texture. In order not to attack the friction material, the texture had to be machined precisely while suppressing swelling due to the heat-affected zone (HAZ). The selection of this machining technique achieved the intended texture (Fig. 8).

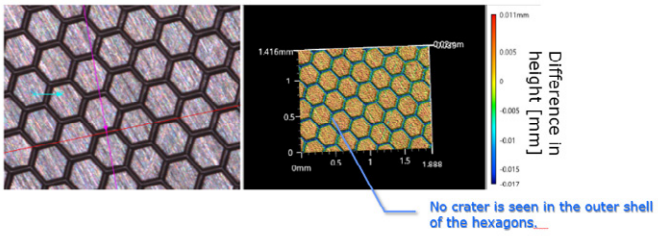

Fig. 8 Appearance of texture prototype

4.2.1 Result: effect on improving the coefficient of friction (μ)

The μ-V characteristic is a performance index obtained by plotting μ on the vertical axis in relation to differential rotation, i.e., sliding velocity, on the horizontal axis.

A characteristic that trends downward to the right is referred to as a negative gradient, which is a factor causing stick-slip. A clutch with a negative gradient tendency was prepared, and it was confirmed that replacing the steel plate with a textured plate obtained a characteristic with a positive gradient. Robustness against the fluid temperature and surface pressure was also improved, and performance stabilized under conditions of a low temperature and low surface pressure where a negative gradient tends to appear. Figure 9 shows the characteristics obtained at 40°C and 0.2 MPa.

Because the measured results did not show any large difference between the CS and SS orientations, the following discussion focuses on the CS orientation.

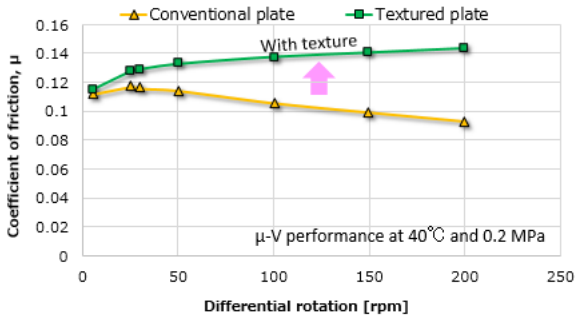

Fig. 9 μ-V performance

4.2.2 Result: Durability lifetime until reaching a negative μ gradient

Durability tests were conducted using a low-velocity friction apparatus (LVFA) for measuring clutch service life. The temperature of the test transmission fluid was adjusted to 120°C, and friction characteristics were measured at 40°C, 80°C and 120°C at certain specified intervals. Compared with clutches with ordinary steel plates, it was found that clutches with a textured steel plate extended by 65% the time until the μ-V characteristic showed a negative gradient and fell below the performance criterion. The lifetime extension was especially prominent under a low surface pressure condition (Fig. 10).

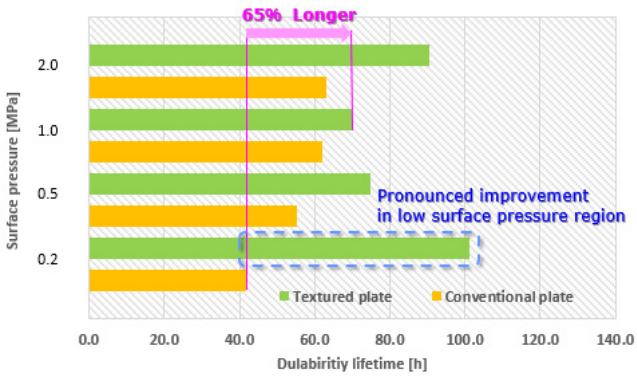

Fig. 10 Difference in service life due to the effect of the texture

4.2.3 Consideration

The foregoing results were due to the functionality and benefits imparted by the texture, which ordinary steel plates have not possessed. It is assumed that the following factors were effective in improving friction characteristics and extending clutch service lifetime:

A) the hexagonal pads stabilized the μ characteristic in the region of high differential rotation;

B) the grooves stabilized the μ characteristic in the region of a low temperature and low surface pressure by helping to optimize the fluid film on the frictional surface;

C) moreover, the transmission fluid in the grooves enhanced cooling performance,

which had the effect of improving friction characteristics and extending durability lifetime.

5. Toward mass production

Forming grooves of 50 μm in width and 20 μm in depth on steel plates having even larger undulations requires considerable technical skill. Production scale and production speed are also critical elements in adopting the texture on automotive parts. A survey was conducted at the planning stage concerning manufacturers possessing both the requisite technical capabilities and production scale. A company with precision press processing technology was found in Japan. Following prototype validation, a prototype die was fabricated at that company and press processing trials were launched. Development work is still under

way at present, including a review of the press processing conditions while making repeated improvements.

The smooth progress of trials of the mass production method enabled other studies to be undertaken ahead of schedule that were not limited to single-part experiments and included confirmation of in-vehicle process control and an examination of process variation.

6. Conclusion

(1) The stability of clutch friction characteristics was markedly improved by applying a surface texture inspired by two types of creatures. It is expected that adaptation to low-temperature conditions in particular will contribute to use on electric vehicles that have little waste heat following vehicle start-up. It is believed that this surface texture technology can contribute to new ways of using vehicles, including lengthening their usable lifetime.

(2) It is difficult to create a motif when applying properties of creatures to industrial products. The simple hexagonal structure on the bottom of the creatures' feet enabled a design based on Fermi estimates, making it possible to obtain the intended functionality.

7. References

(1) Stanislav Gorb, Biological microtribology: anisotropy in frictional forces of orthopteran attachment pads reflects the ultrastructure of a highly deformable material, Proceedings of the Royal Society B, pp. 1239-1244 (2000).

(2) Masatsugu Shimomura, "New Trends in Next-generation Biometric Materials Engineering: Learning from Biodiversity," Science and Technology Trends, May 2010, No. 110, pp. 9-28 (2010) (in Japanese).

(3) Huaway Chan, Bioinspired Surface for Surgical Graspers Based on the Strong Wet Friction of Tree Frog Toe Pads, ASC APPLIED MATERIALS & INTERFACES, Volume 7, Issue 25, pp. 13983-13995 (2015).

(4) Alexey Tsipenyuk, Use of biomimetic hexagonal surface texture in friction against lubricated skin, Journal of the Royal Society Interface, 11, pp. 1-6 (2014).

(5) Fandong Meng, et al., Tree frog adhesion biomimetics: opportunities for the development of new, smart adhesives that adhere under wet conditions, PHILOSOPHICAL TRANSACTIONS OF THE ROYAL SOCIETY A, Volume 377, Issue 2150, p.17 (2019)

(6) Michinori Matsuo, "Clutch texture technology inspired by two types of creatures: From conception to design to mass production method," JSAE Symposium: New Technologies of Power Transmission Systems 2022, Document No. 20224625 (in Japanese).

■ Author ■

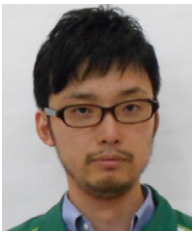

Michinori MATSUO

Construction of a platform for supporting promotion of manufacturing workplace data digitization and improvement of overall equipment effectiveness

Makoto HIROSAKI*

Summary

Improving Overall Equipment Effectiveness (OEE) in manufacturing workplaces will be essential for overcoming the severe cost and quality competition in the years ahead due to vehicle electrification. To accomplish that, it necessary to use Internet of Things (IoT) tools to digitize, visualize, analyze and effectively utilize factory floor data. This article presents a platform that has been constructed to consistently support the collection, transfer, storage and visualization of such data for improving OEE.

1. JATCO's aimed for Smart Factory

JATCO is promoting efforts to improve Overall Equipment Efficiency (OEE) by digitizing GENBA data. These efforts are called Smart Factory activities and involve the three steps defined below and shown in Fig. 1.

Step 1: Factory that minimizes defects and equipment downtime

Step 2: Factory that does not pass on defects and does not stop production lines

Step 3: Factory that maintains maximum efficiency

As of 2022, the state of progress of the activities was between Step 1 and Step 2, and the target is to transition to Step 3 in the 2030s.

In order to achieve a factory that maintains maximum efficiency, efforts must be made to substantially improve OEE from the current level. JATCO's current OEE level is around 80%. We must aim to attain a level of 90% in Step 2 and 100% in Step 3.

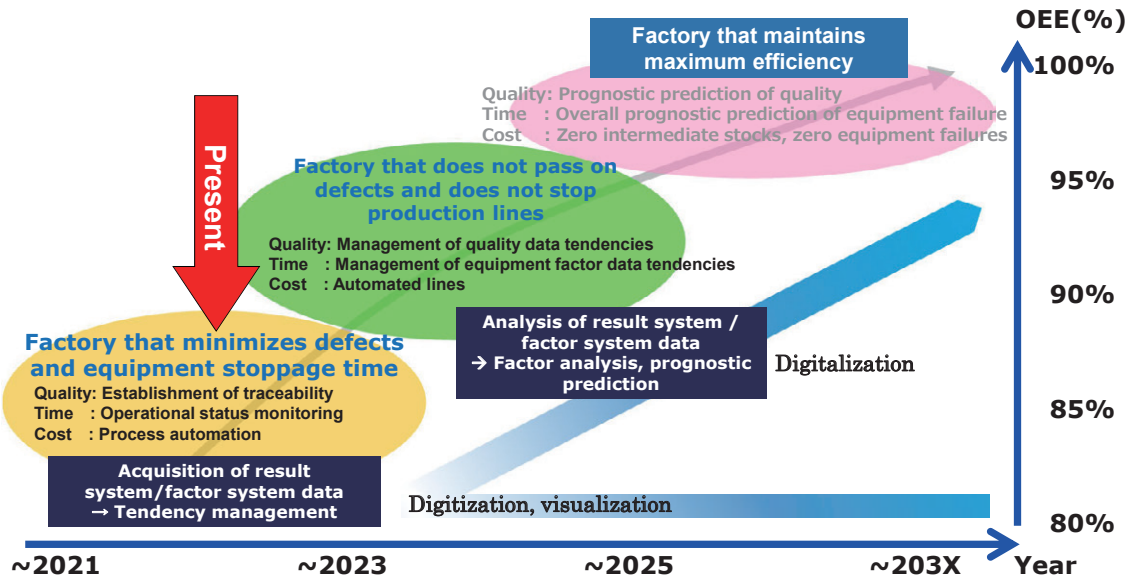

Fig. 1 Roadmap to JATCO's Smart Factory

* Promotion Digital Innovation Department

2. Ascertaining the current situation

2.1 Six large OEE losses in manufacturing workplaces

The question of how to minimize losses is a key factor for improving OEE. The following six large equipment losses can be cited as loss factors that lower OEE.

- Breakdown loss
- Setup and adjustment loss
- Idle time and short stop loss
- Speed reduction loss
- Defect and reworking loss
- Start-up and yield loss

In order to eliminate these losses, they must be discovered early and dealt with quickly. It is also necessary to take advance preventive measures.

2.2 Issues and measures concerning workplace data collection

Eliminating losses requires quick collection of manufacturing workplace data, identifying losses indicated by the data, and implementing countermeasures. However, the following factors in the current situation are delaying the elimination of losses.

- Employees do not realize the line has stopped and neglect losses.
- Checking the equipment takes time, so dealing with line issues is delayed.
- Long lead time is needed for investigation when a problem occurs, thus prolonging losses.

An analysis of these three factors revealed the issues shown in Table 1.

As countermeasures, the operational status of the line must be ascertained in real time and advance preventive measures must be taken based on the implementation of tendency management. To accomplish these tasks, an Internet of Things (IoT) tool was used to promote digitization of manufacturing workplace data in this project.

2.3 Benefits of using IoT tools

The following benefits are gained by using IoT tools.

- Because data are treated digitally, not like paper-based analog data, data searches, processing and visualization can be done flexibly.
- IoT tools can replace human employees for processing data on equipment and quality without relying on people.
- Large improvements in cost effectiveness can be obtained because many inexpensive IoT tools have been put on the market in recent years.

Table 1 Issues delaying elimination of losses and countermeasures

Present situation	Issues	Countermeasures
Employees do not realize the line has stopped and neglect losses.	Employees have no means of confirmation except looking at the line directly.	Automatically collect and visualize data on the operational status of the line.
Checking the equipment takes time, so dealing with line issues is delayed.	Checking equipment is time consuming because many items have to be written on paper by hand.	Digitize hand-written tasks to shorten employee man-hours and increase their line monitoring time.
Long lead time is needed for investigation when a problem occurs, thus prolonging losses.	It takes a long time to find the true cause of a problem after it occurs because of investigations.	Predict problems in advance or take immediate action based on management of equipment and quality tendencies

2.4 Necessity of constructing a data platform

Implementation of the countermeasures in Table 1 makes it possible to obtain and utilize data from different inputs such as from equipment and PCs connected to measuring instruments. However, if the collected data are in different formats, it can be troublesome to visualize and analyze the data later, so it is necessary to convert data to a unified format.

In addition, the scope of data utilization is limited if the collected data are stored in independent storage devices such as the separate PCs of individual employees. It is necessary to have a unified data storage location so that data can be shared, analyzed and utilized with other departments. A platform needs to be constructed that enables company-wide visualization of data.

3. Platform development concept and construction

3.1 Platform concept

The following concept was formulated for the platform described here.

- It must allow importation of different types of inputs.
- It must be possible to visualize different types of data in the same format.

To achieve these capabilities, the processing flow of the platform was defined as follows.

- Different types of inputs are digitized.
- Digitized data are converted to the same format.
- Converted data are stored in same location.
- Data can be visualized in an identical format.

This processing flow is illustrated in Fig. 2.

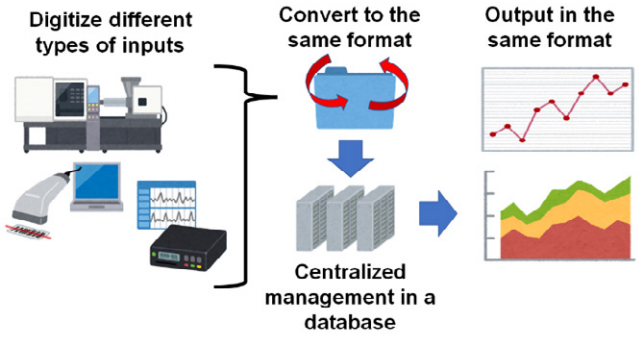

Fig. 2 Platform development concept

3.2 Examples of digitization of different types of inputs

This section explains specific examples of the different types of inputs mentioned in the previous section.

1) Data on equipment operational status

The signals of the programmable logic controller (PLC)[*1] that is used to control each piece of equipment are collected.

The internal signals of the PLC are monitored and suitably output in real time to ascertain the operational status of equipment. This method can be adopted on any line if it is possible to monitor PLC signals.

2) Check sheet data

The hand-written check sheets of employees are collected.

The input format is imported to a PC, and employees' hand-written elements up to that point are converted to PC inputs, and the input data are summarized.

This method can be adopted on any job line if the input format of check sheets can be imported to a PC.

3) Measured quality data

The data measured with 3D measuring instruments or other devices and accumulated on PCs connected to the instruments or in storage devices are collected.

PCs and storage devices are connected to JATCO's in-house network. The data they accumulate internally are saved on an in-house data server.

This method can be adopted for any measurement instrument if the measured results are saved as digital data.

3.3 Platform construction

This section explains how the platform was constructed based on the development concept. The overall configuration of the platform is shown in Fig. 3.

The platform constructed in these activities is called EQ_Connect, a name coined from the words “easy, quick, equipment and connect.” The name is now applied as a unified in-house standard.

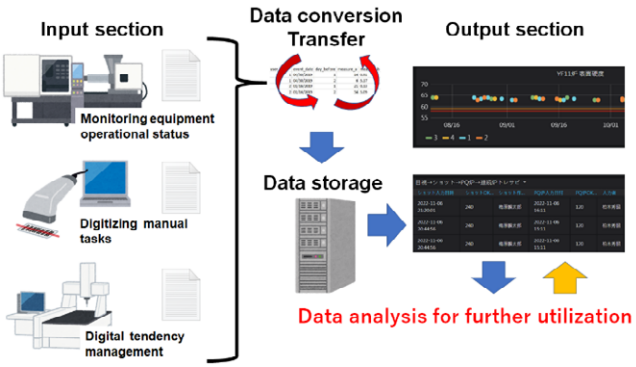

Fig. 3 Platform configuration

1) Input section

An IoT tool has been adopted for importing into the platform the various types of input data mentioned in the preceding section.

Discussions were held with the users[*2] of the platform for each matter in order to identify the necessary data items, and a data specification was developed.

2) Data conversion section

Input data are converted to a common list format composed of rows and columns using a programming language that is well-suited to character string processing.

At the time of conversion, there are instances when unexpected data may be input such as abnormal values output by the equipment or data input errors by the employees. Platform robustness has been enhanced by creating a program that envisions various types of error countermeasures so as to ensure that the conversion program does not stop when such instances occur.

3) Data transfer section

The converted list data mentioned above are transferred from each terminal to a storage server. Data are transferred in batch files[*3] that are executed at specified time intervals by the task scheduler.

This operation is a standard Windows function that enables data to be transferred reliably.

4) Data storage section

The storage server is one that has been installed in-house and is connected to the in-house network.

A relational database[*4] (RDB) has been created on the storage server.

Whenever data are transferred to the server, a program developed in-house writes the lists contained in the data into tables.

The specifications of the in-house program allow the imported lists to be modified easily, which facilitates easy horizontal deployment to other departments or plants.

5) Output section

A commercially available business intelligence (BI) app[*5] called WebAccess was adopted for visualizing data. This software reads data from the RDB for representation in tables and graphs.

4. Results obtained with EQ_Connect

4.1 Effect on OEE

As of December 2022, EQ_Connect has been implemented on approximately 40% of JATCO's main production lines. The following benefits have been revealed by visualizing and analyzing data from lines equipped with EQ_Connect.

- Data visualized by WebAccess are displayed on monitors installed in plants and offices, enabling the line operational status to be ascertained in real time. This now makes it possible to take corrective action immediately whenever a loss occurs.
- The collection of equipment data reduces the time employees have to spend checking equipment, thereby increasing the time they have for tending to the line.
- Highly accurate data that have already been collected and accumulated can be analyzed and utilized whenever a problem occurs, enabling a loss countermeasure to be

implemented in a short lead time..

- It is not necessary for employees to prepare data, so they can spend more time on analyzing and correcting problems that occur..

The measures mentioned above have improved OEE by approximately 5% on the lines where EQ_Connect has been implemented.

4.2 Secondary benefits of the activities

The activities described here have made it possible to visualize and utilize data effectively, enabling users to realize for the first time the value and importance of data. Users who now know the importance of data have requested that various types of data be visualized by EQ-Connect. More users are seeking advice about data analysis, and the number of users who are conscious of using data has been increasing.

In the course of proceeding with efforts to deploy EQ_Connect, it was found that many departments simply store data they have already visualized. Importing such data into EQ_Connect for visualization now enables the data to be deployed horizontally for use by other departments.

5. Future prospects

The platform constructed in this project is designed to be easy to operate, but a certain educational period is needed to gain consistent operational proficiency. It is desired to develop a certain number of employees capable of operating the platform to ensure continuous use going forward.

Activities for implementing the platform quickly are also needed to establish EQ_Connect throughout the company. Patterns can be created for each matter based on the types of inputs involved. It is desired to quicken horizontal deployment by preparing packages that can be varied for connecting to EQ_Connect according to the matter concerned.

Footnotes

*1: PLC

This is an acronym for programmable logic controller. It has an embedded microprocessor and is used to control production equipment by means of programs that users can modify.

*2: Users

The target users of this platform are manufacturing employees, manufacturing managers, engineers and others who require data.

*3: Batch files

These are files in which a series of commands are described, such as for connecting to a server, copying data or other tasks; they are executed automatically in serial order.

*4: RDB

A relational database is a collection of data consisting of interrelated rows and columns.

*5: BI app

This software is used for visualizing and analyzing various types of data possessed by a company in order to assist management in making decisions about business and operations.

■ Author ■

Makoto HIROSAKI

Development of methods for automating the mounting/removal operations of heat treatment jigs

Suguru FURUTANI*

Summary

JATCO aims to automate all the manual operations on the CVT pulley production line for the purpose of reducing costs. However, automation of the process of loading pulleys on heat treatment trolleys has not been accomplished yet. This process includes the work of mounting and removing heat treatment jigs that are stacked in two levels. Heat treatment jigs are repeatedly put into the heat treatment furnace during mass production; the effect of repeated heating gradually increases the amount of jig deformation and bending. This makes it extremely difficult to automate the operations of mounting and removing the jigs. This article describes the development of methods that enable automatic mounting and removal even of heat treatment jigs that are greatly deformed or bent.

1. Introduction

JATCO is promoting the automation of the CVT pulley production line for the purpose of reducing costs. Figure 1 shows the production processes of the pulley line. The processes in the blue frames have already been automated; the ones in the red frames have yet to be automated and are still performed manually at present. The unautomated processes have various issues such as detection of whether pulleys are present on the trolleys and detection of trolley position deviation. Among these processes, there is an especially strong need from an ergonomic standpoint to automate the mounting/removal of heat treatment jigs in the process indicated in the double red frames. This article describes newly developed methods that automate these operations.

2. Mounting/removal of heat treatment jigs

2.1 Heat treatment jigs and heat treatment trolleys

Heat treatment jigs are made of heat-resistant alloys, and pulleys are arranged on them for transport into the heat treatment furnace. Heat treatment jigs are put into the furnace together with the pulleys. The appearance and constituent parts of a heat treatment jig are shown in Fig. 2.

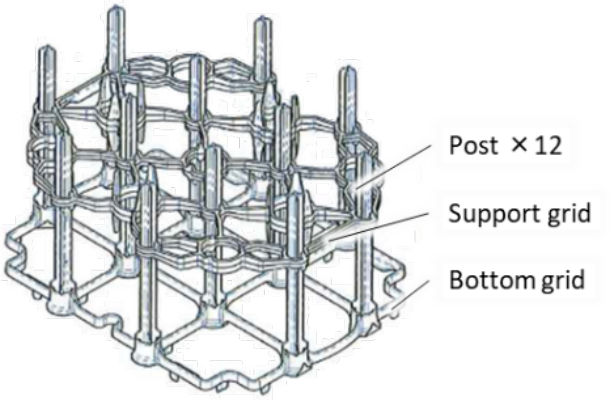

Fig. 2 Heat treatment jig

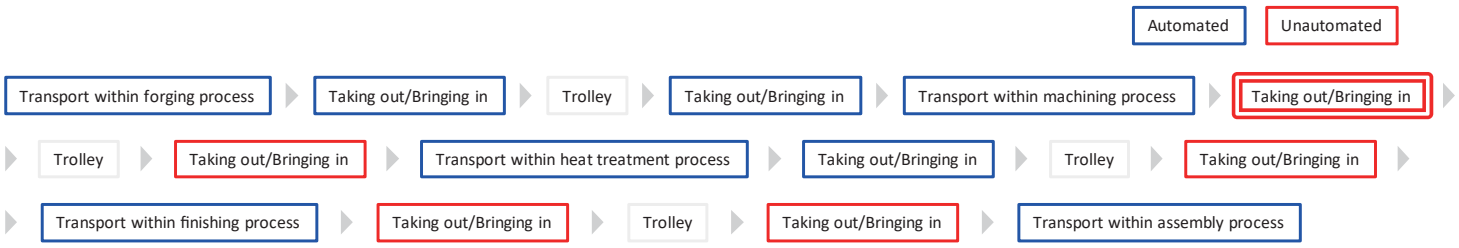

Fig. 1 Pulley production line processes

* Hardware System Development Department

A heat treatment jig consists of posts, a bottom grid and support grids. The posts are screwed to the bottom grid and the support grids are fastened to the posts. Figure 3 shows the appearance of a heat treatment trolley. The trolley is stacked with two rows and two levels of heat treatment jigs into which pulleys are loaded.

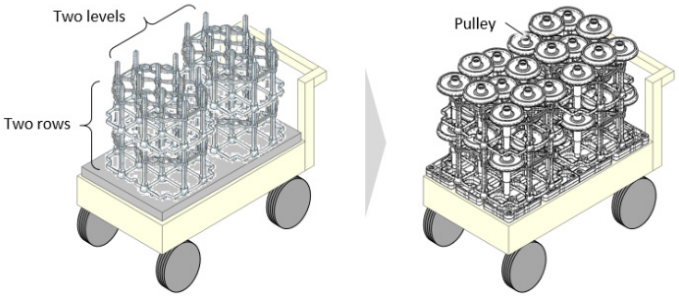

Fig. 3 Heat treatment jig trolley

2.2 Mounting/removal of heat treatment jigs

Figure 4 shows the work flow of the process for loading pulleys on a heat treatment trolley. These tasks are performed on the trolley shown in Fig. 3. A heat treatment jig has two levels stacked one above the other, so the upper level must be removed in order to load pulleys into the lower level and then remounted. These operations are repeated twice for each trolley. Because a heat treatment jig is heavy, weighing approximately 15 kg, there is a strong need to automate the work from an ergonomic perspective.

2.3 Deformation and bending of heat treatment jigs

Pulleys are heat treated to increase their surface hardness because they must function to transmit torque. Heat treatment jigs made of heat-resistant alloys also incur deformation induced by heating during the heat treatment process. The heat treatment furnace is heated to approximately 900°C in the pulley heat treatment process and then cooled. The amount of deformation induced by one heat treatment is around several tens of μm, but because heat treatment jigs are repeatedly put into the heat treatment furnace during mass production, their deformation and bending gradually become larger.

Figure 5 shows examples of heat treatment jigs that have experienced large deformation and bending. Posts show significantly large bending, with the largest bending being approximately 10 mm.

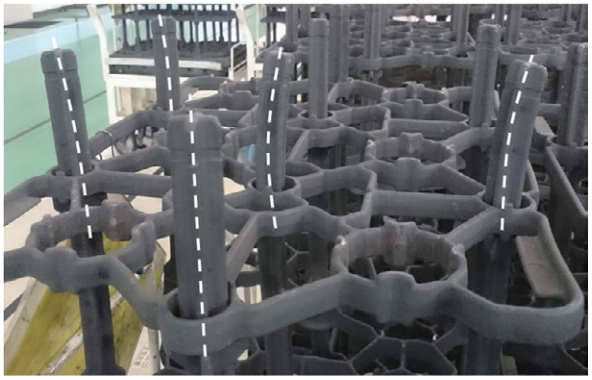

Fig. 5 Heat treatment jig

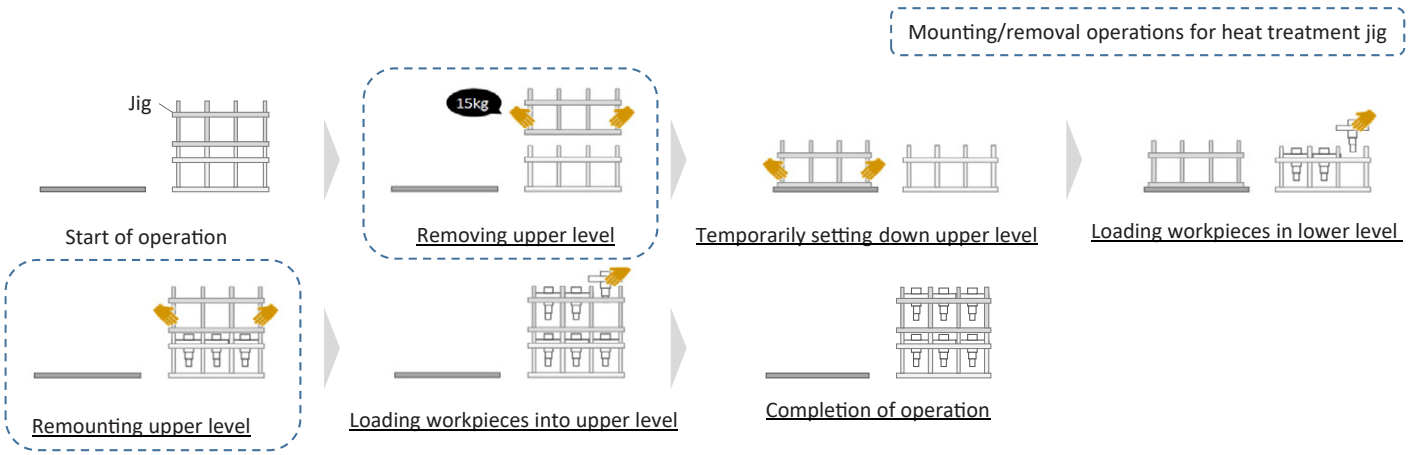

Fig. 4 Process of loading pulleys in jigs on trolleys for heat treatment

2.4 Issues in automating the work of putting pulleys into the furnace

Figure 6 shows examples of deformed and bent heat treatment jigs. Several tens of heat treatment jigs are used on the pulley production line. The amount of deformation and bending that jigs incur is not uniform for all of them.

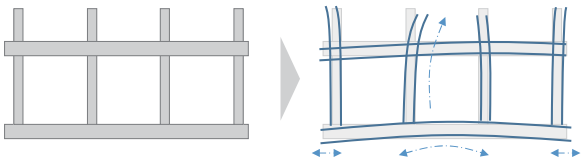

Fig. 6 Deformation/bending of heat treatment jigs

Heat treatment jigs must be clamped in order to automate the mounting/removal operations. Pneumatic cylinders are generally used to actuate clamps. Based on the configuration of the heat treatment jigs, it was assumed that the most suitable location for clamping them would be the sides of the bottom grid. However, the following problem can be cited in this regard. In case a pneumatic cylinder is used to clamp a heat treatment jig, a sensor installed in a fixed position would be used to confirm the completion of clamping. However, when the bottom grid of a greatly deformed or bent heat treatment jig is clamped, a stationary sensor would not be able to confirm the completion of clamping. It can be predicted that a clamping defect might occur (Fig. 7). This is an issue in trying to automate the work of putting pulleys into the heat treatment furnace,

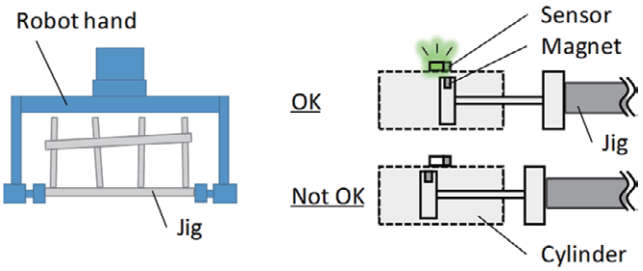

Fig. 7 General clamping system

3. Investigation of specifications

3.1 Equipment specifications

Figure 8 shows an outline of the equipment specifications.

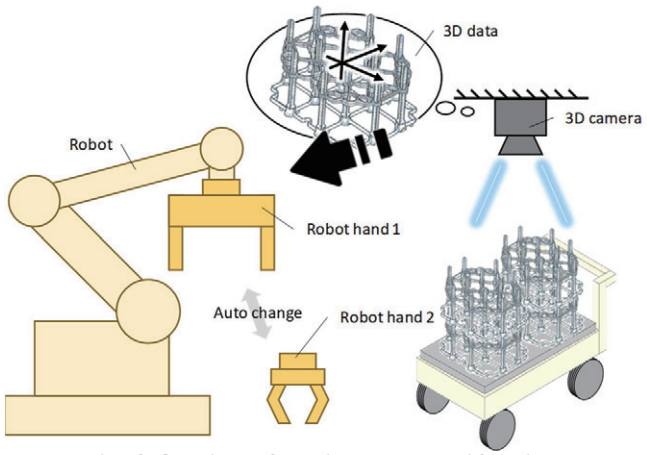

Fig. 8 Outline of equipment specifications

In this project, a study was made of equipment specifications involving the use of an articulated robot and a 3D camera. A 3D camera is capable of capturing in three dimensions the shape, position and orientation of the object being photographed. The trolley and the heat treatment jigs on it generally experience several tens of mm of positional deviation each time the trolley is changed. It was envisioned that the 3D camera would capture the positional information of the heat treatment jigs and input that information into the robot. The robot hand can approach a heat treatment jig in the space over the jig. Putting pulleys into the furnace requires a robot hand for mounting/removing heat treatment jigs and a robot hand for loading pulleys into the jigs. The equipment is fitted with a device that enables the attaching/detaching of a robot hand suitable for each task.

3.2 Investigation of a clamping system

As mentioned in section 2.4, it is obvious that general clamping systems would not be able to cope with deformed or bent heat treatment jigs. Accordingly, clamping systems were benchmarked.

Figure 9 presents the benchmarking results.

O :Good X :Poor

Clamping system	Flexibility	Load capacity	Cost	Durability
Suction	O	X	O	X
Spring	O	X	O	O
Interchangeable soft/hard gripper mechanism	O	X	X	X
Cooperative linkage mechanism	O	X	X	X
Locking cylinder	O	O	O	O

Fig. 9 Benchmarking of clamping systems

One function required of the clamping system in this project is flexibility for reliably clamping even deformed or bent heat treatment jigs. In addition, it must have the load capacity to transport heavy heat treatment jigs weighing 15 kg apiece. Moreover, cost and durability are also important indices for application to mass production. Based on these perspectives, it was reasoned that a locking cylinder would be best suited for the clamping system.

Figure 10 shows an outline of a locking cylinder. A locking cylinder has a mechanism for holding the rod at the position where the cylinder stops. Unlike ordinary cylinders, there is no need for a locking cylinder to stop at a pre-determined position, so it can clamp a heat treatment jig by following the jig's shape.

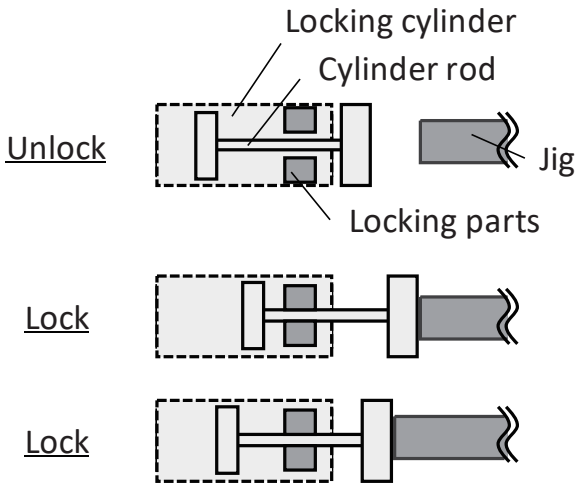

Fig. 10 Locking cylinder

3.3 Investigation of robot hand specifications

Figure 11 illustrates the concept of clamping the bottom grid of a heat treatment jig using a locking cylinder.

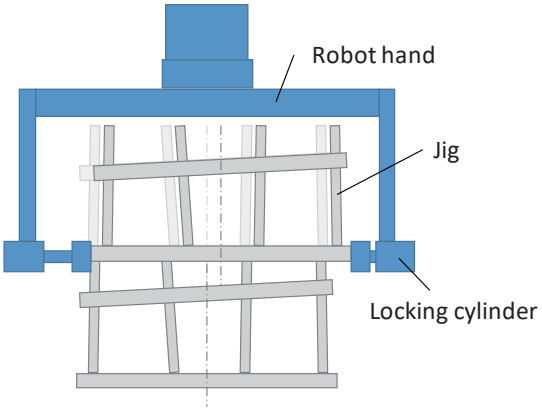

Fig. 11 Clamping system using a locking cylinder

A locking cylinder is characterized by continuing to move forward to its full-stroke position so long as a certain level of reaction force is not applied to it. Accordingly, it might shift the position of the upper level of the heat treatment jig when clamping the bottom grid. This means that it would not be able to reproduce the position for remounting the upper level. Therefore, a study was made of a clamping system capable of following the shape of the heat treatment jig while keeping the jig stationary. Figure 12 illustrates this clamping method.

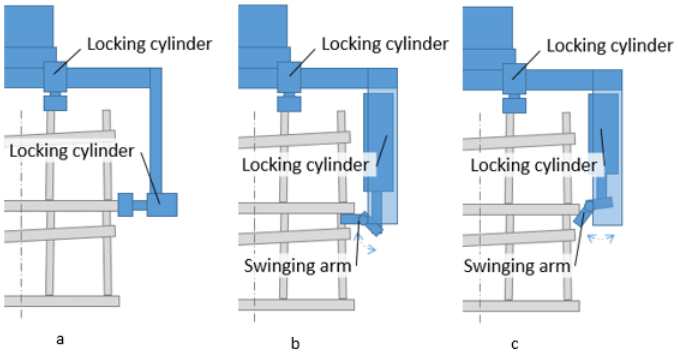

Fig. 12 Clamping method

To keep the heat treatment jig stationary, first, the upper level of the jig is pressed against the lower level. The adoption of a locking cylinder is also advantageous here because it can accommodate deformed posts. The "post holding device" attached to the front end of the cylinder was designed with a size that can handle deformed or bent posts at the time a heat treatment jig is removed.

Next, the bottom grid is clamped. There was concern that if the grid was clamped horizontally, the clamping force might be insufficient against inertial force during transport and a heat treatment jig might fall down. To prevent that, a specification was devised for sandwiching jigs from above and below by adopting a swinging arm, as shown in Fig. 12-b. However, because the swinging arm would interfere with the heat treatment jig at the lower level, clamping would be impossible. Accordingly, to avoid that interference, a method was devised for pushing the swinging arm diagonally by offsetting its fulcrum (Fig. 12-c). It was reasoned that this would not only avoid interference, it would also prevent positional deviation vertically and laterally. Figure 13 shows a 3D model of the robot hand that was designed on the basis of the proposed methods.

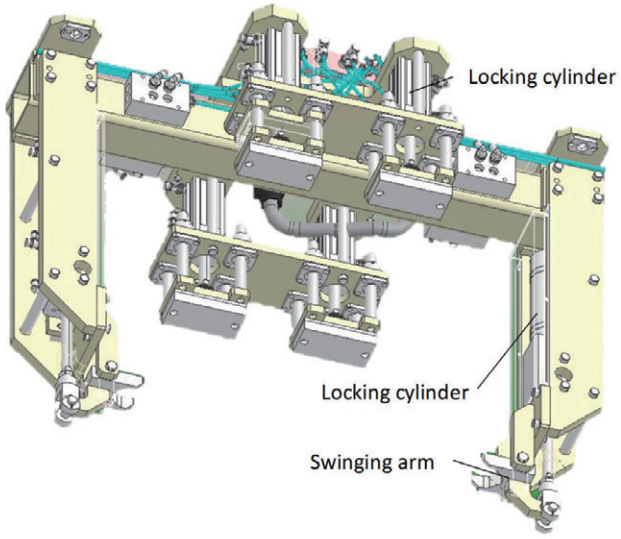

Fig. 13 Robot hand

3.4 Investigation of heat treatment jig specifications for temporary upper level removal

An investigation was made of the operation of "temporarily removing the upper level" shown in Fig. 4. In order to automate this operation, after the robot hand removes the upper level of the heat treatment jig, the hand must be switched to the robot hand for loading pulleys into the lower level of the jig. At that time, as shown in Fig. 14-a, temporarily setting down the heat treatment jig and the robot hand separately might cause their positional relationship to deviate, making it impossible to reproduce the position for remounting the upper level of the jig. Therefore, a method was devised for temporarily setting them down together in a state with the robot hand clamping the heat treatment jig (Fig. 14-b). That was accomplished by using the characteristic of the locking cylinder that it locks when the air supply is stopped. This method makes it possible to suppress any deviation in the positional relationship when temporarily removing the upper level of the jig.

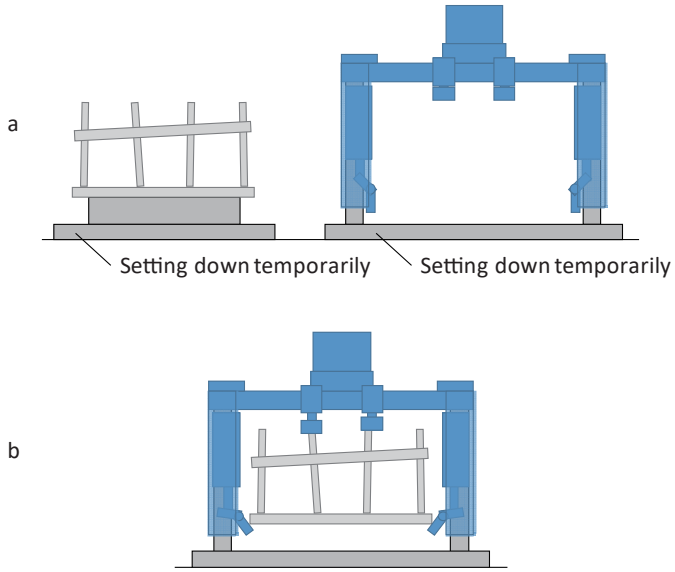

Fig. 14 Specification for temporarily setting down heat treatment jig

4. Application to mass production

Equipment was designed and built to achieve the devised methods and installed on the pulley production line to conduct a mass production trial. Figure 15 shows the appearance of the equipment installed on the pulley production line. The trial was conducted using multiple heat treatment jigs having different amounts of deformation and bending. The results confirmed that even heat treatment jigs with various amounts of deformation and bending were clamped stably. All operations of the pulley input process were automated including jig removal and remounting, thus achieving successful application to mass production.

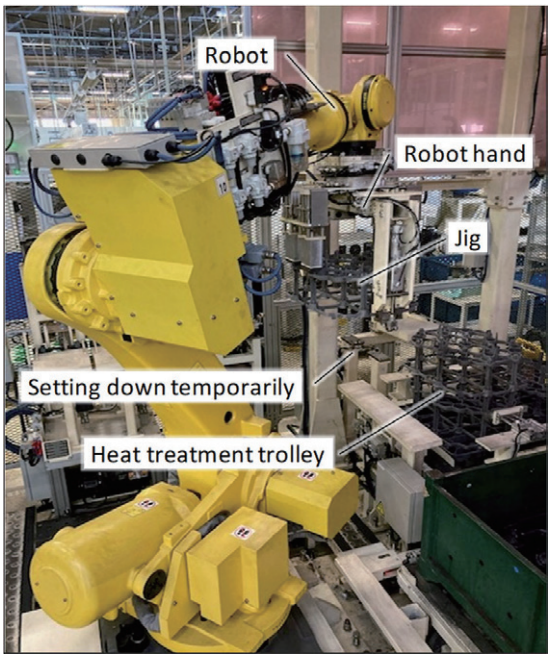

Fig. 15 Appearance of equipment

5. Conclusion

The development of the methods described here has made it possible to automate the operations of mounting/removing heat treatment jigs having large amounts of deformation or bending. As a result, this eliminates the manual work of handling heavy heat treatment jigs when putting them into the furnace, thereby reducing costs and improving the work environment.

The equipment installed in this project was developed for use on the pulley production line, but it is also applicable to the gear production line as well as to jigs. It is planned to use these methods in the future to achieve further cost reductions and work environment improvements.

■ Author ■

Suguru FURUTANI

Countermeasure against black scale residue by defining conditions for detecting the groove for start of machining of roller grooves on CVT pulleys

Naoki HAMAGUCHI* Kazuki KOTANI* Masahiro NAKAGAWA** Takefumi YAMAMOTO** Makoto HIRATA**

Summary

The fixed secondary pulley half of a continuously variable transmission (CVT) for vehicle use has three grooves called roller grooves for sliding the movable pulley half smoothly in the axial direction. In the initial period following production launch, a black scale residue occurred on one side of some of the roller grooves, causing a chronic problem.

This article describes a study conducted to visualize and validate the effect of the machining allowance on the positional relationship between shaft outer diameter runout and roller grooves. Detection of roller groove positions and newly measured values of shaft outer diameter runout were combined to create a countermeasure for resolving the occurrence of the black scale residue.

1. Introduction

A black scale residue on the roller grooves of the fixed half of the secondary pulley refers to an unmachined material that remains because grinding cannot be done owing to unbalanced or absence of machining allowance on the right and left shoulders of the roller grooves due to outer diameter runout of the workpiece shaft. A black scale residue can occur even if the split angle, curve (R), contact angle and over ball diameter (OBD) of the three grooves are machined completely within the standard.

2. Overview of black scale residue on roller grooves

2.1 Outline of pulley machining processes and roller groove machining

The black scale residue on the fixed secondary pulley half and the pulley machining processes are shown in Figs. 1-1 and 1-2, respectively.

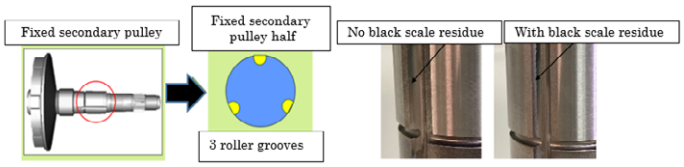

Fig. 1-1 Diagram of fixed secondary pulley half and appearance of black scale residue

After raw material machining, heat treatment and curve correction, center hole correction is performed as the first process of finishing machining. Roller grooves are ground in a subsequent process.

In the roller groove grinding process, the roller grooves on the shaft outer circumference are detected with a proximity indexing sensor. The center of the roller grooves is determined and the first groove is machined.

The remaining two groves to be machined are executed at 120° divisions from the position of the first groove (Fig. 2). Because the position of the grooves may be misaligned relative to the position of the grinding wheel, the machining allowance becomes unbalanced, causing unmachined scale to remain.

* Production Section No.2 Yagi ** Engineering Management Department

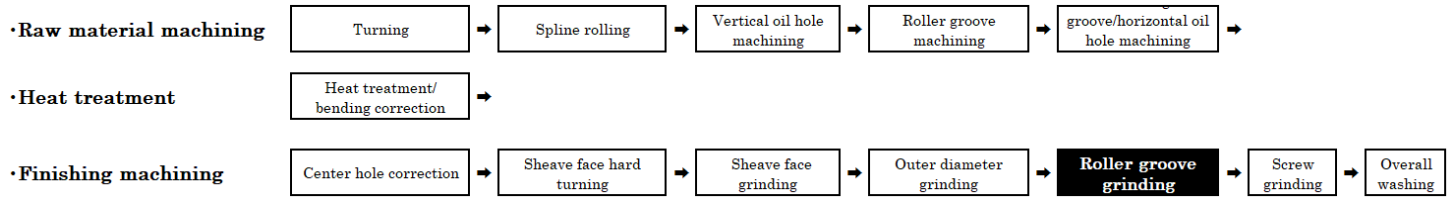

Fig. 1-2 Diagram of machining processes

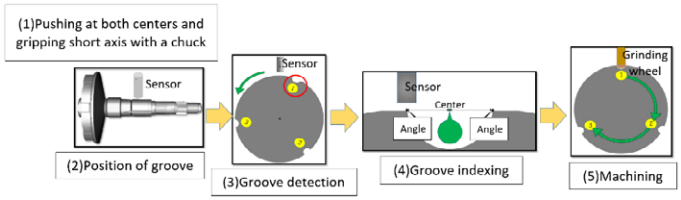

Fig. 2 Indexing motion for machining roller grooves

2.2 Relationship between workpiece outer diameter runout and black scale residue on roller grooves

Shaft outer diameter runout was investigated for workpieces that displayed the black scale residue on the roller grooves. The results revealed that the defect rate was 90% or more for workpieces with large runout.

A test was conducted to reproduce the black scale residue for workpieces displaying large shaft outer diameter runout. It was found that there were workpieces on which the black scale residue occurred and those where it did not occur.

2.3 Relationship of eccentricity between machine center and workpiece center

It was found that workpieces displaying the black scale residue had the following characteristics (Fig. 3).

(1) Large shaft outer diameter runout.

(2) The phase of the maximum convex portion or minimum concave portion of shaft diameter runout was close to the phase of the roller groove position.

(3) Eccentricity was caused by the effects of heat treatment distortion and the center correction performed in the first finishing process.

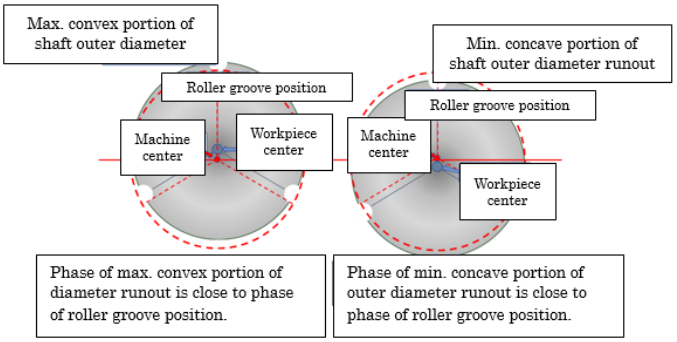

Fig. 3 Positional relationship between shaft outer diameter runout and roller groove

Figure 4 shows the results of the investigation of workpieces for which the phase of the maximum convex portion of shaft outer diameter runout and the phase of the roller groove position were close. Designating the groove where the phases were close as the 0-deg. groove, grooves were defined as the 120-deg. groove and the 240-deg. groove in the clockwise direction.

- The black scale residue did not occur on workpieces machined from the 0-deg. groove, as shown in the top row in the figure.
- The black scale residue occurred at the 240-deg. groove for workpieces machined from the 120-deg groove, as shown in the middle row in the figure.
- The black scale residue occurred at the 120-deg. groove for workpieces machined from the 240-deg. groove, as shown in the bottom row in the figure.

For workpieces displaying the black scale residue, eccentricity occurred between the workpiece center position and the machine center position owing to the effect of outer diameter runout of the workpiece shaft. In cases where the position of the phase of the maximum convex portion or the minimum concave portion of the

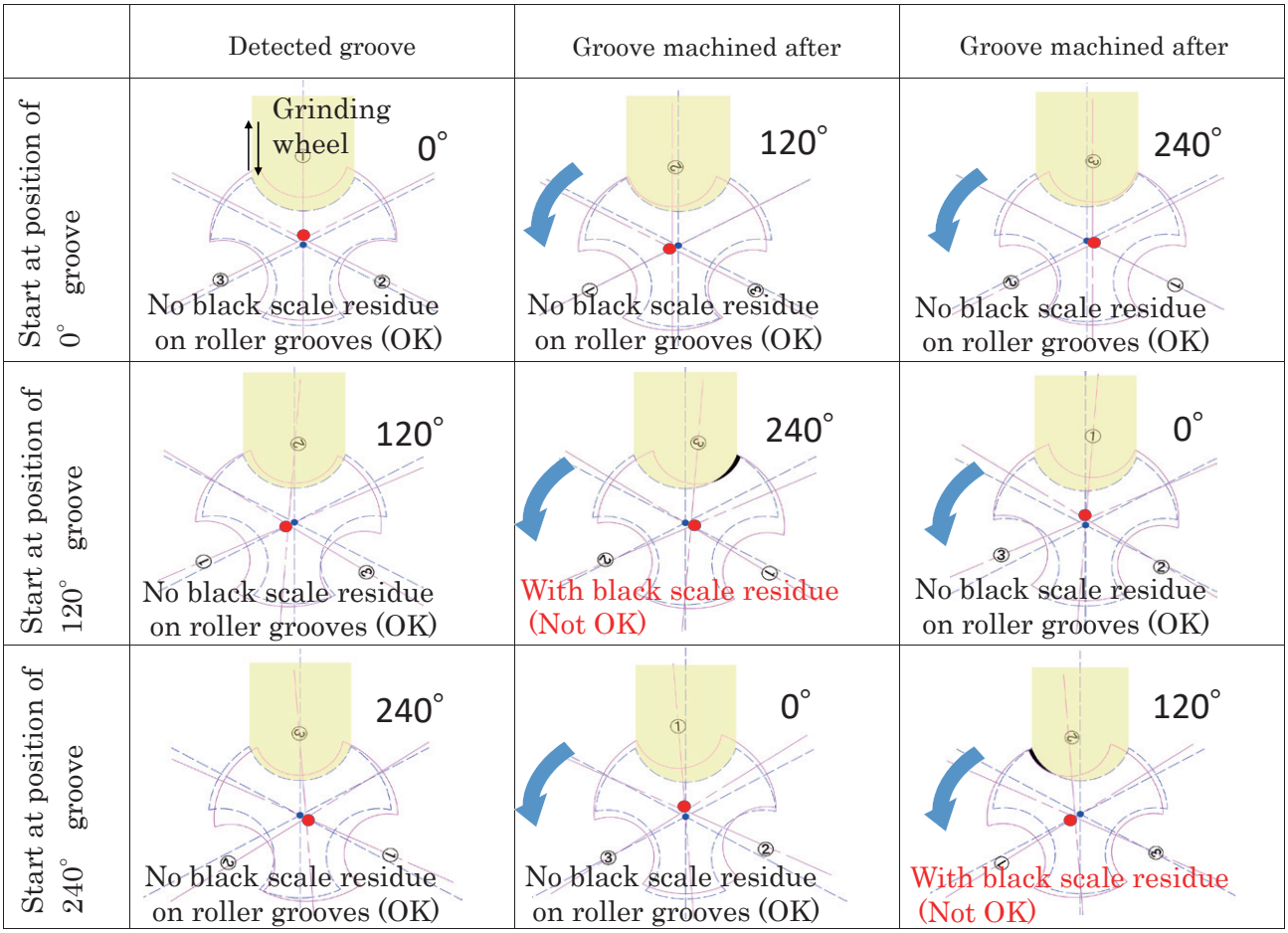

Fig. 4 Validation diagram of misalignment when roller groove is at maximum runout point

runout amount was close to the phase of the roller groove position, it was found that misalignment of the roller grooves increased when machining began at any groove other than the 0-deg. groove.

3. Analysis of mechanism causing black scale residue on roller grooves

3.1 Analysis of roller groove misalignment and black scale residue

Roller groove misalignment was compared for cases where the phases of the roller grooves and the maximum convex portion or minimum concave portion of the runout amount were close and cases where they were distant. In order to investigate if the amount of misalignment became minimum when the phases were close, an equation was formulated based on the related elements for calculating the machining allowance on the right and left roller groove shoulders (Fig. 5).

The related elements refer to the reference shaft diameter, shaft outer diameter and runout amount (concave and convex), roller groove OBD, roller groove position and split angle.

The method of calculating the machining allowance is to find the difference between the intersection of the reference roller groove circle (2) and the reference outer diameter circle (1) and the intersection of the pre-machined roller groove circle (3) and the outer diameter circle (4) at the time runout occurs. Positive coordinates are for the right shoulder machining allowance and negative coordinates are for the left shoulder machining allowance.

The amount of roller groove misalignment was calculated from these machining allowances.

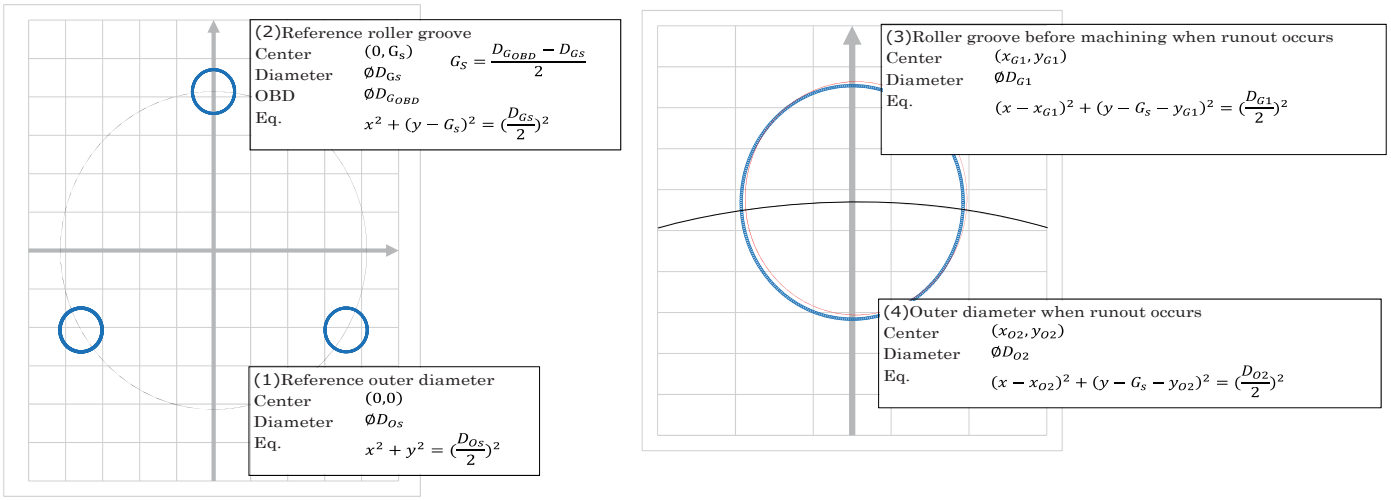

Calculation equation on right shoulder (mm)

$$= x_{S1} - x_{G1} - D_{G1}\cos\left\{\tan^{-1}\left(\frac{y_{O2} - y_{G1}}{x_{O2} - x_{G1}}\right) + \cos^{-1}\left(\frac{(x_{O2} - x_{G1})^2 + (y_{O2} - y_{G1})^2 + {D_{G1}}^2 - {D_{O2}}^2}{D_{G1}\sqrt{(x_{O2} - x_{G1})^2 + (y_{O2} - y_{G1})^2}}\right)\right\}$$

Calculation equation on left shoulder (mm)

$$= -x_{S2} + x_{G2} + D_{G1}\cos\left\{\tan^{-1}\left(\frac{y_{O2} - y_{G1}}{x_{O2} - x_{G1}}\right) - \cos^{-1}\left(\frac{(x_{O2} - x_{G1})^2 + (y_{O2} - y_{G1})^2 + {D_{G1}}^2 - {D_{O2}}^2}{D_{G1}\sqrt{(x_{O2} - x_{G1})^2 + (y_{O2} - y_{G1})^2}}\right)\right\}$$

Fig. 5 Calculation equation for machining allowance on right/left shoulders and relate elements

3.2 Validation of machining allowance calculation equation and black scale residue

The calculation equation was used to determine if roller groove misalignment became minimum in cases where the phase of the maximum convex portion or minimum concave portion of the runout amount was close to the phase of the roller groove position. That was done as shown in the phase diagram of the roller grooves and outer diameter runout in Fig. 6 by defining the maximum convex portion and minimum concave portion of the outer diameter runout amount at every 30° from 0°.

- The validation results were identical for 0° and 60° because these positions are on the axis of the roller grooves.
- The validation results were the same for 30° and 90° because these positions are 30° from the roller groove position.

Based on the foregoing results, validation was performed at the positions of 0° and 30°.

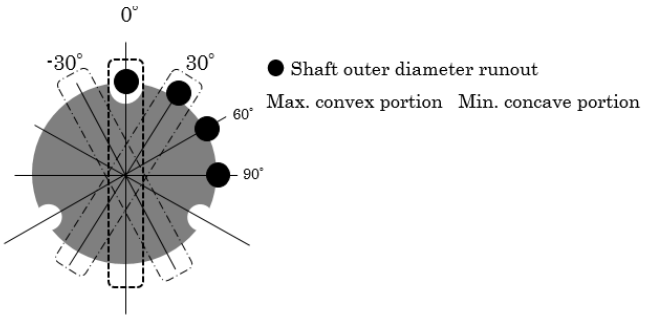

Fig. 6 Phase diagram of roller grooves and shaft outer diameter runout

The vertical axis of the graph in Fig. 7-1 is the amount of misalignment of the roller groove position found by CAD software and the horizontal axis shows the amount of roller groove misalignment calculated with the calculation equation. Good agreement is seen between the two sets of results.

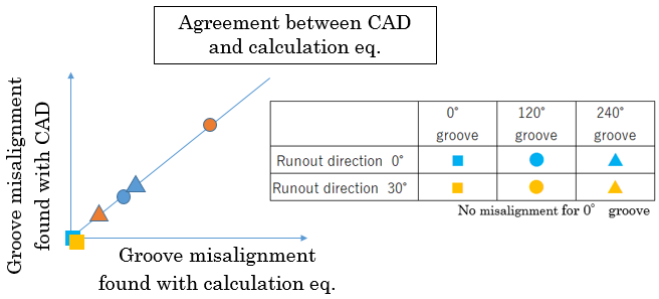

Fig. 7-1 Validation of misalignment found with CAD and with calculation equation

The vertical axis of the graph in Fig. 7-2 is the amount of roller groove misalignment found with the calculation equation. The upper level of the horizontal axis shows the angles of the maximum convex portion and minimum concave portion of the outer diameter runout amount, and the lower level indicates the groove for the start of machining.

The results reveal that misalignment becomes the smallest if machining starts from the 0-deg. groove when the phase is 0°. Misalignment also decreases if machining starts from the 0-deg. groove when the phase is 30°.

Accordingly, if machining starts from the 0-deg groove, misalignment becomes minimum for both the 0° and 30° phases, making it possible to suppress the occurrence of the black scale residue.

4. Countermeasure and effect

4.1 Machining start groove and construction of a detection method

A program was constructed for using the first detected groove as a reference for measuring shaft outer diameter runout. The roller groove in the region of the maximum convex portion or the minimum concave portion of shaft outer diameter runout is automatically detected and machining starts from that groove.

The groove for the start of machining is specified, and machining begins from the groove where the phases of the roller groove and the maximum convex portion or minimum concave portion of the diameter runout amount are the closest. This method suppresses misalignment, making it possible to suppress the occurrence of the black scale residue (Fig. 8).

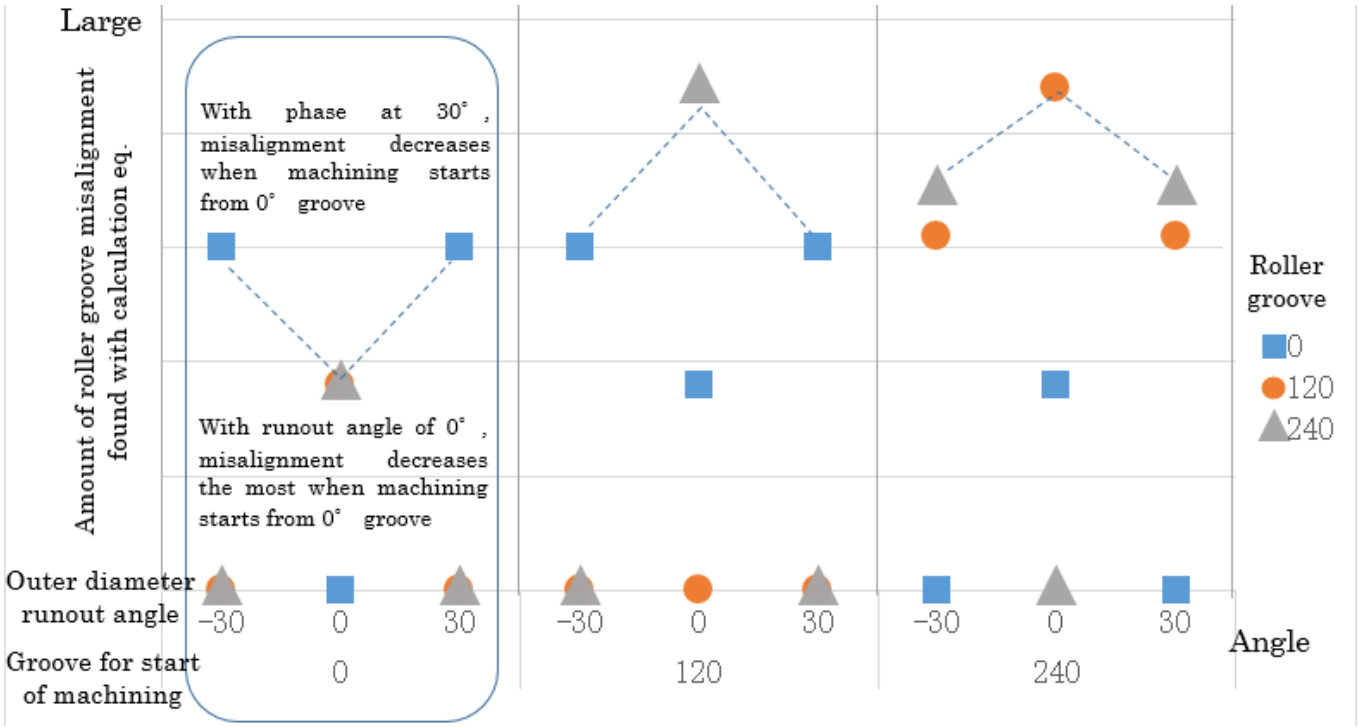

Fig. 7-2 Validation of risk for occurrence of black scale residue

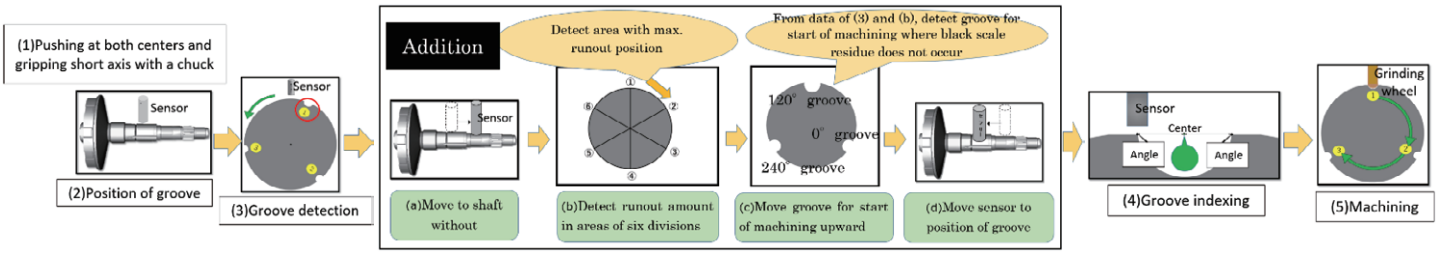

Fig. 8 Indexing motion after addition of actions for specifying groove for start of machining

4.2 Improvement effect

Since the implementation of the program for automatically detecting the groove for the start of machining prior to roller groove grinding, the previous occurrence of chronic black scale residue defects has been reduced to zero.

The operation delay due to the addition of the automatic detection program has been compensated for by shortening the cycle time.

5. Conclusion

Misalignment of each roller groove in relation to the start of machining at different grooves was calculated with an equation and compiled into a chart. This resulted in clarification of the mechanism causing the black scale residue on the roller grooves.

The adoption of the program for specifying the groove for the start of machining resulted in an effective measure for preventing the occurrence of the black scale residue.

■ Authors ■


Naoki HAMAGUCHI


Kazuki KOTANI


Masahiro NAKAGAWA


Takefumi YAMAMOTO


Makoto HIRATA

Development of an application for analyzing vehicle sounds

Satoshi SAITOH*　Tsuyoshi ENDO*

Summary

Analyses of worrisome sounds occurring in vehicles are not widely conducted by the general public because they require specialized equipment and software. Accordingly, it was hypothesized that using a smartphone would enable anyone to analyze sound data easily. An application has been developed that can automatically analyze sound data recorded in the videos which contains the dashboard gauges movement obtained with a smartphone. An application has been developed that can automatically analyze sound data and dashboard instrument videos obtained with a smartphone.This article describes the activities undertaken to develop this application.

1. Introduction

When drivers hear a worrisome sound in their vehicles while driving, they may take their vehicles to the nearest car dealer because they want to get advice or have some improvement made. A technician at the dealer where the vehicle is brought determines the source of the indicated sound and implements a measure to improve the problem if the vehicle owner so desires. However, there are often cases where it is very hard to determine the sound source because sound analysis involves an extremely high degree of difficulty.

In such cases, the dealer technician may use a voice recorder or some similar device to record the sound in question and then sends the sound data to the vehicle manufacturer's service center to get advice.

An engineer at the service center who receives the inquiry analyzes the sound data in place of the dealer technician. If the engineer has a clue about the sound source, that information is conveyed back to the dealer technician. However, like the dealer technician, there are cases when service center engineers also have a hard time determining the sound source based solely on the sound data received.

In order to resolve such problems, we have developed an application that makes it easy to determine sound sources even for people who are not sound specialists. This article describes the development activities that were undertaken.

2. Difficulty of sound analysis

What is the inherent difficulty in sound analysis? The difficulty lies in representing sound visually. The conventional approach to visualizing sound is to first conduct a fast Fourier transform (FFT) analysis of the sound data. After the FFT analysis, a spectrogram is then drawn based on the data obtained (Fig. 1).

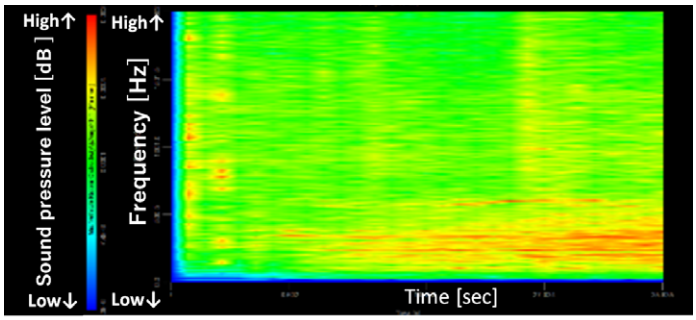

Fig. 1 Spectrogram analysis

The horizontal axis of a spectrogram represents time, the vertical axis shows the frequency, and the shades of color express sound pressure levels. Drawing a spectrogram provides the following benefits.

- The frequency of the indicated sound can be confirmed.
- The change in the frequency with time can be confirmed.

* Quality Assurance Department, JATCO Engineering Ltd

In addition, if engine speed data and vehicle speed data have been recorded simultaneously with the sound data, a rotational order ratio analysis can also be performed.

As mentioned here, many benefits can be obtained by conducting an FFT analysis and drawing a spectrogram. However, performing such analyses generally requires specialized devices, software and knowledge of sound, and for that reason they are not widely conducted at present.

3. Determinable range by visualization

Let us assume that a service center received over 100 inquiries about sounds during the past one year and that the sounds recorded at car dealers were visualized at the center. An investigation was made of the extent to which sound sources could be determined at the service center.

As the results in Fig. 2 show, it was estimated that sound sources could be determined based on only a spectrogram in approximately 21% of the total number of cases. If engine speed data and vehicle speed data can be viewed simultaneously with the spectrogram, the percentage of cases in which it is estimated sound sources can be determined increases further by approximately 37%. Adding the two percentages together, the results reveal that sound sources are determinable at service centers in approximately 58% of the cases.

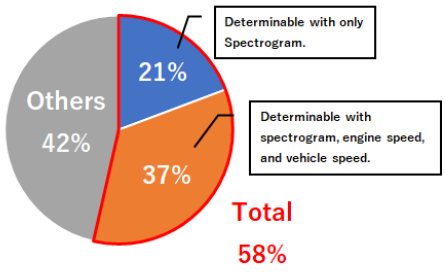

Fig. 2 Breakdown of sound sources determinable by visualization

Development activities aimed at the two objectives below were carried out for the purpose of enabling sound source determination at service centers 58% of the time.

- Establishment of a method for obtaining engine speed data, vehicle speed data and sound data simultaneously
- Development of an application enabling simple visualization of sound data

4. Investigation of a recording tool

4.1 Definition of the requirements for a data recorder

The following requirements were defined for a data recorder in order to achieve the objective of establishing a method for simultaneously obtaining engine speed data, vehicle speed data and sound data.

- Inexpensive
- Capable of simultaneously obtaining engine speed data, vehicle speed data and sound data
- Capable of recording sounds in a frequency range of 300 Hz to 8 kHz, which is required for measurement of vehicle noise and vibration

4.2 Selection of a recording tool

It was decided to use a smartphone as the recording tool for satisfying the requirements listed above. A major advantage of using a smartphone is that it eliminates the need to buy a new device because smartphones have already penetrated society widely in general. Accordingly, it would substantially reduce the cost of purchasing a recording tool.

In addition, simultaneous recording of engine speed data, vehicle speed data and sound data can be accomplished by taking videos of the dashboard instruments within the photographable range of a smartphone camera (Fig. 3). This is another major reason why a smartphone was selected as the recording tool.

Fig. 3 Simultaneous recording of engine speed, vehicle speed and sound data

With regard to recording capability, the microphone built into smartphones usually has a recording frequency range of approximately 100 Hz to 10 kHz. This is narrower than the frequency range of the microphones used by vehicle manufacturers and others, which is typically 20 Hz to 20 kHz. However, this frequency range of approximately 100 Hz to 10 kHz is equal to the level of the voice recorders used by car dealer technicians. Moreover, because the frequency bandwidth required for measuring vehicle noise and vibration is around 300 Hz to 8 kHz, it was judged that smartphones could be used as the recoding tool without any problem.

5. Application development

5.1 Definition of application requirements

The following requirements were defined for the application in order to achieve the objective of developing an application enabling simple visualization of sound data.

- Easy to operate
- Allowing simultaneous viewing of a spectrogram and a vehicle instrument video
- Linking of the spectrogram cursor and the video playing time
- Enabling a comparison of spectrograms of recorded sound data and sample sound data
- Enabling a comparison of auditory perceptions of recorded data and sample sounds

The specifications were determined based on the requirements listed above, and the application was then developed.

5.2 Development of the application

A desktop application that runs on a PC was adopted in consideration of screen visibility and ease of operation (Fig. 4). In addition, usability was improved by adopting specifications that allow all operations to be performed automatically, from FFT analysis to drawing of a spectrogram by just dragging and dropping photographed videos onto the application.

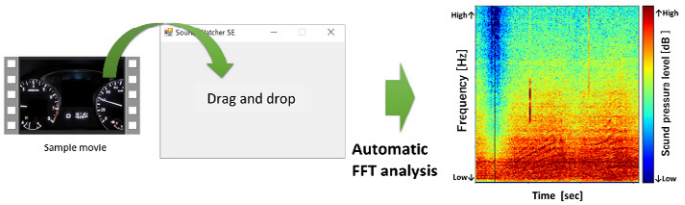

Fig. 4 Application for automatic FFT analysis

The design adopted for the user interface positions the spectrogram on the left side of the screen and a video taken with a smartphone on the right side. This allows an analysis to be conducted while constantly comparing vehicle behavior and the spectrogram (Fig. 5).

Moreover, the cursor is positioned such that it moves over the spectrogram in concert with the playing time of a video, making it easy to confirm the moment when a sound occurs.

Thanks to these measures, the frequency of the sound of interest can easily be confirmed based on the shades of color and the time when the sound occurs.

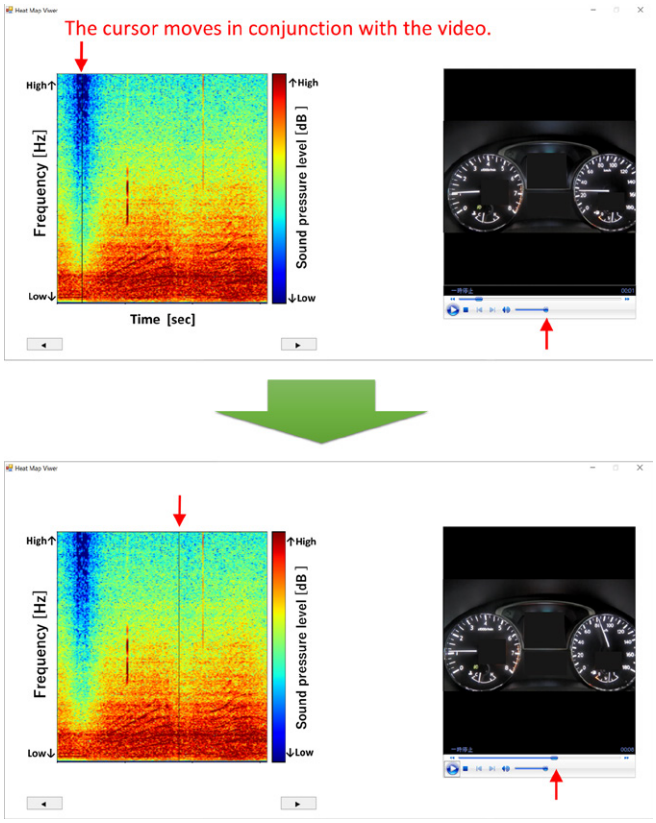

Fig. 5 Movement of spectrogram cursor linked to video of vehicle instruments

The application also incorporates sample images of past data appended with additional information such as sound sources, frequencies, sound magnitude, onomatopoeia, and characteristic visual aspects of spectrograms, among other things.

This makes it easier to narrow down sound sources by comparing the spectrogram of the sound recorded at a car dealer with the sample images already incorporated in the application in advance (Fig. 6).

Comparing frequencies and other information in addition to characteristic visual aspects of spectrograms enables judgment of sound sources with even higher accuracy.

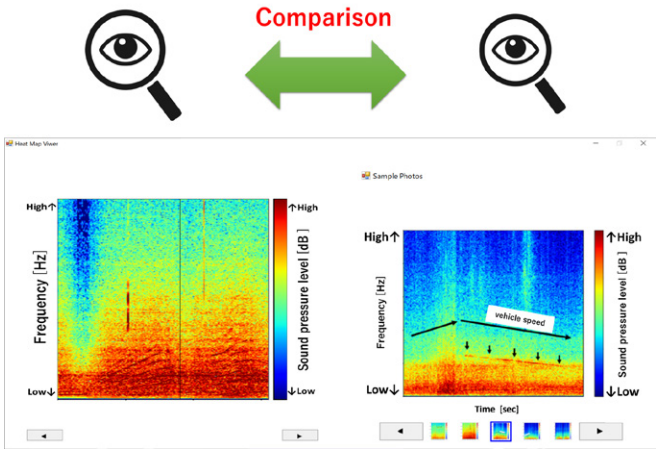

Fig. 6 Comparison of recorded data and previous data

Because sample sounds can be heard in addition to seeing sample images, auditory judgments can also be added to visual judgments. This is another factor that improves judgment accuracy (Fig. 7).

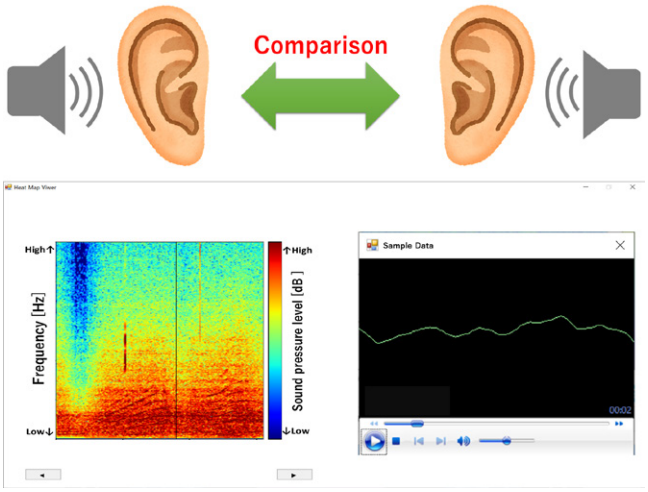

Fig. 7 Comparison of recorded sound and sample sound

6. Conclusion

Conventional FFT analysis has required specialized equipment and software. However, the newly developed application uses a smartphone as the recording tool and automatically analyzes videos taken with the smartphone camera. Consequently, this application enables determination of over 50% of the sound sources which could not be identified heretofore at vehicle service centers. Going forward, we will continue our development activities with the aim of developing a tool that will automate even the final judgment of sound sources.

■ Authors ■

Satoshi SAITOH

Tsuyoshi ENDO

AI-based metallographic determination

Tomoya SUZUKI*

Summary

Metallographic examinations are essential for confirming the performance of metal parts. However, examination results varied depending of the proficiency of the examiner because the complexity of the examination details requires sufficient experience. Therefore, a tool was made for classifying metallographic structures using artificial intelligence (AI) for the purpose of assisting the determination of iron-based metallographic structures. This article describes the AI-based tool that has been confirmed to be effective to a certain extent in classifying metallographic structures.

1. Introduction

Metallographic examinations are essential for confirming whether the metal parts of products like continuously variable transmissions (CVTs), automatic transmissions (ATs) and production equipment satisfy the performance intended by their design. This is especially true for ferrous metals. Metallographic examinations involve specimen preparation, observation and structure determination. However, metallographic structures change in complex ways depending on the type of material, processing conditions and heat treatment conditions, among other factors. Since sufficient experience is required for the examiners, variation of determination result occur depending on the proficiency of the examiners.

This article reports the activity of tool preparation for classifying eight types of metallographic structures using AI for the purpose of assisting the determination of iron-based metallographic structures.

2. Present situation

The procedure and details of a metallographic examination are shown in Fig. 1. The specimen preparation processes for a metallographic examination consist of sectioning, embedding, polishing and etching. Finally, a prepared specimen undergoes microscopic observation for determining the microstructure. Technical skill is required for polishing and etching and metallographic determination requires knowledge.

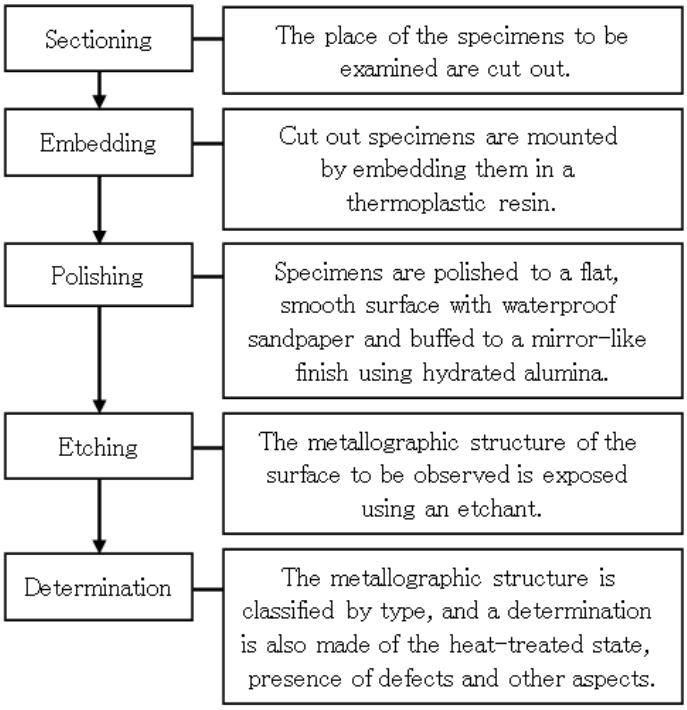

Fig. 1 Metallographic examination procedure and descriptions

The knowledge needed especially for determination requires visual experience. Variation of determination results stemming from insufficient examination experience is an issue. It is also an issue in harmonizing the determination level of metallographic examinations at each testing site including those overseas.

The following two points concern factors causing variation.

*Quality Assurance Department, JATCO Engineering Ltd

1) Factors originating in the images themselves such as scratches occurring during polishing and etchant bleeding caused by insufficient washing.
2) Factors originating in the examiner's experience with the classification of metallographic structures at the time a determination is made.

2.1 Influence of polishing and etching

First, regarding point 1), polishing and etching are critical procedures for the subsequent determination. Proper processing of specimens leads to an accurate determination.

Insufficient polishing gives rise to scratches and unevenness. Excessive or deficient etching as well as insufficient washing can cause etchant bleeding.

These phenomena affect the subsequent determination.

2.2 Classification of metallographic structures

With regard to point 2), the state of metallographic structures changes depending on the type of material and the processing and heat treatment conditions. Consequently, a specimen may look different from general samples of metallographic structures, rendering classification difficult and causing an incorrect determination.

As a typical example in this regard, Fig. 2 shows differences in the general appearance of sorbite.

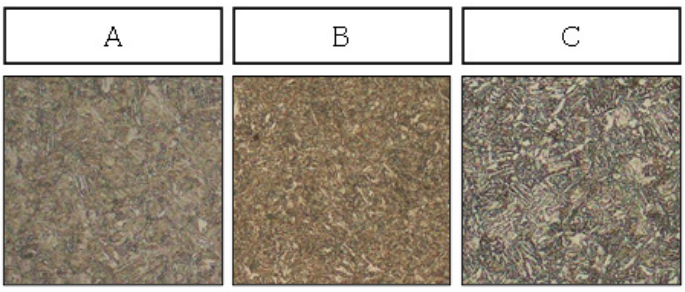

Fig. 2 Metallographic structure of sorbite

3. Preparation of a tool for classifying metallographic structures

In consideration of the factors mentioned in chapter 2 above, it is necessary to classify images of metallographic structures correctly in order to make proper determinations. There are various measures for preventing incorrect determinations, such as making a memo of points requiring attention or preparing a large volume of sample images. However, all of them depend to a large extent on the experience of the examiner.

Therefore, a heat-treated structure was taken as an example in this study in an effort to prepare a tool for automatically classifying if the metallographic structures captured in images are martensite or sorbite.

An examination of various automation methods, including different image processing and logic creation procedures, revealed that making such a tool would involve a high level of difficulty.

Further investigation indicated that automation would be possible by using AI. It was decided to adopt AI because it would involve fewer procedures than the methods mentioned above and provide a higher degree of versatility.

It was envisioned that users of the tool would be examiners having around one or two years of experience with metallographic examinations.

4. Selection of images for training the AI-based tool

Since one examiner would perform all the processes involved in a metallographic examination of a specimen. In order to enable metallographic structures to be classified correctly, low-quality images were also included in training the AI-based tool in consideration of the uncertain elements present at the time of specimen preparation.

Figure 3 shows typical examples of uncertain elements present when specimens are prepared. If the AI-based tool were taught only high-quality images of specimens prepared by proficient examiners, it would not be able to correctly classify actual low-quality images.

Taking scratches as an example, a high-quality image has few scratches while a low-quality image has many scratches. The lower the quality of the image, the more the accuracy rate of the tool would decline.

It was necessary to give the tool versatility by training it both high- and low-quality images so that it would be able to classify even images of poor quality.

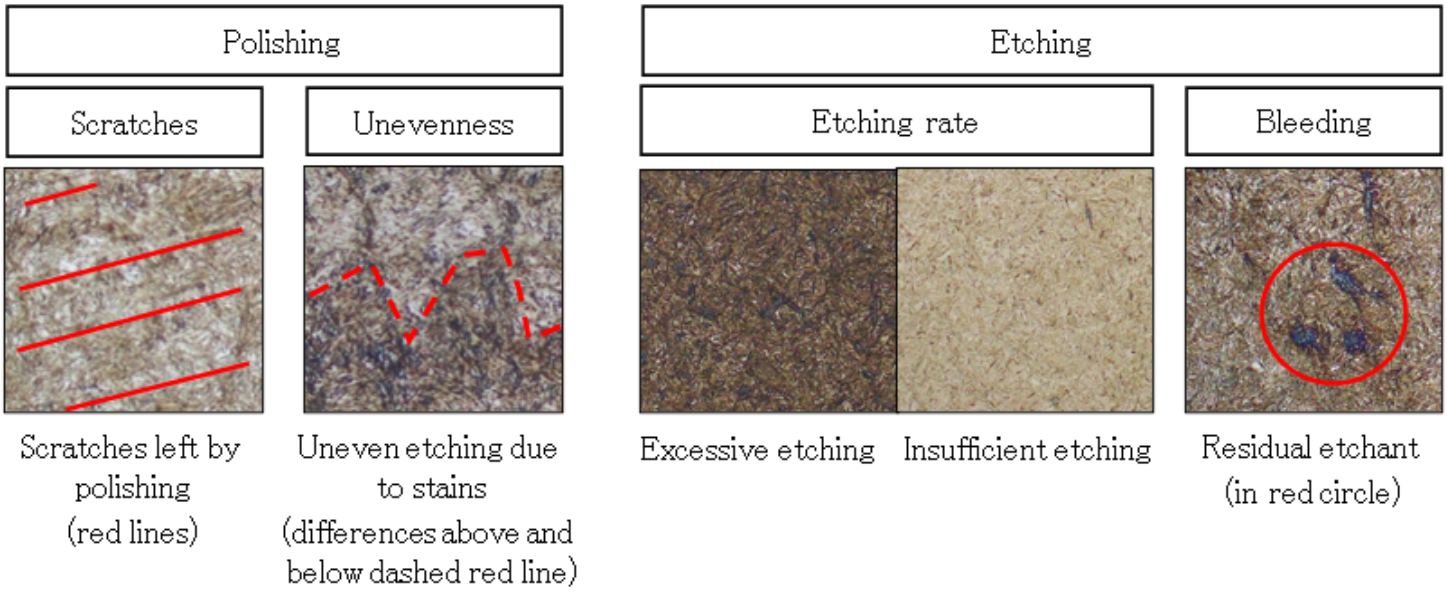

Fig. 3 Typical uncertain elements at the time of specimen preparation

4.1 Scratches

Scratches are often caused by insufficient polishing, among other factors. Images containing scratches were also included with the aim of enabling the tool to classify even images with scratches.

4.2 Unevenness

Unevenness can occur during etching due to insufficient polishing or insufficient washing. The occurrence of unevenness and its degree can vary depending, for example, on the material of the specimen. Therefore, to target materials which unevenness is apt to occur, used images which for containing unevenness for training. The aim was to enable the tool to classify even images in which unevenness is partially shown.

4.3 Etching degree

Etching gradations involve a variety of factors, but the principal factor is variation in the number of seconds a specimen is immersed in the etchant. Images were also included in which etching gradations were intentionally varied by changing the number of seconds for etchant immersion. The aim was to enable the tool to classify even images in which the etching degree differs.

4.4 Bleeding

Bleeding is principally caused by residual etchant that oozes out from a gap in a specimen owing mainly to insufficient washing after etching, among other factors. Images of different degrees of bleeding were also included, limited to materials for which bleeding is apt to occur. The aim was to enable the tool to classify even images showing some bleeding

4.5 Effectiveness of image selection

As explained above, images were selected and taught to the tool for enhancing its versatility. The proportions of the number of images for training were adjusted based on the training results.

As a typical example, Fig. 4 shows the results obtained for training images containing scratches.

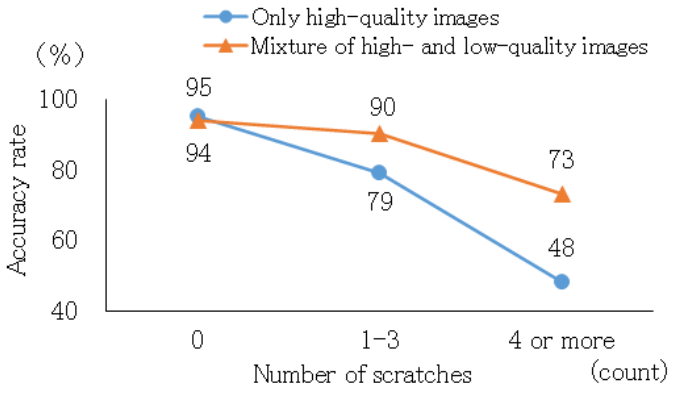

Fig. 4 Accuracy rate as a function of the number of scratches

A comparison was made of the results obtained for training only high-quality images and for training a mixture of both high- and low-quality images. The results revealed that a high correct rate was obtained in the latter case even for images containing scratches.

5. Consideration of effectiveness

Separate from the images used in training, images for tool validation were also prepared in advance and their classification was confirmed by a proficient examiner. Those images were then classified by the AI-based tool. The results showed that the tool achieved an accuracy rate of 90% compared with a rate of 100% for the proficient examiner.

The 90% that were correctly classified also included images in which the appearance of sorbite and other aspects were vastly different. This result confirmed that the purpose of this project was accomplished, which was to assist examiners who make incorrect determinations due to insufficient knowledge. It was concluded that the AI-based tool can reduce variation in classification results.

The 10% inaccuracy was largely due to materials that underwent plastic deformation or contained troostite. Because materials that experience plastic deformation or contain troostite are difficult to classify even for proficient examiners this result could be expected.

6. Conclusion

(1) It was confirmed that using AI can assist in making determinations of metallographic structures.
(2) It was also recognized, in consideration of image quality, that it is important to train the tool images containing confirmed uncertain elements in order to raise its accuracy rate.
(3) Based on the envisioned details, the tool was successfully made. Examinations to be done by human examiners and examinations that can be entrusted to the AI-based tool were confirmed.

7. Future issues

The tool made in this project only has a function for classifying. It is desired to equip it with an additional function for displaying advice in cases where image quality is low because specimen preparation did not go well. Such advice would prompt in correcting the details of preceding processes, such as insufficient polishing or dark etching.

It is also planned to improve the tool so that it can be deployed at other places where similar metallographic examinations are performed.

To make it realized, activities for increasing the accuracy and the number of metallographic structures that can be classified will be continuously taken.

■ Author ■

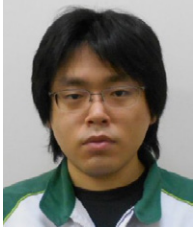

Tomoya SUZUKI

DX Promotion: Digitization of purchasing quotation process

Makoto INOUE* Yuhei MIYAMOTO* Junichi OSHIMI* Mieko KOBAYASHI*

Summary

The Services & Support Purchasing Department inherited previous work procedures involving manual tasks and paper output for carrying out purchasing operations from the issuing of quotation requests to the selection of suppliers. In recent years, JATCO has been proceeding with company-wide efforts to promote digital transformation (DX). This article describes activities for digitizing the purchasing quotation process using cloud computing and apps, which have produced substantial results.

1. Introduction

JATCO has been pushing ahead with efforts to reduce manhours and go paperless by promoting digital transformation (DX) against a backdrop of encouraging working from home under the impact of the Covid-19 pandemic and undertaking activities toward sustainable development goals (SDGs).

The Services & Support Purchasing Department, which arranges for materials, construction and other necessities, has also been moving ahead with various DX promotion activities. Improvement of a dedicated purchasing system and utilization of general-purpose software and applications, among other efforts, have produced various results in this regard.

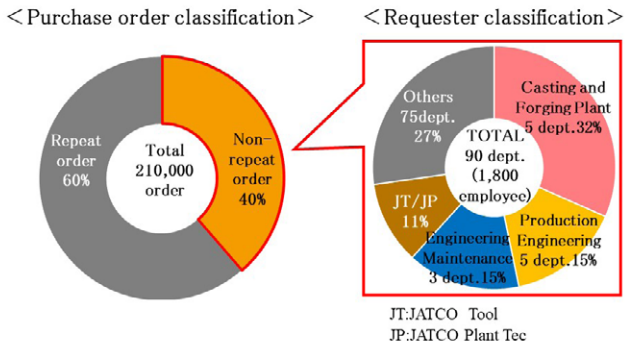

Fig. 1 Purchase order classification

Among these activities, this article focuses in particular on examples of company-wide efforts that have produced enormous benefits and also facilitated low-cost improvements through the use of general-purpose software.

2. Activities of the Services & Support Purchasing Department

2.1 Situation before improvement

The Services & Support Purchasing Department uses JATCO's dedicated purchasing system to determine prices and suppliers for procurement of the company's production facilities, tools, logistics, services, prototype parts, and so on.

Costs are allocated using a purchasing cost system to place orders for the materials used at the plants and for construction projects. Typical items ordered include cutting tools, spare parts for equipment and construction work.

The left-hand pie graph in Fig. 1 shows the total volume of cost quotations. The purchase order volume totals approximately 210,000 purchase orders annually, of which 60% are repeat orders and 40% are non-repeat orders.

Repeat orders refer to things purchased repeatedly on a continual basis. Prices are determined with suppliers in advance and items are ordered each time whenever

* Service & Support Purchasing Department

necessary. For non-repeat orders, a quotation is obtained every time according to the timing for ordering. After the department making a purchase request confirms the details, the final price and supplier are determined and an order is issued.

Non-repeat orders necessarily require manual tasks and paperwork outside of the existing purchasing cost system. The right-hand pie graph in Fig. 1 breaks down the departments making requests for the issuance of limited purchase orders. Approximately 1,800 employees in 90 departments are using the purchasing system.

2.2 Issues

The following is the flow of the process for issuing non-repeat orders. First, the requesting department prepares a quotation request and specification document and sends them to a supplier via the Purchasing Division. The supplier creates a quotation according to the specification document and submits it to the Purchasing Division. Purchasing sends the quotation to the requestor for confirmation of the specifications. After the details are confirmed, the final price and the supplier are approved by Purchasing. The requestor reports that information to a superior and then issues a purchase order via the Purchasing Division (Table 1).

Tasks denoted by the letters a to d in the table constituted issues because they still required manual work and paperwork. Accordingly, it was necessary to reduce the printing of documents and man-hours.

a: printing documents

b: mailing documents

c: creating e-mails

d: stamping on documents

3. Details of improvements

3.1 Data exchange box

The issues of “a: printing documents” and “b: mailing documents” were eliminated by adopting a tool for sharing data with external suppliers. Before the improvement, there were two ways to send specifications. The first method is to put the printed specifications in a box set up at JATCO and ask the supplier to come pick it up, and the other method is to send the documents by mail. Following the improvements made, a dedicated folder is created for each supplier on a cloud server as a data exchange box. Storing documents in folders achieves digitization. A function has also been added that automatically sends an e-mail message to notify a supplier when documents are stored in a folder (Fig. 2).

Table 1 Process flow for issuing non-repeat orders

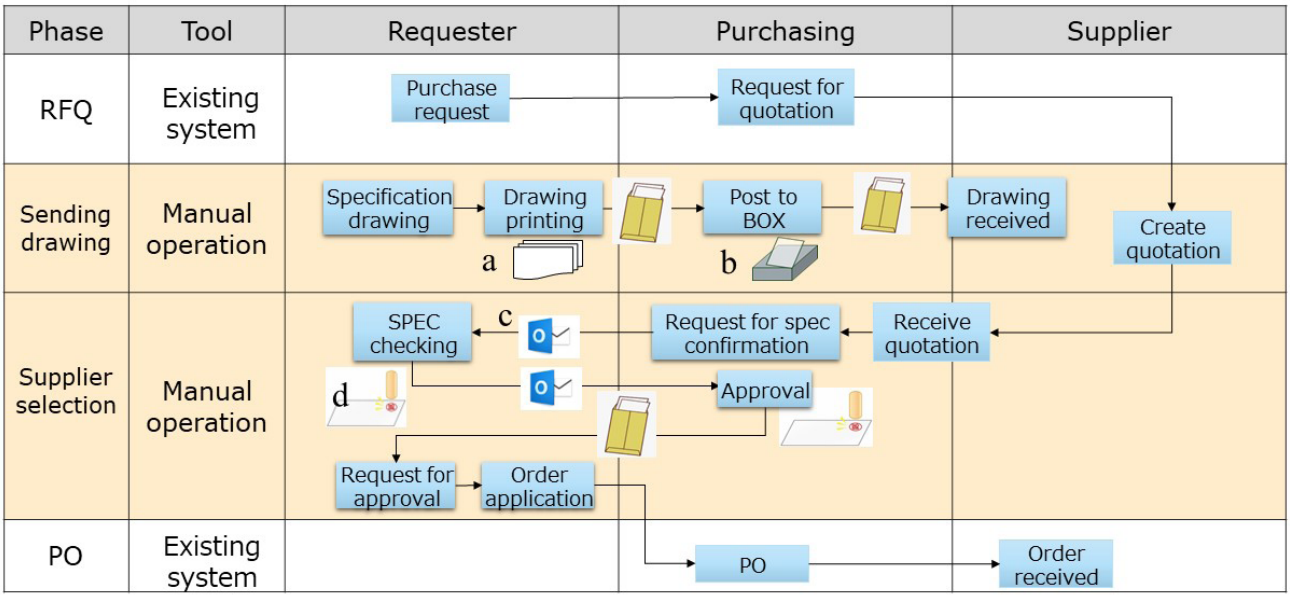

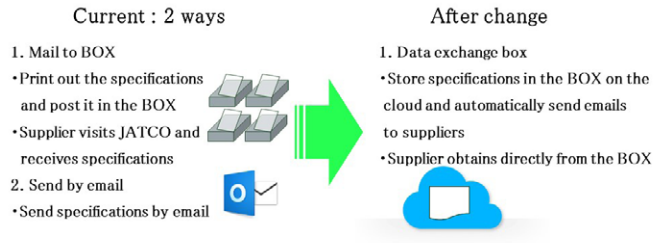

Fig. 2 Methods of sending specification documents

The following benefits have been obtained by using these functions.

(1) Reduction of paper usage

(2) Shortening of lead time for sending documents to suppliers

(3) Suppliers are automatically notified that documents have been sent to them.

In consideration of security, a separate password is established for each supplier to eliminate mistaken transmission of information.

3.2 Work improvement app

A work improvement app was created to eliminate the remaining issues of "creating e-mails," "requesting approval" and "stamping on documents."

3.2.1 Process flow visualization

Based on the organized flow of the existing process, an operational flow was created for the work improvement app to visualize approval routes (Fig. 3). The left-hand diagram shows the flow of the entire process, which is branched into approval routes at four points: "specification approval", "superior approval", "price approval" and "final approval."

The right-hand diagram shows the details of the branch flows in the specification approval phase for a requestor. The specification approval phase is branched into four routes labeled (1)-(4).

Similarly, there are two routes depending on whether a report is made to a superior, price approval is branched into three routes and final approval into three routes. Combining the branches in each phase results in a total of 72 routes.

Visualization of these complex flows established a concept for creating an accurate program without any omissions.

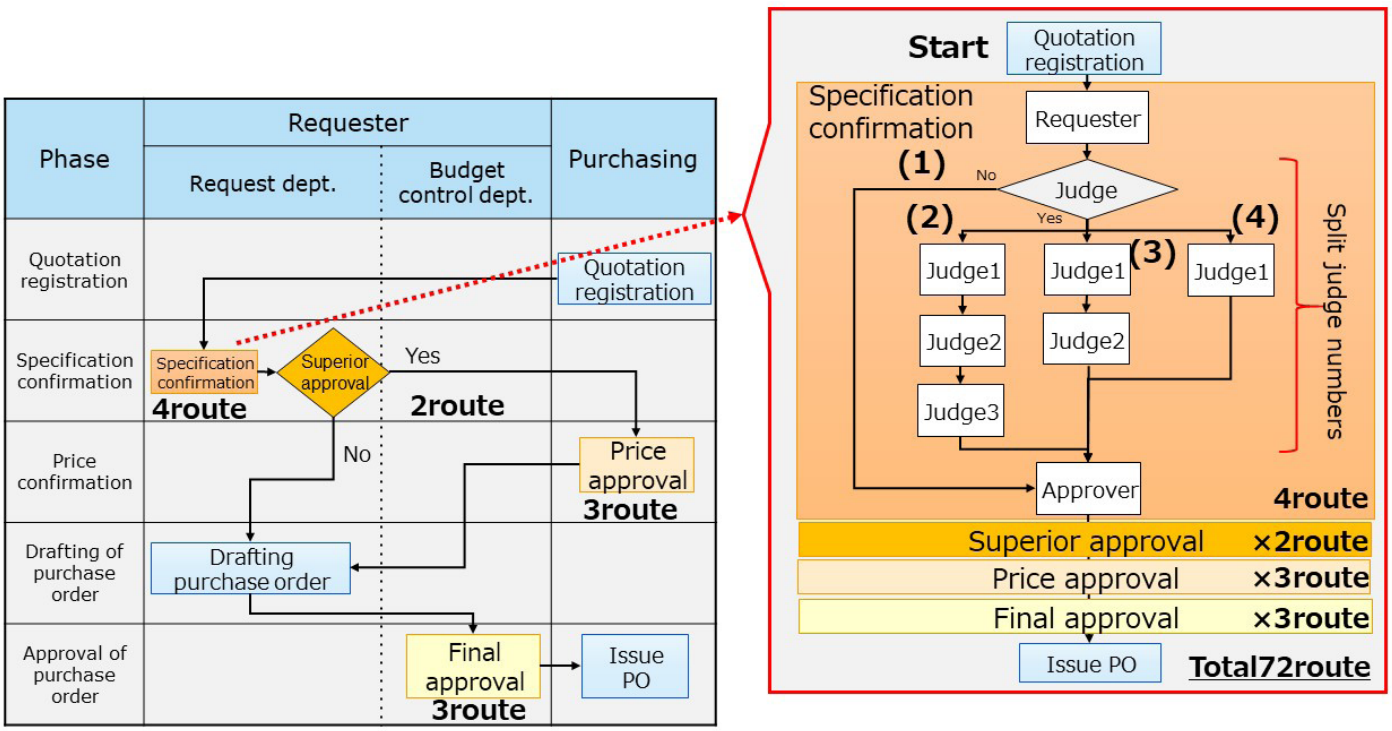

Fig. 3 Visualized approval routes

3.2.2 Process changed to the app

The following is the process that could be changed to the app (Table 2).

A: Registration of quotation information

- The Purchasing Division enters quotation data and quotations into the app.
- An e-mail requesting confirmation is automatically sent to the requestor.

B: Specification confirmation

- The requestor opens the app, confirms the contents, enters any necessary items and registers the information.
- When the approver completes the approval process, an e-mail is automatically sent to the Purchasing Division.

C: Price approval request & approval

- The buyer selects a supplier and requests final approval of the price to approver.
- The approver of the purchase confirms the details and then registers the approval.
- An e-mail indicating the price approval result is automatically sent to the requestor.

D: Approval request to superiors & purchase order issuance request

- The requester requests approval from the superior and registers the approval result in the app.
- An email requesting issuance of a purchase order is automatically sent to the Purchasing Division.

Previously, each department had various approval methods and processes for handling quotations. A system was successfully established by creating request routes satisfying the demands of each department.

3.2.3 Features devised in creating the app

The following features were carefully devised when creating the app.

(1) Screen for registering quotation data

The items to be input via the entry screen for registering quotation data were narrowed down to the minimum necessary in order to avoid increasing data input man-hours.

(2) Function for attaching quotations

A function for attaching quotations was adopted so that quotation contents can be easily confirmed whenever someone wants to know the details.

(3) Authorization

By using the approver table, only those who have approval authority can approve.

Table 2 Process flow after digitization

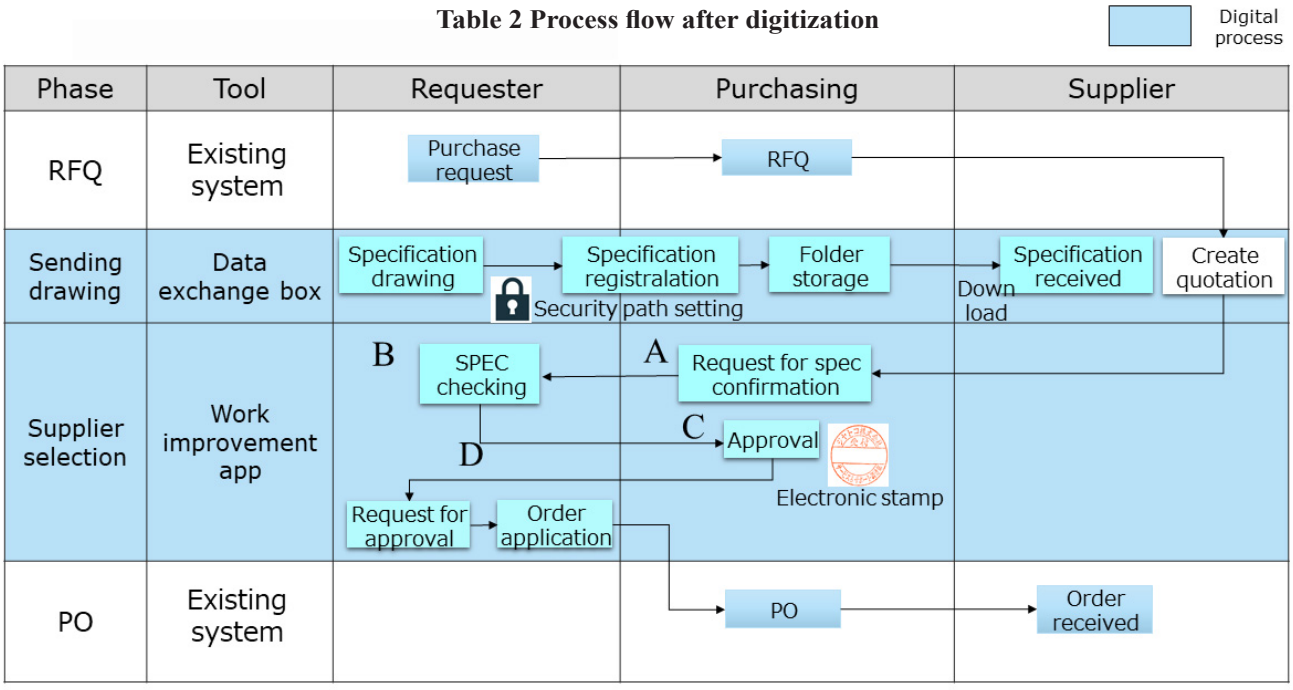

3.2.4 App functions

The following four improvements have been achieved by using the functions of the work improvement app, thus contributing to a reduction of man-hours and elimination of the printing of documents.

(1) Improvement of approval security

Approval security has been strengthened by granting the right to access data (Fig. 4).

Fig. 4 Improvement of approval security

(2) One-click approval without stamp

It is now possible to indicate “approval” or “send back” with one click. This function has eliminated the need to print documents and stamp to them for indicating approval (Fig. 5).

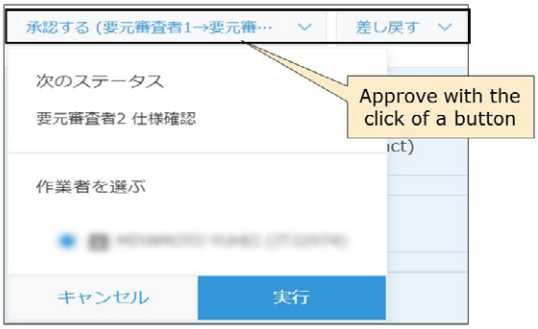

Fig. 5 One-click approval

(3) Status confirmation via a list

Items can be displayed in a list, enabling the status of each one to be visualized. Knowing the status has the effect of preventing work operations from being overlooked (Fig. 6).

Fig. 6 Status confirmation

(4) Automatic e-mail creation for making an approval request

Notification e-mails are created and sent automatically, making it unnecessary to create them manually (Fig. 7).

Fig. 7 Automatic creation of e-mail

3.2.5 Batch approval function

In proceeding with trials with related departments using the work improvement app, it was necessary to open the file of each item in order to approve it. This presented a problem that more man-hours were required than before.

Therefore, a challenge was undertaken to create a batch approval function that would enable multiple items to be displayed for confirming the contents and approving them all at one time. Although programming was complex because of the many branches in the approval process, a total of 40 programs were created to complete a batch approval program.

This batch approval function enables the contents of a displayed list of items to be confirmed, thereby establishing a highly efficient approval process (Fig. 8).

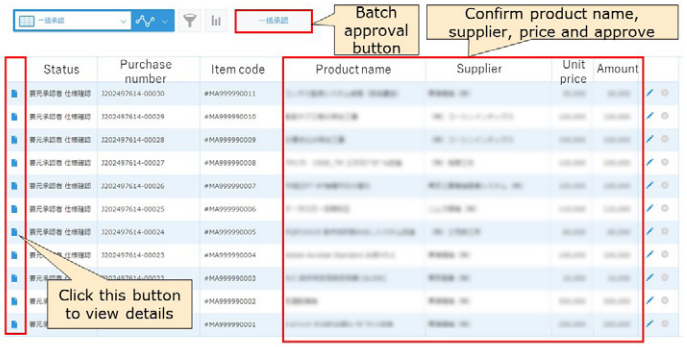

Fig. 8 Screen of batch approval

4. Conclusion

Various improvements were made to the details of the issues mentioned at the beginning, which produced the following substantial results.

1. Sharing the data exchange box with suppliers has eliminated the need to print and mail quotation requests and specification documents.
2. The creation of the work improvement app enabled the entire quotation process to be digitized.

These improvements have produced the following benefits.

a. Reduction of documents printed: 110,000 pages/year
b. Reduction of stamping to documents: 50,000 times/year
c. Reduction of work man-hours: 4,000 hours/year

As a final result, an effective cost reduction of 20 million yen per year was obtained. In addition, the following qualitative benefits were also achieved.

- Visualization of the work status simplifies progress management.
- The creation of a digitized system prevents work errors due to the loss of paper documents or for other reasons.
- The granting of data access rights has strengthened approval security.
- Lead time for approval and interdivisional communication has been shortened.

5. Future activities

Although overall man-hours have been reduced by the efforts described here, man-hours are still needed for data registration because the quotation information received from suppliers is input into the app manually.

Going forward, we want to utilize the upload function of the work improvement app to register quotation data more efficiently. We also aim to reduce man-hours further by applying robotic process automation to automate the work of attaching quotations, among other improvements.

The Services & Support Purchasing Department intends to promote further DX in pursuing higher efficiency and expansion of robot-based tasks by using various apps, general-purpose software and programs.

■ Authors ■


Makoto INOUE


Yuhei MIYAMOTO


Junichi OSHIMI

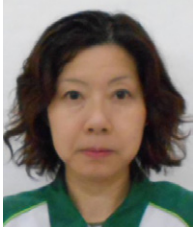
Mieko KOBAYASHI

Introducing the JR711E 7-speed Automatic Transmission for the Nissan Caravan

The JR711E 7-speed automatic transmission (AT) for rear-wheel-drive vehicles is installed on the Nissan Caravan that was released in Japan by Nissan Motor Co., Ltd. in April 2022, fitted with a new diesel engine (4N16).

Compared with the 5-speed AT used on the Caravan heretofore, the wider ratio coverage obtained with the increased number of gear steps provides both excellent power performance and fuel economy along with contributing to improved quietness during high-speed cruising.

Moreover, the added manual shift mode also ensures pleasing driving performance matching the driver's wishes.

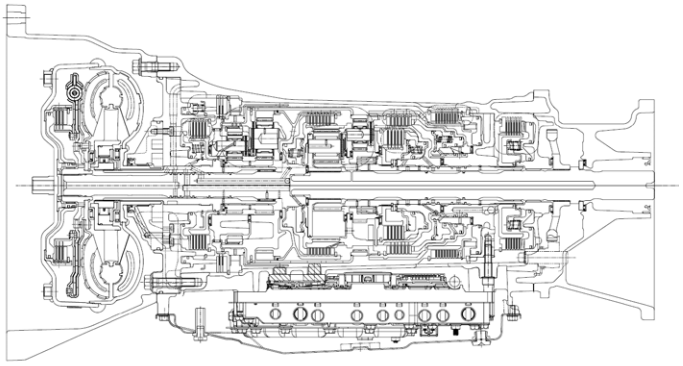

Fig. 1 Main cross-sectional view

Table 1　Specifications of JR711E

Torque capacity		370 Nm
Torque converter size		260 mm
Gear ratios	1st	4.886
	2nd	3.169
	3rd	2.027
	4th	1.411
	5th	1.000
	6th	0.864
	7th	0.774
	Rev.	4.041
Ratio coverage		6.31
Final gear ratio (reference)		3.700
Selector positions		P, R, N, D + Manual shift
Overall length		756 mm
Weight (wet)		101kg

※2.4L 4WD

Nissan Caravan

Introducing the JR913E 9-speed Automatic Transmission for the Nissan Fairlady Z

The JR913E 9-speed automatic transmission (AT) for rear-wheel-drive vehicles is installed on the new generation of the Fairlady Z that Nissan Motor Co., Ltd. released in July 2022.

The new Fairlady Z is mounted with a 3.0-liter direct-injection turbocharged engine that significantly improves power output over that of the previous model. That improvement is combined with the high transmission efficiency of the JR913E, which fully transmits the torque produced by the engine to the tires, to achieve superb power performance.

In addition, reduced shift shock and improved shifting speed deliver shifting performance befitting a sports car, thereby contributing to a dramatic improvement of driving performance.

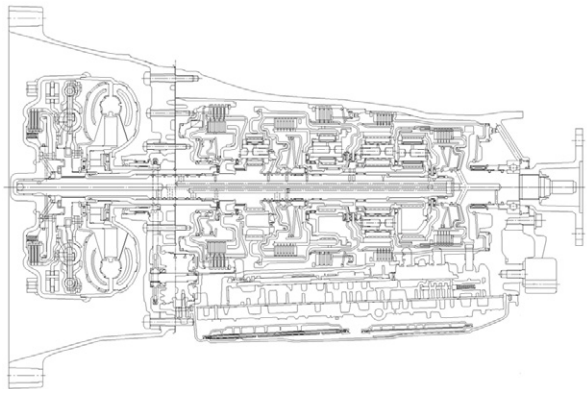

Fig. 1 Main cross-sectional view

Table 1　Specifications of JR913E

Torque capacity		700 Nm
Torque converter size		260 mm
Gear ratios	1st	5.425
	2nd	3.263
	3rd	2.249
	4th	1.649
	5th	1.221
	6th	1.000
	7th	0.861
	8th	0.713
	9th	0.596
	Rev.	4.799
Ratio coverage		9.1
Final gear ratio (reference)		3.133
Selector positions		P, R, N, D + Manual shift (Paddle) (Park & Shift by wire)
Gear box length		439.5 mm
Weight (wet)		99.5 kg

Nissan Fairlady Z

Introducing the Jatco CVT-X(JF022E) for the Renault Austral

The Jatco CVT-X (JF022E) is installed on the new generation of the Renault Austral that was launched in the European market in October 2022 as Renault's flagship model.

Thanks to its wide ratio coverage, friction reduction technologies and twin oil pump system, the JF022E elicits the full performance of Renault's latest 1.3-liter, 4-cylinder, turbocharged engine, thereby contributing to improvement of both fuel economy and driving performance.

Reflecting the needs of the European market, the JF022E incorporates JATCO's first stop-start sailing technology that turns off the engine while the vehicle is coasting. It is also optimally tuned to match the concept of an SUV. These features achieve both excellent fuel economy and dynamic driving performance that are highly acclaimed by customers.

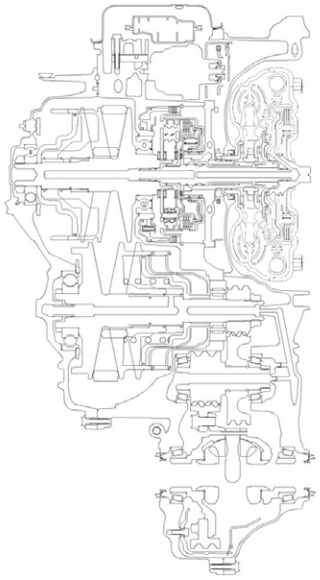

Fig. 1 Main cross-sectional view

Table 1 Specifications of JF022E

Torque capacity	330 Nm
Torque converter size	230 mm
Pulley ratios	2.953 - 0.361
Ratio coverage	8.18
Reverse gear ratio	0.745
Final gear ratio	5.676
Selector positions	P, R, N, D + 7step manual shift mode (Park & Shift by wire)
Overall length	381.8 mm
Weight (wet)	103.4 kg

Renault Austral

Introducing the Jatco CVT-X(JF022E) for the GMMC Outlander

The Jatco CVT-X (JF022E) is installed on the new generation of the Outlander that GAC Mitsubishi Motors Co., Ltd. (GMMC) launched in the Chinese market in November 2022.

Compared with the all-new Outlander that Mitsubishi Motors Corporation released in North America in 2021, the Chinese specification model is equipped with a 1.5-liter direct-injection turbo engine and a 48V mild hybrid system. The JF022E actively uses the region of good engine efficiency and reliably transmits the torque boost provided by turbocharging to the tires as driving force. Moreover, in addition to the torque assist provided by the mild hybrid system, its improved shifting speed ensures quick acceleration response matching the driver's operation of the accelerator pedal.

The shift mechanism of the JF022E has been specifically tuned for the first time to match Mitsubishi Group vehicles, and its mechanical friction has been thoroughly reduced. These features enable the JF022E to contribute to both high power output and excellent fuel economy, qualities that are highly acclaimed by customers.

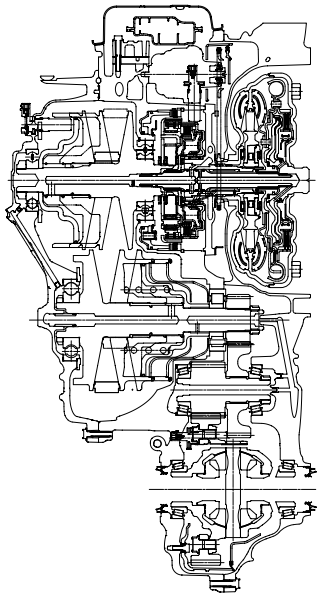

Fig. 1 Main cross-sectional view

Table 1 Specifications of JF022E

Torque capacity	280 Nm
Torque converter size	230 mm
Pulley ratios	2.870 - 0.361
Ratio coverage	8.0
Reverse gear ratio	0.745
Final gear ratio	6.036
Selector positions	R←N←H→N→D/M (Paddle shift only) + P button
Overall length	392.5 mm
Weight (wet)	103.0kg (2WD) / 103.8kg (4WD)

GAC Mitsubishi Outlander

Introducing the Jatco CVT8(JF016E) for the Nissan Serena

The Jatco CVT8 (JF016E) is installed on the new generation of the Nissan Serena that Nissan Motor Co., Ltd. released in Japan in December 2022, following the execution of a full model change.

The JF016E adopts a newly designed control valve that provides both control stability and responsiveness for dramatically improving shift response and substantially reducing friction. As a result, the JF016E brings out the full performance of the MR20 engine, thereby contributing to an enhanced feeling of power and driving performance as well as improving fuel economy.

In addition, the JF0162 adopts a next-generation shift-by-wire system complementing Nissan's first push-button shifter.

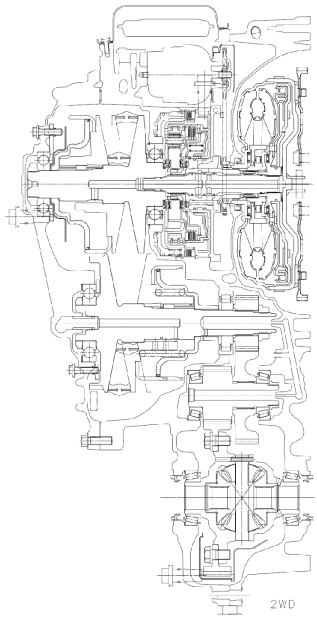

Fig. 1 Main cross-sectional view

Table 1 Specifications of JF016E

Torque capacity	250 Nm
Torque converter size	236 mm
Pulley ratios	2.631 - 0.378
Ratio coverage	7.0
Reverse gear ratio	0.745
Final gear ratio	5.385
Selector positions	P, R, N, D/M + Manual shift (Paddle) (Park & Shift by wire)
Overall length	358.8 mm
Weight (wet)	95.1 (2WD) / 95.6 (4WD)

Nissan Serena

Patent

This patent is related to the improvement of the sound vibration performance of Jatco CVT-X that is introduced in the technical report "Development of a new CVT featuring high efficiency and wide ratio coverage".

1. AUTOMATIC TRANSMISSION

(Fig. 1)

Application Number :2017-138492
Application Date :14.7,2017
Patent Number :7117831
Registration Date :4.8,2022
Title :AUTOMATIC TRANSMISSION
Inventors :Yukawa Hirohisa,
Yamashita Katsunori

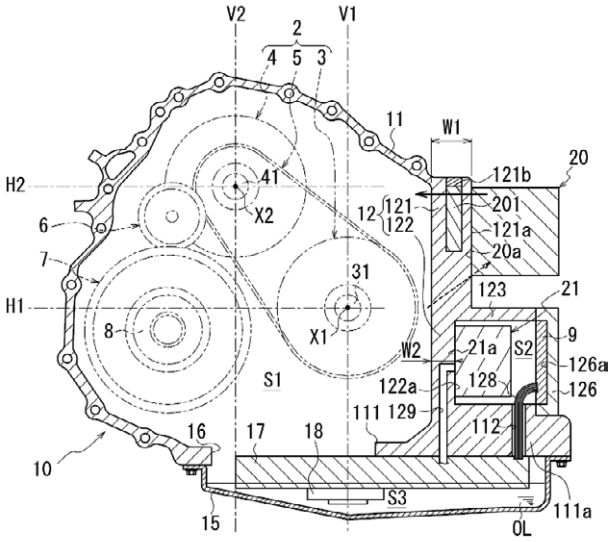

Fig. 1

【SUMMARY OF THE INVENTION】

When an electric oil pump is attached to the outer circumference of the automatic transmission case, the further away from a rotating axis X1 of the primary pulley, which is the node of power plant resonance (the point of small amplitude), there is the issue that the worse the sound vibration performance becomes.

In the automatic transmission of the present invention, the primary pulley side end 21a of the electric oil pump 21 is positioned closer to the primary pulley 3 than the primary pulley side end 20a of the oil cooler 20.

This allows the electric oil pump 21, which has a higher sound power level than the oil cooler, to be placed closer to the node of the power plant resonance of the power plant, thereby reducing the deterioration of the sound vibration performance.

ジヤトコ・テクニカル・レビュー　No.22

JATCO Technical Review No.22

発　　行　2023年3月
発 行 所　ジヤトコ株式会社
　　イノベーション技術開発部
　　〒417-8585
　　静岡県富士市今泉700-1
　　TEL: 0545-51-0047（代）
　　FAX: 0545-51-5976
編　　集　E−グラフィックス コミュニケーションズ株式会社
　　東京都三鷹市牟礼6丁目25番28号

March 2023
Distributor　Inovative Technology Development Department
JATCO Ltd
700-1 Imaizumi, Fuji City, Shizuoka
417-8585, Japan

JATCO Ltd

700-1, Imaizumi, Fuji City, Shizuoka 417-8585, Japan
TEL: +81-545-51-0047 FAX: +81-545-51-5976

www.jatco.co.jp/english